NASA Contractor Report 175092

Analytical Determination of Propeller Performance Degradation Due to Ice Accretion

(NASA-CR-175092) ANALYTICAL DETERMINATION OF PROPELLER PERFORMANCE DEGRADATION DUE TO ICE ACCRETION Final Report (Sverdrup Technology, Inc.) 138 p HC A07/MF A01 CSCL 01C G3/03
N86-23577
Unclas 05976

Thomas L. Miller
Sverdrup Technology, Inc.
Lewis Research Center
Cleveland, Ohio

April 1986

Prepared for
Lewis Research Center
Under Contract NAS 3-24105

NASA

National Aeronautics and
Space Administration

TABLE OF CONTENTS

	Page
LIST OF SYMBOLS	iii
CHAPTER 1. INTRODUCTION	1
CHAPTER 2. SUMMARY OF PREVIOUS WORK	5
A. Early Work	
1. Experimental Effort	5
2. Analytical Effort	7
B. Recent Work	
1. Experimental Effort	10
2. Analytical Effort	12
CHAPTER 3. CODES EMPLOYED	17
A. Theodorsen Transformation	17
B. Droplet Trajectory Code	19
C. Aerodynamic Coefficient Correlations	22
1. Gray Correlation	30
2. Bragg Correlation	32
3. Flemming Correlations	34
4. Miller Correlation	36
D. Propeller Performance Code	37
CHAPTER 4. PERFORMANCE DEGRADATION CODE ASSEMBLY	39
CHAPTER 5. RESULTS	44
A. Bragg	48
B. Gray	49
C. Flemming	51

	Page
SUMMARY AND CONCLUSIONS	54
REFERENCES	57
FIGURES	62
TABLES OF EXPERIMENTAL & ANALYTICAL DATA	80
APPENDIX 1. PROGRAM FLOWCHART	85
APPENDIX 2. USER'S GUIDE	88
APPENDIX 3. SAMPLE CASE	100

LIST OF SYMBOLS

a	speed of sound
Ac	accumulation parameter
b	propeller section chord
B	number of propeller blades
BHP	propeller power absorption
c	airfoil section chord
C_d	section drag coefficient
C_l	section lift coefficient
C_p	propeller power coefficient = $\frac{P}{\rho n^3 D^5}$
C_T	propeller thrust coefficient = $\frac{T}{\rho n^2 D^4}$
D	propeller diameter
E	total collection efficiency = $\frac{\Delta Y_0}{h}$
Fr	Froude number = $\frac{U}{\sqrt{cg}}$
g	gravitational constant
h	airfoil project height
I	airfoil drag constant
J	propeller advance ratio = $\frac{V}{nD}$
K	inertia parameter = $\frac{\sigma \delta^2 U}{18 c \mu}$
k/c	particle roughness height
K_o	modified inertia parameter = $K(1 + .0967\,(R_u)^{0.6397})$
M, M_x	local Mach number

n, N	propeller revolutions per minute
r	leading edge radius of curvature
R_u	droplet Reynolds number = $\rho \lvert \bar{u} - \dot{\eta} \rvert U \delta / u$
S	airfoil surface arc length
t/c	airfoil thickness to chord ratio
T_o	freestream temperature
u	local air velocity
U, V	freestream velocity
w	liquid water content
x	propeller radial location in fraction of tip radius
Y_o	initial droplet y-coordinate
α	airfoil section angle of attack
α_i	induced angle of attack
β	impingement efficiency = dy_o/ds; propeller twist angle
βmax	maximum local impingement efficiency
δ	droplet diameter
η	propeller efficiency = $\frac{J C_T}{C_p}$
$\dot{\eta}$	local droplet velocity vector
μ	absolute air viscosity
ρ	air density
ρice	ice density
σ	droplet density
σ_p	section solidity = $\frac{Bb}{\pi D}$

τ icing time

ϕ resultant advance angle

CHAPTER 1

INTRODUCTION

The accretion of ice on the lifting or propulsive surfaces of an aircraft is a phenomenon which can have severe, if not disastrous, consequences if it is not dealt with properly and in a timely fashion. In many cases, this accretion may produce a serious reduction in lift and increase in drag, requiring more power than is available and resulting in a serious departure from the mission profile. Although measures and devices exist which generally prevent this worst-case scenario from happening, ice accretion on airfoils is still a common occurrence in certain atmospheric conditions and as such merits further study because of the significant negative effect which it has on airfoil and aircraft performance. It is the objective of this thesis to provide a single computer code which will accurately predict the degree of performance degradation, primarily with respect to drag increment, which will result from the exposure of an airfoil to some set of atmospheric and flight conditions conducive to ice formation.

Two basic types of ice are found to occur as a result of exposing an airfoil in forward motion to supercooled water droplets in a sub-freezing environment (Fig. 1). The type of ice which will form may be determined by a variety of factors including freestream velocity, liquid water content of the cloud, droplet size distribution, and freestream temperature. Based upon an investigation of the data currently available, the two latter factors appear to be the most influential in determining the resulting ice type. The first kind of ice, known as rime ice, occurs at relatively low velocities, low liquid water content values (typically 0.5 to 1.0 grams per cubic meter), and temperatures well below freezing. Due primarily to the very cold temperatures associated with rime ice formation, the droplets tend to freeze on impact to form a fairly smooth addition to the leading edge of the airfoil. At some point with respect to the combination of flight and atmospheric conditions present, ice type transitions from rime to glaze ice. Not only is the crystalline structure of these ice types different, but glaze ice is also produced by higher freestream velocities, higher liquid water content values (on the order of 1.5 to 3.0 grams per cubic meter), and temperatures near, but below, freezing. Again, due chiefly to the warmer temperatures involved, the water droplets impacting the surface tend not to freeze on impact but rather to strike the airfoil or existing ice formation and run back somewhat in a chordwise direction before freezing.

Both types of ice cause significant performance degradation of the airfoil. When compared to the aerodynamics of an airfoil in the clean, or non-iced, configuration, the iced airfoil will virtually always exhibit a decrease in lift, an increase in drag, and a change in pitching moment which will yield a detrimental effect on aircraft stability. Examination of the available icing data base indicates that the degree of performance degradation, specifically with respect to drag increment, is generally more severe for the glaze ice condition. This may be attributed to the more drastic alteration of the leading edge of the airfoil as a result of glaze ice formation, as compared to the typically smoother and less obtrusive rime ice formation. Increases in drag coefficient in excess of 100% or more are not unusual for either type of accretion.

Both rime and glaze ice act to negatively influence airfoil performance by physically altering the shape of the airfoil, thereby changing the flowfield around the airfoil. In computing this flowfield for the propeller case, the rotational and induced components of velocity, as well as the forward component, must be taken into account as exhibited in Figure 2. The reshaping of the airfoil surface by the ice accretion and the rough peaks and surfaces commonly present in ice accretions, especially in the glaze ice case, serve to induce premature transition and often separation of the flow around the airfoil, thus spoiling its designed aerodynamic characteristics. The associated ice roughness also acts as an energy loss device. For the propeller configuration dealt with in this thesis, these effects may occur along the entire span of the propeller and have the same effect on propeller aerodynamics as they are found to have with respect to fixed wing aircraft. Ice accretion on a propeller may then translate for example into an increase in power required to maintain a given flight condition when ice is allowed to form on the propeller blades. As a pilot, passenger, or other concerned party it would therefore be desirable before undergoing an icing encounter to have some idea of just how much power would be required to maintain a flight condition with ice accreting on the propeller and other aircraft components, so that some decision could be confidently made regarding the safety of undergoing or avoiding such an encounter. In addition, information provided by this code may be used in establishing propeller ice protection system specifications, as well as potentially in future icing certification efforts.

CHAPTER 2

SUMMARY OF PREVIOUS WORK

Much work has already been done in attempting to better understand ice accretion and its effect on aircraft performance. However, due to the very complicated physics which govern the ice accretion process, many questions remain unanswered in this area and it is still difficult with present technology to accurately predict the degree of performance degradation which will result from an arbitrary icing encounter. Several recent developments have made the prediction of performance degradation, especially in terms of drag increase, more reliable and have expanded the range of conditions over which relatively accurate predictions can now be made. Yet much of the groundwork for these developments was laid thirty to forty years ago. This initial work involved both experimental and analytical investigations of ice accretion, and much of the icing data used in current correlation development work was actually collected during this early period, from roughly the late 1940's to the late 1950's.

A. Early Work

1. Experimental Effort

Early propeller performance degradation data was gathered using both simulated ice and actual natural icing encounters. Corson and Maynard (1) in 1946 used simulated ice on propeller blades and measured average efficiency losses on the order of three percent, with maximum losses of fifteen percent noted. In 1948, Preston and Blackman (2) undertook a flight test program in which they also noted average decreases of roughly ten percent in propeller efficiency due to ice formation, as well as the associated increase in drag. This study was of special significance due to the fact that an attempt was made to examine the effects of ice accretion on all major components of the aircraft. Possibly the most complete and informative work relative to ice accretion on propellers was performed and documented by Neel and Bright (3) in 1950. In a flight test program in which efficiency loss was measured during actual natural icing encounters, they observed losses of roughly ten percent in most cases, with maximum losses on the order of twenty percent. The performance degradation data of Neel and Bright is still used by present researchers to develop or verify analytical propeller performance degradation codes.

Also of note with respect to experimental investigations of airfoil icing are a series of test programs undertaken in the Icing Research Tunnel at the NASA Lewis Research Center and documented by a variety of NACA personnel in the early and mid-1950's. Gray and von Glahn (4,5) looked at the effects of ice on the performance of NACA 65A004 and 65_1-212 airfoils, and lesser increases were noted for both airfoils with rime ice accretions. Brun, et. al. (6,7,8) and Brun and Vogt (9) produced a series of reports dealing with experimental measurements of performance degradation of NACA 65A004, 65_1-208, and 65_1-212 airfoils due to ice formation. These reports focused on the impingement characteristics of these airfoils, which in turn relate directly to drag increment and decreased performance. Included in their investigations were the effects of airfoil thickness and angle of attack on droplet impingement values, noting that thickness tends to increase the volume of water collected and decrease the rearward limit of droplet impingement, and as expected total impingement increases with increasing angle of attack.

Gelder, Smyers, and von Glahn (10) in 1956 investigated droplet impingement properties on several airfoil sections of various thickness and concluded in part that the total and maximum local collection efficiencies were strong functions of first of all the modified inertia parameter, a parameter which takes into account factors such as freestream velocity, droplet density and diameter, airfoil chord, absolute air viscosity and air density, and also of thickness ratio and angle of attack.

These early experimental programs not only provided valuable insight into the process and effects of ice accretion, but also established a data base from which analytical ice growth and performance degradation predictions could be developed or verified.

2. Analytical Effort

In the report by Neel and Bright (3), the authors attempted to predict analytically the degree of propeller performance reduction to be expected as a result of ice accretion. Using blade element theory as the basis for their analysis, and by relating the change in airfoil drag/lift ratio to efficiency loss, they predicted efficiency losses which agreed at least to the same order of magnitude with the experimentally obtained values.

Bergrun (11) in 1951 offered a method for determining droplet impingement characteristics on an airfoil by solving a set of simultaneous differential equations which described the particle dynamics of a water droplet moving in an air stream. This same principle forms the basis for present droplet trajectory codes also. Along with Lewis in 1952 (12), Bergrun also investigated using probability analysis the atmospheric factors responsible for ice formation and identified with a quite limited data base the three parameters still felt to be of primary importance in the ice accretion process: cloud liquid water content, water droplet size, and ambient temperature.

In 1958, Gray undertook an icing study of the NACA 65A004 airfoil (13) and attempted to develop a drag coefficient correlation which would relate ice nature and droplet impingement rates to the associated aerodynamic penalties for this airfoil. Using experimental icing data, he obtained a dimensional correlation which he found to be accurate at all but angles of attack greater than four degrees, presumably due to the flow separation occurring at the higher angles of attack. Gray then published in 1964 a report (14) in which he examined available aerodynamic icing data for other airfoils and modified his correlation to make it applicable to these other airfoils as well. He accomplished this through the introduction of the factor 'r' which represents the airfoil leading edge radius of curvature in percent of chord. This modified correlation represented the only available icing drag coefficient correlation at that time, and saw widespread use for several years. Only recently has its validity as a general icing correlation been questioned, and it will most probably remain in use until a suitable replacement is offered.

The formulation of Gray's drag coefficient correlation represented the last major development with respect to ice accretion effects for several years. The advent and use of the jet engine and turbofan on the propulsion scene then deemphasized the use of the propeller as a propulsive device and subsequently drew much attention away from the problem of ice accretion, which was of lesser importance for the large commercial transports and military aircraft of that time. However, with recent increased fuel costs and a renewed interest in commuter aircraft and all-weather helicopters, new interest in ice protection systems and a need to better understand the phenomenon of ice accretion have again come about.

B. Recent Work

1. Experimental Effort

Researchers involved in the renewed study of ice accretion recognized the need to expand the quite limited experimental data base, especially to include tests of ice accretion on the newer airfoils designed for use on current general aviation aircraft, propellers, and helicopter rotors. Shaw, Sotos, and Solano in a 1982 report (15) discussed the results of one such program in which aerodynamic performance degradation data was obtained for a NACA 63_2-A415 airfoil. Glaze and rime ice formations were studied in both cruise and climb configurations and significant performance degradation was noted for all cases. Also evaluated was the effect of aft frost growth on airfoil performance, and this phonomenon was found to significantly increase section drag coefficient. This project was also of importance because it provided new data with which to test Gray's drag coefficient correlation. The authors found that the correlation was as accurate in most cases for the new data as it was for the old data upon which the correlation was developed, but it became poorer in accuracy for higher liquid water content values. This conclusion again pointed out the need for a better, more accurate drag coefficient correlation.

Also in 1982 at the Ohio State University, Bragg and Gregorek (16), along with Zaguli (17), used simulated ice shapes to investigate various aspects of the ice accretion problem. In one test a simulated rime ice shape was applied, with and without surface roughness, to a NACA 65A413 airfoil and the ensuing performance degradation was measured. Surface roughness was determined to be an important factor in modelling ice shapes, affecting drag coefficient and $C_{\ell_{max}}$. In the second test, they also demonstrated the feasibility of using wood shapes to model ice accretions on a NACA 63_2-A415 airfoil in order to ascertain the effects of the ice shape on the aerodynamic flowfield.

Flemming and Lednicer in 1983 (18) tested a series of scale models of helicopter airfoils to investigate the effects of artificial ice accretion on airfoils at high speeds. Aerodynamic performance degradation of all the airfoils was noted, with the authors citing drag coefficient increases of up to roughly 300% in some cases. Also accomplished in this test were better definitions of the boundaries for ice growth and ice type in terms of static temperature, Mach number, and liquid water content.

Motivated by a desire to find a relatively simple, economical means of collecting performance degradation data relative to rotating systems, Korkan, Cross, and Cornell (19,20) and Korkan, Cross, and Miller, (21,22) in 1984 undertook a test program utilizing a model helicopter with a 53.375-inch diameter, 2.5-inch chord NACA 0012 main rotor with a simulated ice shape attached and measured main rotor performance degradation. Trends identical to those previously seen on larger or full-size airfoils and rotors were noted, with increases of up to 300% in torque coefficient found to be required to maintain a given thrust coefficient after the addition of the simulated ice to the rotor blades. The sensitivity of the tip region of the rotor to the adverse effects of ice formation was also seen, with an increase in torque coefficient required to maintain a given thrust coefficient of as much as 150% measured when the simulated ice was extended from the 85% rotor radial location out to the 100% location.

Just prior to this model helicopter test, the issue of Reynolds number effects on aerodynamic data was also addressed by the same authors (20,22). In a 2-D airfoil test using a NACA 0012 airfoil section with a simulated ice formation geometrically identical to that used in the model helicopter test, the authors collected aerodynamic data for the airfoil in both clean and iced configurations over a Reynolds number range which included the operating range of the model helicopter rotor tip. Reynolds numbers effects appeared significant only at the highest Reynolds number tested, 3.4×10^6.

2. Analytical Effort

Much has been learned in recent years as a result of these experimental programs, and a major contribution of these tests has been in the expansion of the icing data base to provide more current data with which to develop and evaluate analytical methods for prediction of icing-related performance degradation. As in the experimental area, many analytical advances have also been recently made. These advances have taken the forms of both better methods of predicting droplet impingement characteristics as well as better aerodynamic performance degradation correlations.

Bragg et. al. recently developed a computer program to calculate water droplet trajectories and thereby determine airfoil impingement efficiencies and theoretical ice shapes (23). Development of this code represented a major step toward the goal of analytical prediction of airfoil performance degradation due to ice accretion and the code is now often used for this purpose. The code itself will be discussed in more detail in a later chapter as it is one of the major components of the code development which is the subject of this report. Along with this droplet trajectory code, Bragg and Gregorek have also formulated a drag coefficient correlation for the rime ice condition (16). In this correlation, the change in drag due to ice is given as a function of several variables related to flight and atmospheric conditions, airfoil geometry, and duration of ice accretion. This correlation has seen widespread use since its development and has only recently been studied in any detail to better define its range of applicability. An unpublished investigation performed by this author shows the correlation to in several cases significantly overpredict drag increment for icing data which appears to be rime-oriented.

Canadale and Gent in a 1983 report (24) detailed the development of another two-dimensional airfoil icing code.

Unlike the Bragg code, the effects of compressibility, kinetic heating, and water runback are taken into account in this code, thus making it applicable to both rime and glaze ice conditions. Designed to be applied to helicopter configurations, the code employs a heat balance analysis to calculate the kinetic heating and runback effects. The authors have reported good agreement between predicted and experimentally obtained ice shapes, temperature distributions, and icing threshold conditions.

Flemming and Lednicer (25) have used experimental icing data to formulate new rime and glaze ice drag coefficient correlations. In addition, this data was also used to formulate separate lift and moment coefficient correlations. These correlations, recently published in final form (25), have shown some promise in preliminary evaluations and are discussed in more detail in a later section.

Using Bragg's droplet trajectory code, Korkan, Dadone, and Shaw (26) have developed a method for predicting performance degradation of rotating systems under the influence of ice accretions. Limited currently to the rime ice condition, the effects of ice formation on helicopter rotor or propeller thrust coefficient, torque coefficient, and efficiency may be calculated. Originally restricted to the helicopter hover mode, extension of the method to include forward flight calculations has been performed and documented in a recent AIAA paper by Korkan, Dadone, and Shaw (27). The method essentially involves first obtaining non-iced values of angle of attack and Mach number as a function of radial location, then determining impingement efficiency and accumulation parameter for a given set of icing conditions for each radial location, and finally determining the resulting drag increment at each radial location. An existing propeller or helicopter performance code with the iced drag increment input then will produce values of iced performance which may be compared with known or calculated clean values to ascertain the degree of performance degradation which results from the given icing encounter. Good agreement between theory and experiment has been obtained for both the propeller and helicopter rotor configurations.

Korkan et. al. have also developed a method of averaging (27) to compute rotor or propeller disk performance in which angle of attack and Mach number are first averaged around the disk. From these averaged values, collection efficiency, accumulation parameter, and finally drag increment are calculated for given icing conditions. This procedure has been shown to be virtually as accurate as the previously described method but provides a significant reduction in the number of necessary calculations and hence computer run time.

Miller, Korkan, and Shaw in 1983 (28) attempted to develop a drag coefficient correlation for the glaze ice condition using statistical analysis of icing data as a basis of the correlation development. Although a resulting correlation was presented, it represented only the state of the study at the time and showed a need for much further modification and analysis. Feasibility of using such an analysis as the basis for correlation development was demonstrated, but the results of such an analysis must be interpreted correctly and in tandem with physical observations of the associated phenomenon to make the method truly beneficial.

Bragg (29) has also recently documented a study in which he predicted airfoil performance with both simulated rime and glaze ice shapes. Various codes were examined for possible use in calculating pressure distributions on an airfoil with glaze ice attached. The potential flow code of Bristow was determined to be suitable for this purpose and provided good agreement between predicted and experimental pressure distributions. Bragg also investigated the effects of surface roughness in the laminar boundary layer on drag increment and offered promising results for predicting drag increase by this method.

CHAPTER 3

CODES EMPLOYED

A. Theodorsen Transformation

The first step in the performance degradation determination process is computation of the flowfield about the airfoil section being investigated. The method used in this code is a Theodorsen technique of conformal mapping which translates the airfoil coordinates to a circle plane and from that plane determines the velocity distribution about the airfoil. The calculations involved in this method make the assumption of potential flow, in which no viscous effects are considered. This has been found to be an acceptable assumption, allowing the method to yield accurate results, due to the fact that viscous effects existing in the boundary layer near the leading edge of the airfoil have little effect on droplet trajectory for all but the smallest of droplet sizes. The magnitude of the inertia force associated with the larger droplets greatly predominates over any viscous deflection or interaction phenomena in this region.

This particular flowfield calculation technique is limited to incompressible flow, which is acceptible since compressibility effects on droplet trajectory have been found to be negligible up to the airfoil section critical Mach number for all but the smallest of drop sizes. In recent joint studies between NASA and the Royal Aircraft Establishment (RAE) (30), back-to-back comparisons were made between the impingement efficiency values generated using the incompressible Theodorsen method at NASA and those calculated using the compressible flowfield code of Garabedian and Korn for supercritical airfoil sections at the RAE. Good agreement was observed between the two methods, thereby deemphasizing any compressibility effects and validating the use of the Theodorsen transformation in computing the flowfield about airfoil sections exposed to icing.

Theodorsen's method makes use of the Karman-Trefftz transformation to relate the airfoil geometry to a near circle plane. This particular transformation is used because it has been found to yield a better near circle for airfoils with finite trailing edge angles by avoiding any cusp atthe trailing edge. It is given by the formula

$$z = nb \frac{(z_1+b)^n + (z_1-b)^n}{(z_1+b)^n - (z_1-b)^n} \qquad (1)$$

where z is a vector which may define some profile such as an airfoil section, and z_1 is a vector from the origin, O, to some arbitrary point on the circle. Here, b represents a vector directed along the positive x-axis with length OB', where B' is a point at which the circle and x-axis intersect. The value of n is typically just less than two, and it may be observed that for n=2, the Karman-Trefftz transformation simplifies to the more familiar Joukowski profile, given by

$$z = z_1 + \frac{b^2}{z_1} \qquad (2)$$

Finally, an iterative procedure calculates the Fourier coefficients in the Theodorsen mapping to the exact circle.

Using a Newton root-finding scheme, the point in the circle plane corresponding to a particular point on the airfoil may be determined and from this the flow velocity at that point may be obtained given the section angle of attack.

B. Droplet Trajectory Code

The droplet trajectory code employed in this analysis was developed by Bragg (31) in 1980. Using basic theory and equations developed several years earlier as its foundation, the code extends the earlier work to include the results of more recent studies as well as much improved computer technology. Essentially, the code is used to compute single droplet trajectories and points of impingement on a given airfoil, and from these calculations it is able to determine both total and maximum local collection efficiencies as well as a predicted ice shape if desired.

Again, the initial step in the trajectory calculation process requires a computation of the potential flowfield about the airfoil under investigation. This flowfield information, calculated using the Theodorsen transformation method described in the previous section, is passed to the trajectory calculation portion of the code in the form of the aforementioned Fourier coefficients, which yield the flow velocity at any given point in the airfoil flowfield for a specific angle of attack. With this flowfield information available, droplet trajectories may then be computed.

The trajectory calculation requires solving a differential equation which results from the application of

Newton's Second Law to a water droplet moving in an air stream. This equation is given as

$$K\ddot{\eta} = \frac{C_D R}{24}(\bar{u}-\dot{\bar{\eta}}) + \frac{1}{Fr^2}\frac{\bar{g}}{g} \tag{3}$$

where K and Fr are nondimensional parameters known respectively as the inertia parameter and Froude number. They are given by

$$K=\frac{\sigma\delta^2 u}{18c\mu} \tag{4}$$

and

$$Fr=\frac{U}{\sqrt{cg}} \tag{5}$$

From Equation 3 a set of four simultaneous first order ordinary differential equations result, which when solved yield the droplet trajectory.

Once the droplet trajectories are known, impingement efficiencies may then be calculated. Airfoil local impingement efficiency, β, physically represents a ratio of airfoil surface droplet mass flux to freestream mass flux, and is

$$\beta = \frac{dy_0}{ds} \tag{6}$$

Here, y_0 is the initial particle y-coordinate and S is the airfoil surface arc length from the leading edge to the point of impact. Figure 3 illustrates graphically the calculation of β, and Figure 4 shows a typical β-S curve. If y_0 is plotted versus S, it may be seen that β is simply the slope of the y_0-S curve at a given point. Total, or overall, collection efficiency of an airfoil is also an important icing parameter and is defined by

$$E = \frac{\Delta Y_0}{h} \tag{7}$$

where Y_0 is the distance between the initial y-coordinate of the upper and lower droplet tangent trajectories and h represents the maximum airfoil projected height. Total collection efficiency is then a ratio of the amount of water mass collected by the airfoil to the amount in the freestream sector which is swept out by the airfoil. Figure 5 exhibits typical variation of collection efficiencies with radial location, and Figure 6 is an example of the radial variation of local angle of attack and Mach number.

Other capabilities exist within the droplet trajectory code, perhaps most significantly the ability to develop a theoretical rime ice shape using a time-stepping routine, but this function is not necessary in the present study and will not be employed or further discussed here. Although it is true that the formation of an ice shape on an airfoil will indeed alter the flowfield about the airfoil, and hence the β curve for that airfoil, this phenomenon is not considered in this analysis because the values of β and E used in later calculations are taken for the clean airfoil. The importance of the collection efficiencies will be manifested in the following section dealing with aerodynamic coefficient correlations.

C. Aerodynamic Coefficient Correlations

Prior to the initiation of the present study, an effort was made to identify all of the dimensionless parameters relevant to an icing encounter using Buckingham's Pi Theorem, with the goal of identifying and/or justifying the use of certain variables in empirical correlations. The Pi theom of Buckingham, presented first in 1914, provides a means of creating a dimensionless variable set from an initial group of dimensional variables. The theorem states that any function of N variables, of the form

$$f(P_1, P_2, P_3, \ldots P_N) = 0$$

may also be given in terms of (N-K) dimensionless Pi products, such that

$$f(Pi_1, Pi_2, \ldots Pi_{N-K}) = 0$$

Here K represents the number of dimensionally independent quantities necessary to fully express the dimensions of the N variables, and each Pi term is a dimensionless combination of an arbitrarily chosen set of K dimensionally independent variables. The Pi theorem will be used here to nondimensionalize parameters relevant to an airfoil icing encounter.

The procedure is initiated by first listing all of the suspected relevant dimensional parameters. In an icing encounter, these are taken to be as given in Table 1.

Table 1. Dimensional parameters considered in the ice accretion process.

Symbol	Denotes	Units
T	temperature at which ice is formed	t
T_0	reference temperature	t
τ	icing time	T
w	liquid water content	ML^{-3}
d	droplet diameter	L
V_0	freestream velocity	LT^{-1}
ρ_{ice}	ice density	ML^{-3}
ρ_{air}	air density	ML^{-3}
μ	absolute air viscosity	$ML^{-1}T^{-1}$
c	airfoil chord	L

(t=temperature, T=time, M=mass, L=length)

Here, ten dimensional variables (N) and four fundamental dimensions (K) are given. Therefore, N-K = 10-4 = 6 Pi products will result. It should be noted that although other parameters such as total and local collection efficiencies are also thought to be important parameters in an icing encounter, they are not included in the above variable set because they are already dimensionless and would not be affected by the Pi theorem which deals only with dimensional quantities. They can, however, be added to the final list of nondimensional variables which will result from the use of the Pi theorem.

Certain other physical characteristics of the airfoil which may affect ice accretion and resulting aerodynamic performance losses, namely leading edge radius of curvature, airfoil thickness, and camber, are not included in the above variable set even though they are dimensional quantities. This is because the only seemingly meaningful way to nondimensionalize these terms is with respect to airfoil chord, so that for the purposes of this analysis it will be assumed that these parameters are all initially nondimensionalized by chord and hence are not included in the variable set. Instead they may be added to the list of nondimensional variables at the conclusion of the application of the theorem if desired.

It may be noted that the chord term makes its influence felt in the nondimensionalization of these airfoil geometry terms, and has also been included in the dimensional variable set to allow for the possible development of dimensionless terms which will be consistent with or similar to dimensionless quantities already in existence. For example:

$$AC = \frac{V_0 w \tau}{\rho_{ice} c} \qquad \text{(Accumulation Parameter)}$$

$$K_0 = f(K, R_u) \qquad \text{(Modified Inertia Parameter)}$$

where

$$K = \frac{\rho_{ice} d^2 V_0}{18 c \mu}$$

$$R_u = \frac{V_0 \rho_{air} d}{\mu}$$

The next step in the procedure is to formulate a K set of four (equal to the number of fundamental dimensions) dimensionally independent variables, from which the Pi products will be developed. To form the set, any four variables may be chosen from the dimensional variable list, with the restriction that they may not themselves combine to form a dimensionless combination. A K set consisting of

$$K = (T, \tau, w, V_0)$$

is initially chosen. With this K set, the six resulting Pi products are:

$$Pi_1 = f(T, \tau, w, V_0, T_0)$$

$$Pi_2 = f(T, \tau, w, V_0, d)$$

$$Pi_3 = f(T, \tau, w, V_0, \rho_{ice})$$

$$Pi_4 = f(T, \tau, w, V_0, \rho_{air})$$

$$Pi_5 = f(T, \tau, w, V_0, \mu)$$

$$Pi_6 = f(T, \tau, w, V_0, c)$$

To create nondimensional terms from these sets, the following procedure, as illustrated by an example using Pi_1, is employed. The Pi product is first written as a product of all of its terms, each raised to some power.

$$Pi_1 = (T)\ (\tau)^a\ (w)^b\ (V_0)^c\ (T_0)^d$$

It is then rewritten in terms of the fundamental dimensions involved:

$$Pi_1 = (t)\ (T)^a\ (ML^{-3})^b (LT^{-1})^c (t)^d$$

For this product to be nondimensionalized, all of these dimensions must go to zero, i.e., the exponents on each dimension must sum to zero.

$$t: \quad 1+d = 0$$

$$T: \quad a-c = 0$$

$$M: \quad b = 0$$

$$L: \quad -3b+c = 0$$

This set of equations is then solved for a, b, c, and d.

$$d = -1 \qquad b = 0 \qquad c = 0 \qquad a = 0$$

The Pi product is then rewritten with these values included.

$$Pi_1 = (T)\,(T_0)^{-1} = \left(\frac{T}{T_0}\right),$$

which is the first dimensionless quantity.

Likewise, the other Pi products are found to be

$$Pi_2 = \frac{V_0\tau}{d}$$

$$Pi_3 = \frac{w}{\rho_{ice}}$$

$$Pi_4 = \frac{w}{\rho_{air}}$$

$$Pi_5 = \frac{wV_0^2}{\mu}$$

$$Pi_6 = \frac{V_0}{c}$$

The resulting set of dimensionless variables as determined by the Pi theorem is then

$$f(t/T_0,\ V_0\tau/d,\ w/\rho_{ice},\ wV_0^2/\mu,\ V_0\tau/c) = 0,$$

or in the case of predicting drag coefficient change due to these variables,

$$f(T/T_0, \;\ldots\ldots\ldots\ldots\ldots\ldots\ldots,\; V_0\tau/c) = \Delta C_d$$

At this point, any other dimensionless variables such as collection efficiencies or airfoil geometry terms may be included in the equation of desired. The user may then apply some correlation development technique to determine the exact relationship between these dimensionless variables and the associated dependent variable(s).

It may be demonstrated that the resultant set of dimensionless variables is dependent on both the set of dimensional variables which is used and on the K set which is initially chosen. Since there are a finite number of dimensional variables and a finite number of K sets which can be chosen, there will be a finite number of dimensionless variables which will result for a given problem. However, not all of these variables will necessarily be produced by one K set. For the icing encounter problem discussed here, this can be illustrated by choosing a second K set:

$$K = (\; T,\; w,\; c,\; V_0\,)$$

This particular K set is especially noteworthy for the icing encounter problem since it contains parameters which are thought to be of primary importance in the ice accretion process: temperature, liquid water content, freestream velocity, and airfoil chord length. The Pi products for this set are:

$$Pi_1 = f(T,\ w,\ c,\ V_0,\ T_0)$$

$$Pi_2 = f(T,\ w,\ c,\ V_0,\ \tau)$$

$$Pi_3 = f(T,\ w,\ c,\ V_0,\ d)$$

$$Pi_4 = f(T,\ w,\ c,\ V_0,\ \rho_{ice})$$

$$Pi_5 = f(T,\ w,\ c,\ V_0,\ \rho_{air})$$

$$Pi_6 = f(T,\ w,\ c,\ V_0,\ \mu)$$

Following the procedure previously outlined for nondimensionlizing these products, the resultant set of dimensionless variables is:

$$f(T/T_0,\ V_0\tau/c,\ c/d,\ w/\rho_{ice},\ w/\rho_{air},\ wcV_0/\mu) = 0,$$

which differs somewhat from the set produced by the other K set used. So for any given problem it is necessary to consider all of the possible K sets to obtain a complete list of dimensionless variables which may be produced. Knowledge of the physics of the problem under consideration should then provide a starting point in the analysis of these variables as they relate to the given dependent variable(s).

In the icing encounter problem, it was desired to use the Pi theorem to provide some justification for the use of the terms AC and K_0, previously defined, in the development of a glaze ice drag coefficient correlation. Although the Pi theorem does not produce these terms directly, it does provide the following dimensionless terms:

(1) $V_0 \tau / c$

(2) w / ρ_{ice}

(3) $\dfrac{\rho_{ice} V_0 d}{\mu}$

(4) d/c

(5) $\dfrac{\rho_{air} V_0 d}{\mu}$

It may be noted that AC is simply the product of terms (1) and (2). K_0 is a function of K, the product of terms (3) and (4), and R_u, which is identical to term (5), e.g.,

$$AC = \underbrace{\frac{V_0 \tau}{c}}_{(1)} \quad \underbrace{\frac{w}{\rho_{ice}}}_{(2)}$$

$$K = \underbrace{\frac{\rho_{ice} V_0 d}{\mu}}_{(3)} \quad \underbrace{\frac{d}{c}}_{(4)} = \frac{\rho_{ice} V_0 d^2}{\mu c}$$

$$R_u = \underbrace{\frac{\rho_{air} V_0 d}{\mu}}_{(5)}$$

Should the reader wish to verify that these terms are indeed obtainable from the original set of dimensional variables, they can be found as follows:

(1) - from K set (T, τ, w, V_0)

(2) - from K set (T, τ, w, V_0)

(3) - from K set (T, d, V_0, ρ_{ice})

(4) - from K set (T, w, c, V_0)

(5) - from K set (T, d, V_0, ρ_{air})

It can be seen that the Pi theorem does indeed provide some justification for the use of the variables AC and K_0 in developing a correlation, and any correlation which does result will be in terms of dimensionless variables obtainable by Buckingham's Pi theorem.

At present, the only means available for analytically determining performance degradation of an airfoil in terms of its aerodynamic coefficients is through the use of empirical correlations. As previously indicated, several individuals have attempted development of one or more of these correlations and generally have met with only limited success in terms of accuracy and range of application. Incorporated into the present study are the two correlations currently most widely used to predict drag increment, as well as a series of new correlations. These empirical correlations represent only an interim solution to the problem of assessing aerodynamic performance losses due to ice formation. A potentially more precise solution technique currently under development involves a Navier-Stokes solution for the flowfield around an iced airfoil (32).

1. Gray Correlation

The first correlation, formulated by Gray (14) roughly twenty years ago is of the form

$$\Delta C_D = [8.7 \times 10^{-5} \frac{Tu}{c} WB_{max} (32-T_0)^{0.3}] (1+6 \{1+2.52r^{0.1} \sin^4 12\alpha)$$

$$\sin^2[543\ w\ \left(\frac{E}{32-T_0}\right)^{1/3} - 81 + 65.3\left(\frac{1}{1.35^{\alpha i}} - \frac{1}{1.35^{\alpha}}\right)]$$

$$\frac{-0.17}{r}\sin^4 11\alpha)) \qquad (8)$$

where here ΔC_d represents the actual numerical value of drag coefficient increment; i.e., $\Delta C_d = C_d(\text{iced}) - C_d(\text{clean})$. As can be seen, this correlation involves combinations of various dimensional parameters, and the dimensionless total and local collection efficiencies calculated in the droplet trajectory code previously discussed also appear. This correlation also has the capability of computing drag coefficient increment at angles of attack other than that at which the ice was formed, through the use of the α and α_i terms. Here α represents the angle of attack at which the experimental data was taken, or the angle at which the effects of the ice accretion are to be evaluated, and α_i represents the angle of attack at which the ice was formed.

The dimensional variables have not in all cases been grouped so as to form dimensionless quantities, and this has evoked some criticism by various persons since the correlation's development. This criticism is based on the idea that any correlation which involves dimensional quantities will be to some extent a function of the data set from which it was formulated. Thus, if the correlation was applied to some other set of data in which the range of one or more of the relevent parameters differed from that of the original data set, the variable affected may have an undue effect on the prediction which was not accounted for in the original, limited data set. Indeed, as is seen in Figure 7, Gray's correlation has been found to predict quite poorly for much of the recently generated NASA glaze ice data, which is typefied by significantly higher liquid water content values than are found in the data set used by Gray in developing his correlation. Nevertheless, since no other glaze ice drag coefficient existed until quite recently, Gray's correlation still sees widespread use and has been included in this program as an option available to the user.

Because Gray's correlation accounts for only changes in drag coefficient, modification of C_ℓ has been added to take into account the decambering effect of ice accretion, resulting in a shift in the C_ℓ-α curve and a decrease in $C_{\ell_{max}}$ due to flow separation on the airfoil upper surface. Trial values tested by the author have indicated that reducing C_ℓ to 95% of its clean configuration value yields an acceptable approximation for iced C_ℓ. This factor is incorporated into the present study for both Gray's and Bragg's correlations.

2. Bragg Correlation

A correlation has been developed by Bragg (16) for the rime ice condition. It has the form

$$\Delta C_d = 0.01\ (15.8\ \ln(k/c) + 28000\ A_c E + I) \qquad (9)$$

where Ac is accumulation parameter, given by

$$Ac = \frac{uw\tau}{\rho_{ice} c} \qquad (10)$$

and I represents a drag constant which varies according to airfoil type as shown in Table 2.

Table 2. Constants in Bragg Drag Coefficient Correlation

Airfoil Type	Drag Constant, I
NACA 4 and 5 digit	184
NACA 63 series	218
NACA 64 series	232
NACA 65 series	252
NACA 66 series	290

In this correlation, ΔC_d represents a fractional change in, rather than an actual numerical value of, drag coefficient. Here ΔC_d may be used to find the iced airfoil drag coefficient using

$$C_{d_{iced}} = (1+\Delta C_d)C_{d_{clean}} \tag{11}$$

Previous studies of this correlation applied to NACA and NASA 2-D icing data have indicated a strong tendency for the correlation to overpredict drag increment. Because the predictions are commonly off by a relatively constant percentage with respect to the Neel and Bright propeller performance data, a factor was introduced which reduces the degree of drag coefficient increase calculated by the Bragg correlation. Replacement of the initial constant in the equation, 0.01, by 0.0008 produced much more acceptable predictions and was therefore incorporated into the present analysis.

Bragg has also recently proposed a new, modified form of his correlation (33) which has also been included in the present study. This new form of the correlation given below, appears to work well for the cases examined to date, but it has not yet been applied to the 2-D NACA and NASA icing data with which the other correlations were tested.

$$\Delta C_d = 0.01\ (15.8\ln(k/c) + 1171\ \ AcE + I) \qquad (12)$$

3. Flemming Correlations

The third correlation, or more precisely set of correlations, are those developed by Flemming (25). Whereas Gray and Bragg dealt strictly with drag coefficient correlations, Flemming has also formulated correlations for lift and moment coefficients for both glaze and rime encounters. These correlations are of the forms:

For a glaze ice encounter,

$$\Delta C_d = KD_1\,[.00686\ K_0\,(t/c)^{1.5}(\alpha+6) - .0313(r/c)^2 + KD(.006)M^{2.4}]$$
$$[w\tau_c(\frac{c}{.1524})^{0.2}/(\frac{c}{.1524})^{1.2}]\,[1-8\Delta C_d{}'(\frac{V_{helo}}{278})] \qquad (13)$$

For a rime ice encounter,

$$\Delta C_d = [.158\ln(k/c) + 175(\frac{V}{\rho_{ice}c})W\tau_c E + 1.70](\frac{\alpha+6}{10})$$
$$[1-8\Delta C_d{}'(\frac{V_{helo}}{278})]\,C_{d_{clean}} \qquad (14)$$

and for both glaze and rime encounters,

$$\Delta C_l = (-.01335K_0\,(t/c)\,[\alpha+2+KL_1(.00555)(\alpha-6)^2]\,KL]\,[W\tau_c$$
$$(\frac{c}{.1524})^{0.2}/(\frac{c}{.1524})^{1.2}] \qquad (15)$$

and

$$\Delta Cm = [(.00179-.0045M)(.00544)K_0\alpha/(t/c)^{2.7} + .00383M(1-63.29r/c)] \quad (16)$$

$$[W\tau_c(\frac{c}{.1524})^{0.2}/(\frac{c}{.1524})^{1.2}]$$

where K_0 is the modified inertia parameter, given by

$$K_0 = K(1+.0967\ R_u{}^{.6397}) \quad (17)$$

and KL, KL_1, and KD, and KD_1 are functions of temperature and angle of attack and are defined within the subroutine.

These correlations were developed using data obtained in a series of tests conducted in the Canadian National Research Council's High Speed Icing Wind Tunnel in late 1982. The ten airfoil scale models tested, with typical chords of roughly six inches, were designed primarily for use in helicopter applications and cover a wide range of helicopter airfoil shapes. For correlation development purposes this range should enable the resulting correlations to adequately account for airfoil geometry as a factor in aerodynamic coefficient increments due to icing.

The correlations are, however, dimensional in nature and again were developed using model data for high speed applications. The full effects of these two items on the range of applicability of the correlations remains to be seen. The correlations have been found in a recent study to underpredict ΔC_d in many cases however. In spite of this, Flemming's correlations still hold promise and do in fact work well in many cases.

4. Miller Correlation

A fourth general drag coefficient correlation development has been attempted by Miller, et. al. Described in detail in Reference 28, this effort used as the basis for the correlation formulation the method of statistical analysis as applied to a set of experimentally obtained icing data. Although a correlation was presented in Reference 28, it represented only a status report and not a final result. Further study and modification of this correlation is necessary before it may be deemed useable, and no modifications made to date have proven satisfactory. The method of statistical analysis is a powerful tool in correlation in development and should yield greater success at some future date, but because the present form of the correlation is not acceptable in terms of accuracy of prediction it will not be incorporated into the code.

So there are presently available three correlations or sets of correlations which are integrated into the code. They provided values of drag, lift, and/or moment coefficient increment for both glaze and rime ice encounters. These increments may then be passed to a propeller performance code, described in the following section, to evaluate the ensuing propeller rotor performance degradation.

D. Propeller Performance Code

The propeller performance code which is integrated into the performance degradation program is based upon a linearized inflow propeller strip analysis, developed by Cooper (34) in 1957. Strip analysis involves the calculation of aerodynamic forces at selected spanwise blade locations for a given operating condition and propeller geometry. From these differential forces, given in terms of thrust and torque coefficients by

$$\frac{dC_T}{dx} = k \frac{c}{D} M_x^2 (C_l \cos\phi - C_d \sin\phi) \tag{18}$$

where $k = \dfrac{900a^2 b}{N^2 D^2}$ (19)

and

$$\frac{dC_Q}{dx} = \frac{x}{2} \frac{dC_T}{dx} \frac{C_d \cos\phi + C_l \sin\phi}{C_l \cos\phi - C_d \sin\phi} \tag{20}$$

thrust and torque coefficients may be obtained by integrating these terms along the blade. Propeller efficiency and power absorbed may then be calculated by

$$\eta = J \frac{C_T}{C_p} = \left(\frac{V}{nD}\right) \frac{C_T}{2\pi C_Q} \tag{21}$$

and

$$BHP = \frac{C_p \rho \eta^3 D^5}{550} \tag{22}$$

Cooper's propeller performance analysis is unique due to the fact that it assumes, or actually approximates, a linear induced flow distribution on the propeller blade. Typically an iterative process is required to obtain the induced angle of attack and lift coefficient at a specific radial location since they are interrelated. However, Goldstein (35) has solved for the radial distribution of circulation for a lightly loaded propeller having a finite number of blades and has established the relationship between $\sigma_p C_\ell$ and α_i. Cooper has then approximated the $\sigma_p C_\ell$ - α_i curves by straight lines and has plotted the slopes of these lines versus advance ratio for various spanwise locations. From these plots, and using available aerodynamic data, it is then possible to determine values for an induced angle of attack. When experimental and analytical results obtained using this method were compared, agreement to within three percent was seen for over ninety percent of the cases investigated.

CHAPTER 4

PERFORMANCE DEGRADATION CODE ASSEMBLY

In order to integrate each of the codes involved into a single performance degradation code, heretofore known as ICEPERF, several phases of modifications were required. These modifications were relatively minor in that they did not change the basic functions, operation, or logic of any of the codes but rather served to make the transition from one section to the next more simple and automatic. This automation then eliminated the necessity of any user intervention in the run stream.

The user-friendly nature of the code was a primary objective of this effort, and although several files are necessary to run the code very few changes are required from one run to another, for the same airfoil. The various components of the code were selected on the basis of availability and accuracy of results. Each component was run and tested separately and extensively to demonstrate its capability to consistently function properly, and all displayed good performance in these runs. Also of importance in the component selection and modification was a desire to maintain a high degree of modularity in the code, such that a different flowfield computation, new correlation, different propeller analysis, etc. could be inserted with a minimum of changes to the code. This also permits the code, now applied to propellers, to be relatively easily extended to a helicopter configuration. A flowchart denoting the current major elements of the program is provided in Appendix 1.

The first phase in the code integration process involved combining the flowfield and droplet trajectory codes previously described. Because the droplet trajectory code was designed to operate using much of the output from the Theodorsen transformation code, this step was relatively straightforward. The modified code has been set up to handle a maximum of four input propeller radial locations, and current runs of the code have been made with four input stations, at the 30, 50, 70, and 90 percent radial locations. An investigation of the benefits of using more input stations, offset by the additional cost due to the extra run time required, has not yet been performed.

Next, a set of subroutines was created to predict drag increment due to ice accretion, given the appropriate impingement efficiency values output from the trajectory code. The ΔC_d correlations of Gray, Bragg, and Flemming are included in the subroutines, with Flemming's correlation also being capable of determining lift and moment coefficient increments. The user may select any of these correlations in each run of the program, and the choice of correlation should be dependent on the type of ice formation expected for a given input condition.

The correlations of Gray and Bragg use values of total and maximum local collection efficiencies in computing drag coefficient increment. One value for each of these parameters is generated for each radial location input, so that a maximum of four sets of collection efficiencies are available as output from the trajectory calculation section. However, it is best when using the propeller performance code to include considerably more input radial locations in the calculations (eleven stations are used in the analysis of a propeller utilizing double-cambered Clark-Y airfoil sections which follows in Chapter 5). In order to obtain values for drag coefficient increment at each of these locations, the collection efficiencies at these stations must be known. Rather than running the Theodorsen transformation and droplet trajectory codes eleven times to obtain collection efficiency values at each of these stations however, a curve fit routine is employed which takes the values computed at each of the four input radial locations and fits a curve through them. Flemming's correlations compute values of collection efficiencies empirically, so that it is not necessary to run the Theodorsen and droplet trajectory sections of the code if Flemming's correlations are to be employed.

In this code, a cubic spline fit routine is used to fit separate curves for total maximum local collection efficiencies between the 30% and 90% radial locations, or between the two most extreme sections input by the user. This method has been found to yield good results due to the fact that the collection efficiencies are both smooth, continuous functions or propeller radial location. Due to the nature of the spline fit routine, it is applicable only between the innermost and outermost radial locations input. Outboard of the outermost input station, and inboard of the innermost station, some other technique is required to compute values for the collection efficiencies as a function of radial location. In this analysis a linear fit, computing the slopes at the endpoints of the spline fit and extending straight lines inboard and outboard of these endpoints, is used to approximate the curves where the spline fit is not applicable. With this method, values for both total and maximum local collection efficiencies are available for any radial location.

Cooper's propeller performance code has been utilized to calculate values of propeller thrust, torque, and efficiency for a given condition. The previously mentioned drag increment subroutines have been incorporated into the propeller performance code to modify the drag coefficient and values used by the code in computing iced propeller thrust and torque. In Equations 18 and 20, the C_ℓ and C_d terms are modified by the factors $(1+\Delta C_\ell)$ and $(1+\Delta C_d)$ respectively, such that

$$C_\ell = C_\ell(\text{clean}) * (1 + \Delta C_\ell) \qquad (23)$$

and

$$C_d = C_d(\text{clean}) * (1 + \Delta C_d) \qquad (24)$$

so that iced propeller thrust and torque coefficients as well as propeller efficiency may then be computed. The code first calculates clean, or non-iced, values for these quantities, and then calculates using the user-selected aerodynamic coefficient correlation the iced values for these same parameters. Various input parameters have been altered or omitted from the original code to make it more conducive to the purposes of the present program, but the essence and mechanics of the code remain unchanged.

The entire code then operates by first computing clean propeller performance values for one advance ratio. Next, the Theodorsen transformation is performed, or previously calculated results are read for the first input radial location. The droplet trajectory section then computes impingement efficiency values for the radial location using the flowfield from the Theodorsen transformation and a section angle of attack computed in the propeller performance section. Impingement efficiencies are then calculated for the remaining input radial stations following the same procedure. The code spline fits the impingement efficiency curves and computes using these values and the selected aerodynamic coefficient increment correlation the iced propeller performance data. This entire procedure is then repeated for each additional advance ratio input.

CHAPTER 5

RESULTS

In the Neel and Bright test, a C-46 twin-engine aircraft was used to obtain propeller efficiency losses as a result of ice formation. Ice was allowed to form on the propeller of the right engine while the left engine propeller was kept clean. Following this procedure, data was recorded for twelve natural icing encounters and typical efficiency losses of four to ten percent were noted. The propellers on the C-46 utilized double-cambered Clark-Y airfoil sections, for which airfoil coordinates used in ICEPERF were obtained from Borst (36).

The Neel and Bright experimental data provided a data base with which to evaluate the ICEPERF iced propeller performance code. For ten of the twelve encounters documented in the test program report (Table 3), calculations were performed for the propeller in both clean and iced configurations. Results and comparison of analytical and experimental performance values are here presented for each of the three correlations employed, specifically those of Bragg, Gray, and Flemming. It should be noted that in all performance calculations presented in this report, consideration was given to the radial extent of icing such that no ice was allowed to accrete analytically outboard of the experimentally observed radial icing extent. These results therefore differ from previous calculations shown by this author (37) in which no restriction was placed analytically on the radial extent of icing.

The results presented in this paper may also be compared directly with calculations performed by Korkan, et. al (27). Their work involved generation of propeller performance predictions for the Neel and Bright data as well, using the Theordorsen transformation flowfield code, Bragg droplet trajectory code, and Cooper propeller performance codes separately. In this initial study by Korkan, et. al., pressure altitude was input and the standard atmospheric pressure, temperature, and density were then used in the calculations rather than the experimentally obtained values for these parameters. The use of actual flight conditions, as employed in all calculations presented in this report, was found to alter the computed thrust and power coefficients by roughly one percent. Potential differences in blade angle specification from study to study may also have a significant impact on the predictions. Finally, the initial constant in the original Bragg correlation was decreased in both studies in an attempt to produce reasonable performance values. This then introduces additional variation between the corresponding iced calculations.

Clean performance predictions were found to agree well with the experimental data for all of the encounters investigated. (Tables 4-6 summarize the analytical and experimental data for Encounters 2, 7, and 12 respectively.) In all cases, calculated thrust and power coefficients were found to agree with the corresponding experimental values within an average of 12.5 percent. C_T and C_p for a given encounter and advance ratio tended to be underpredicted by roughly the same percentage, so that resulting propeller efficiencies compared with experimental measurements to within six percent. Since propeller efficiency is essentially a ratio of thrust coefficient to power coefficient however, errors of similar magnitude in C_T and C_p should then cancel so that the resulting efficiency values would be much less sensitive to error in performance calculations and would not be as good an indicator of analytical prediction accuracy. Therefore statements herein relate primarily to thrust and power coefficient calculations rather than propeller efficiency.

The results shown in this report all involved use of the actual blade angles as measured and reported in the experimental test program. It was found however that by increasing the reported blade angle setting by 0.7 degrees, much better agreement between theory and experiment could be obtained for all encounters. Figures 8-10 are illustrations of the effect of blade angle variation on clean thrust and power coefficients for Encounter 2. This anomaly could be an indication of a deficiency in the performance calculations, but because a constant increase in blade setting produces much better correlation with experiment for several encounters over a range of flight conditions, it more likely signifies the existence of a bias error in the experimental measurement of blade angle. These calculations serve also to indicate the sensitivity of propeller performance predictions to propeller geometry.

The code was found to often overpredict the clean propeller efficiency at the higher advance ratios. Typically, performance predictions agreed with experiment to within a few percent at the lowest advance ratios and gradually worsened to the point where they were often off by roughly twenty percent at the highest advance ratios investigated. It is postulated that this may be due to an inability of the code to adequately account for compressibility effects, which become more significant as advance ratio increases (via increased forward velocity for a fixed rpm). This effect should be studied further in subsequent efforts.

When the restriction on radial icing extent was imposed in the present study's calculations, better agreement with the experimental data was obtained than was previously presented. Currently there is no mechanism in the code for determining the actual radial icing extent. Rather, the user must specify the desired or assumed radial location inboard of which iced calculations are to be performed. In this study, approximate radial icing extent for each encounter was reported by Neel and Bright and these values were then input for the iced performance calculations. The following discussion details results obtained by each correlation for the several encounters investigated.

A. BRAGG

Two forms of Bragg's basic rime ice correlation are available in ICEPERF, as discussed in a previous section. The first of these is a modified form of Bragg's original equation, in which the leading constant was changed from 0.01 to 0.0008 in an effort to produce more realistic drag coefficient increments. This change was made after initial runs of the code indicated that the original equation was producing quite unreasonably large performance changes due to ice formation, as a result of inordinately large predicted ΔC_d values. The 0.0008 constant was arrived at by best-fitting the correlation's performance predictions to Encounter 2 data and was then found to perform acceptably for the other encounters as well. Future use of the correlation may suggest additional modifications of this constant.

This modified form of Bragg's original correlation was then applied to all of the available Neel and Bright data regardless of assumed rime or glaze ice type, as was Bragg's new form of the correlation. Reasonably good agreement between experiment and theory was obtained using both correlations for all encounters. In all cases the original but modified Bragg correlation produced more accurate results than did the newer correlation, but the differences were generally small. The fact that the newer, unmodified correlation gave results almost as accurate as those of the older form which was specifically modified to better fit the propeller data indicates that the changes made by Bragg in forming the new correlation improved the quality of the correlation significantly. Both correlations handled the less severe icing encounters (icing extents below 60%) well (i.e., Encounter 7, Figures 14-16), much better than did the Gray or Flemming correlations. In the most severe case however (Encounter 12, Figures 17-19) both correlations seriously overpredict the degree of degradation, especially in terms of C_p, and produce C_p-J curves which inflect upward at the lower advance ratios rather than downward as would be expected.

It should also be noted that Bragg's equations are for ΔC_d only. Lift coefficient will also generally decrease as a result of ice formation at the leading edge as the flow there is spoiled to some extent, but this is not accounted for in the Bragg equations. A factor was therefore introduced to provide a simple representation of this phenomenon by assigning the iced section lift coefficient a value equal to 95% of its clean value. Although this seems to be a reasonable typical value for ΔC_ℓ, it would be desirable to incorporate a more discriminating form of determining ΔC_ℓ in future calculations.

B. GRAY

As was the case with the Bragg correlations, the Gray correlation also provides its most accurate performance predictions when radial icing extent is small. It is difficult to make any inference regarding the quality of the correlation under such conditions due to the fact that the propeller is loaded most heavily at the tip and its performance will be most sensitive to geometry changes (i.e., ice accretions) in the tip region. Farther inboard, even quite severe ice growths will have much less effect on the overall performance and consequently any correlation, regardless of how great its predicted ΔC_d values may be, will appear to work well in low radial icing extent cases. Thus the true measure of the quality of these correlations comes in the more severe icing encounters such as Encounters 2 and 12. In these two encounters, as can be seen in Figures 11-13 and 17-19, the Gray correlation fails to accurately predict the iced performance, yielding values which overpredict the degree of degradation. Indeed, upon examining the actual ΔC_d values predicted by Gray for Encounter 12 it was found that this correlation was predicting drag coefficient increases of typically 300% at lower advance ratios to as much as 6000% at the outer stations at high advance ratios. The Gray correlation, like that of Bragg, also predicts only drag coefficient increment, so the same five percent reduction in C_ℓ for the iced configuration was again employed when Gray's correlation was used. The Gray correlation itself was unmodified for use in this study, and it is likely that introducing some constant into Gray's equation to affect a constant percentage decrease in its calculated ΔC_d values, as was done with the original Bragg equation, would greatly improve its ability to calculate iced drag coefficient increment and hence iced propeller performance.

C. FLEMMING

The Flemming correlations were applied twice to each encounter, once with icing restricted by the user-input value and then allowing the Flemming correlations to predict the radial icing extent. The second runs were performed to check the no-icing capability of the correlations and to ascertain whether this capability would properly reflect existence of ice under the influence of 3-D, rotating forces (kinetic heating and shedding). Instead of properly predicting radial icing extent however, this feature dictated no icing in the first 30% of propeller radius for any encounter, and then overpredicted the radial icing extent outboard of the 30% station for eight of the ten encounters (Table 7).

In the case of the user-input icing extent, the no-icing problem manifests itself in an underprediction of the propeller performance degradation for all encounters. As the figures illustrate, many of the Flemming-predicted iced thrust and power coefficient values are identical or virtually identical to the clean values, indicating analytically little if any degradation. While these results may appear reasonable at first glance in cases where the actual degradation is minimal, they actually serve only to mask the underlying problem and reason for the negligible degradation prediction. It should also be noted that in Figures 11 through 19, in cases where the clean theoretical curve is not easily visible, it has been hidden by the Flemming correlation curves which are often virtually coincident with the clean data curve.

When no restriction is imposed upon radial icing extent, Flemming's correlations still tend to underpredict the degree of iced performance degradation in several cases. This occurs even though Flemming's correlations predict more extensive icing radially than was seen experimentally, which would indicate that the percentage decreases in thrust and power coefficients predicted by Flemming are actually smaller than the experimental values. For the encounters in which the non-restricted Flemming correlations do predict C_T and C_p well, the predicted radial icing extent is always greater than the measured extent, sometimes by as much as 60%.

It would therefore appear that the Flemming correlations have two significant deficiencies. The first of these is the no-icing calculation which has failed in this study to properly indicate either ice existence or icing extent. In fairness to the correlations it should be pointed out though that various forces not stressed in the 2-D correlation development (i.e., centrifugal forces leading to ice shedding) may have a significant effect on the radial icing extent, and in only one out of ten encounters did the Flemming correlations actually underpredict the extent of ice. The second apparent shortcoming of the correlations is the underprediction of section drag and possibly lift coefficient increments. This same trend toward underprediction of section C_d has also been seen in application of the Flemming correlations to available NACA and NASA 2-D icing data in a separate study (38).

SUMMARY AND CONCLUSIONS

Application of the ICEPERF code to the Neel and Bright experimental data base has provided much insight into the code's performance prediction capability for both clean and iced configurations. The code has been shown to run properly and to produce realistic thrust and power coefficient values, especially when radial icing extent is known and input. As a result of this study several areas of future development and potential improvement, discussed in the following paragraphs, have been identified.

Currently restrictions and simplifications exist within the code which, if removed or modified, should yield better performance evaluations. Development of a ΔC_ℓ correlation to be used in conjunction with the Bragg or Gray correlations would provide a more precise and complete representation of the effects of ice formation on section aerodynamics. Secondly, incorporation of some computational mechanism of predicting the transition from rime to glaze ice, or vice versa, on the blades would enable the code to use the proper correlation at each radial computational station, rather than assuming all rime or all glaze ice in any given encounter. Because of the generally moderate radial icing extent and only slight degree of ensuing degradation, this change will probably have only a very minor effect on the predicted propeller performance. This is in contrast to the helicopter rotor icing situation in which radial icing extent and the related performance degradation are typically more severe for a given icing condition.

Another potential area of improvement lies in the accuracy of the experimental data used for comparison with analysis. One such area with respect to the Neel and Bright data is the actual radial icing extent for each encounter. As specified in the report, the true extent is somewhat unclear and may possibly vary by as much as 20%. Values of radial icing extent presented in this report represent a best estimate of the extent as interpreted from the information in Neel and Bright's report.

The present study has also provided insight into the type and accuracy of experimental data which would be desirable in future test programs. Additional propeller icing data of any type would be useful in further validating and analyzing the code at the present time. Future tests though should include, in addition to flight and atmospheric parameters and icing time, specification of icing extent as accurately as possible. Also desirable would be some photographic or other indication of the ice type so that the proper correlation could be applied at each radial location. Finally, sensitivity of propeller performance to blade angle setting also has indicated the need for quite accurate blade angle measurements. Certainly it is desirable to have a high degree of accuracy in the thrust and power measurements as well.

With respect to the empirical lift and drag correlations used in this code, results obtained in this study concurred with previous work done involving these correlations in indicating deficiencies which exist in each correlation. Overall, the Bragg correlation(s) produced the most reasonable iced propeller performance predictions but overprediction of drag coefficient increment by Bragg's correlation(s) remains a problem, as illustrated in the more severe icing encounters. Overprediction also remains a problem with Gray's correlation, whereas Flemming's correlations typically underpredict the aerodynamic coefficient increments. It is evident then that much more 2-D validation of all these correlations is necessary before iced propeller performance can be predicted consistently using this method and before results of this analysis can be fully evaluated. It should be realized that any ultimate analytical treatment of ice accretion on rotating systems will potentially involve much less empiricism than is currently required and that the use of these correlations represents an interim approach to the problem, which will continue to be used until more sophisticated analytical procedures such as Navier-Stokes or interactive boundary layer analyses of iced airfoil flowfields become available.

REFERENCES

1. Corson, B. W. and Maynard, J. D., "The Effect of Simulated Ice on Propeller Performance," NACA TN 1084, 1946.

2. Preston, C. M. and Blackman, C. D., "Effects of Ice Formation on Airplane Performance in Level Cruising Flight," NACA TN 1598, May 1948.

3. Neel, Jr., C. B. and Bright, G. L., "The Effect of Ice Formations on Propeller Performance," NACA TN 2212, October 1950.

4. Gray, V. H. and von Glahn, U. H., "Effect of Ice and Frost Formations on Drag of NACA 65_1-212 Airfoil for Various Modes of Thermal Ice Protection," NACA TN 2962, June 1953.

5. Gray, V. H. and von Glahn, U. H., "Aerodynamic Effects Caused by Icing of an Unswept NACA 65A004 Airfoil," NACA TN 4155, Feb. 1958.

6. Brun, R. J., Gallagher, H. M., and Vogt, D. E., "Impingement of Water Droplets on NACA 65_1-208 and 65_1-212 Airfoils at 4 Degrees Angle of Attack," NACA TN 2952, May 1953.

7. Brun, R. J., Gallagher, H. M., and Vogt, D. E., "Impingement of Water Droplets on NACA 65A004 Airfoil and Effect of Change in Airfoil Thickness from 12 to 4 Percent at 4 Degrees Angle of Attack," NACA TN 3047, November 1953.

8. Brun, R. J., Gallagher, H. M., and Vogt, D. E., "Impingement of Water Droplets on NACA 65A004 Airfoil at 8 Degrees Angle of Attack," NACA TN 3155, July 1954.

9. Brun, R. J. and Vogt, D. E., "Impingement of Water Droplets on NACA 65A004 Airfoil at 0 Degrees Angle of Attack" NACA TN 3586, November 1955.

10. Gelder, T. F., Smyers, Jr., W. H., and von Glahn, U. H., "Experimental Droplet Impingement on Several Two-Dimensional Airfoils with Thickness Ratios of 6 to 16 Percent," NACA TN 3859, December 1956.

11. Bergrun, N. R., "An Empirical Method Permitting Rapid Determination of the Area, Rate, and Distribution of Water-Drop Impingement on an Airfoil of Arbitrary Section at Subsonic Speeds," NACA TN 2476, September 1951.

12. Lewis, W. and Bergrun, N. R., "A Probability Analysis of the Meteorological Factors Conducive to Aircraft Icing in the United States," NACA TN 2738, July 1952.

13. Gray, V. H., "Correlations Among Ice Measurements, Impingement Rates, Icing Conditions, and Drag Coefficients for Unswept NACA 65A004 Airfoil," NACA TN 4151, February 1958.

14. Gray, V. H., "Prediction of Aerodynamic Penalties Caused by Ice Formations on Various Airfoils," NASA TN-D 2166, February 1964.

15. Shaw, R. J., Sotos, R. G., and Solano, F. R., "An Experimental Study of Airfoil Icing Characteristics, AIAA 82-0282, January 1982.

16. Bragg, M. B. and Gregorek, G. M., "Aerodynamic Characteristics of Airfoils with Ice Accretions," AIAA 82-0282, January 1982.

17. Bragg, M. B., Zaguli, R. J., and Gregorek, G. M., "Wind Tunnel Evaluation of Airfoil Performance Using Simulated Ice Shapes," NASA CR 167960, November 1982.

18. Flemming, R. J. and Lednicer, D. A., "High Speed Ice Accretion on Rotorcraft Airfoils," AHS A-83-39-04-0000, May 1983.

19. Korkan, K. D., Cross, Jr., E. J., and Cornell, C. C., "Experimental Study of Performance Degradation of a Model Helicopter Main Rotor with Simulated Ice Shapes," AIAA 84-0184, January 1984.

20. Korkan, K. D., Cross, Jr., E. J., and Cornell, C. C., "Experimental Aerodynamic Characteristics of a NACA 0012 Airfoil with Simulated Ice," to be published in AIAA J. of Aircraft.

21. Korkan, K. D., Cross, Jr., E. J., and Miller, T. L., "Performance Degradation of a Model Helicopter Main Rotor in Hover and Forward Flight with Generic Ice Shape," AIAA 84-0609, March 1984.

22. Korkan, K. D., Cross, Jr., E. J., and Miller, T. L., "Performance Degradation of a Model Helicopter Rotor with a Generic Ice Shape," AIAA J. of Aircraft, Vol. 21, No. 10, October 1984, pp. 823-830.

23. Bragg, M. B., Gregorek, G. M., and Shaw, R. J., "An Analytical Approach to Airfoil Icing," AIAA 81-0403, January 1981.

24. Cansdale, J. T. and Gent, R. W., "Ice Accretion on Aerofoils in Two-Dimensional Compressible Flow - A Theoretical Model," RAE TR 82128, January 1983.

25. Flemming, R. J., and Lednicer, D. A., "High Speed Ice Accretion on Rotorcraft Airfoils," NASA CR 3910, August 1985.

26. Korkan, K. D., Dadone, L., and Shaw, R. J., "Performance Degradation of Propeller Systems Due to Rime Ice Accretion," AIAA J. Of Aircraft, Vol. 21, No. 1, January 1984, pp. 44-49.

27. Korkan, K. D., Dadone, L., and Shaw, R. J., "Performance Degradation of Helicopter Rotor Systems in Forward Flight Due to Rime Ice Accretion," AIAA 83-0028, January 1983.

28. Miller, T. L., Korkan, K. D., and Shaw, R. J., "Statistical Study of a Glaze Ice Drag Coefficient Correlation," SAE 830753, April 1983.

29. Bragg, M. B., "Predicting Airfoil Performance with Rime and Glaze Ice Accretions," AIAA 84-0106, January 1984.

30. Shaw, R. J., Private Communication, NASA Lewis Research Center, Cleveland, Ohio, August 1984.

31. Bragg, M. B., "Rime Ice Accretion and Its Effect on Airfoil Performance," NASA CR 165599, March 1982.

32. Potapczuk, M. G. and Gerhart, P. M., "Progress in Development of a Navier-Stokes Solver for Evaluation of Iced Airfoil Performance, AIAA 85-0410, January 1985.

33. Bragg, M. B., Private Communication, The Ohio State University, Columbus, Ohio, December 1985.

34. Cooper, J. P., "The 'Linearized Inflow' Propeller Strip Analysis," WADC TR 56-615, March 1957.

35. Goldstein, S., "On the Vortex Theory of Screw Propellers," Proceedings of the Royal Aeronautical Society (London), Ser. A, Vol. 123, No. 792, April 6, 1929.

36. Borst, H. V., Private Communication, Henry V. Borst and Associates, Wayne, Pennsylvania, June 1984.

37. Miller, T. L., "Analytical Determination of Propeller Performance Degradation Due to Ice Accretion," AIAA 85-0339, January 1985.

38. Sanchez-Cantalejo, P. G., Private Communication, NASA Lewis Research Center, Cleveland, Ohio, September 1985.

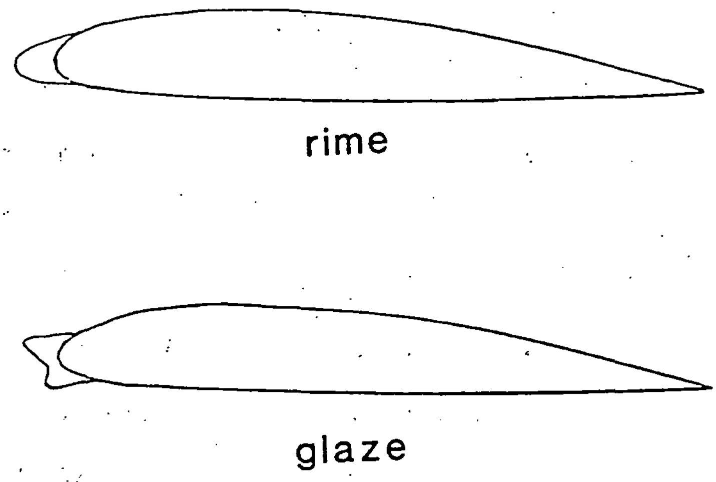

FIGURE 1. The two basic ice types

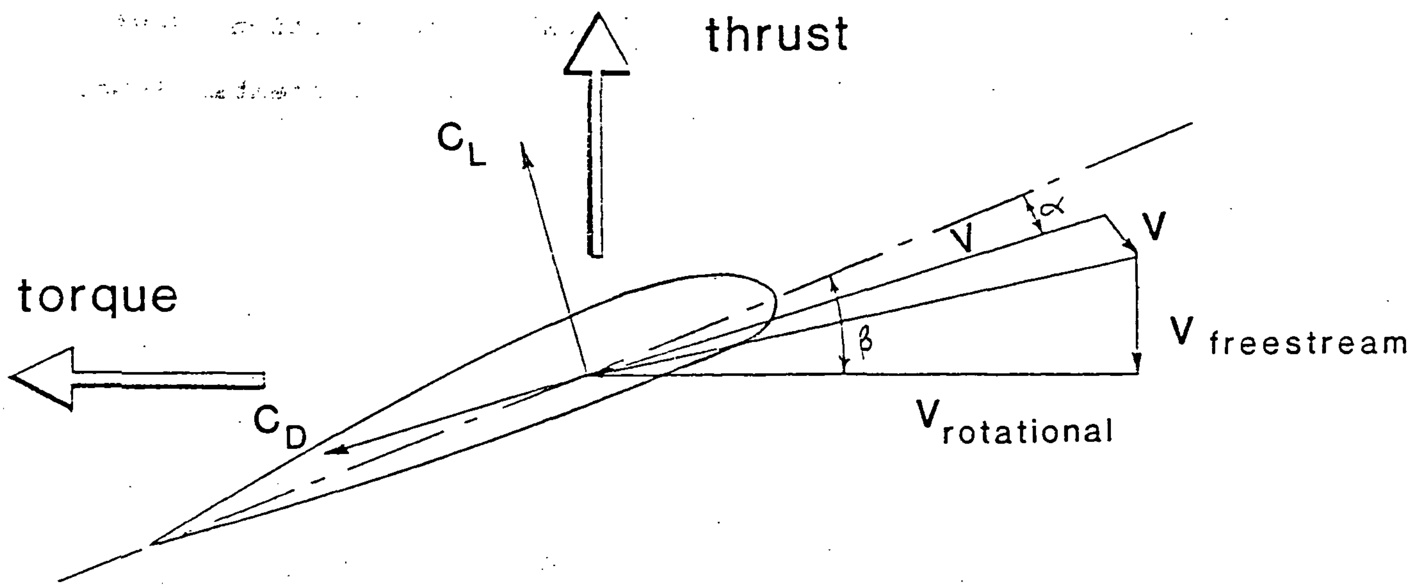

FIGURE 2. Velocity components of propeller section

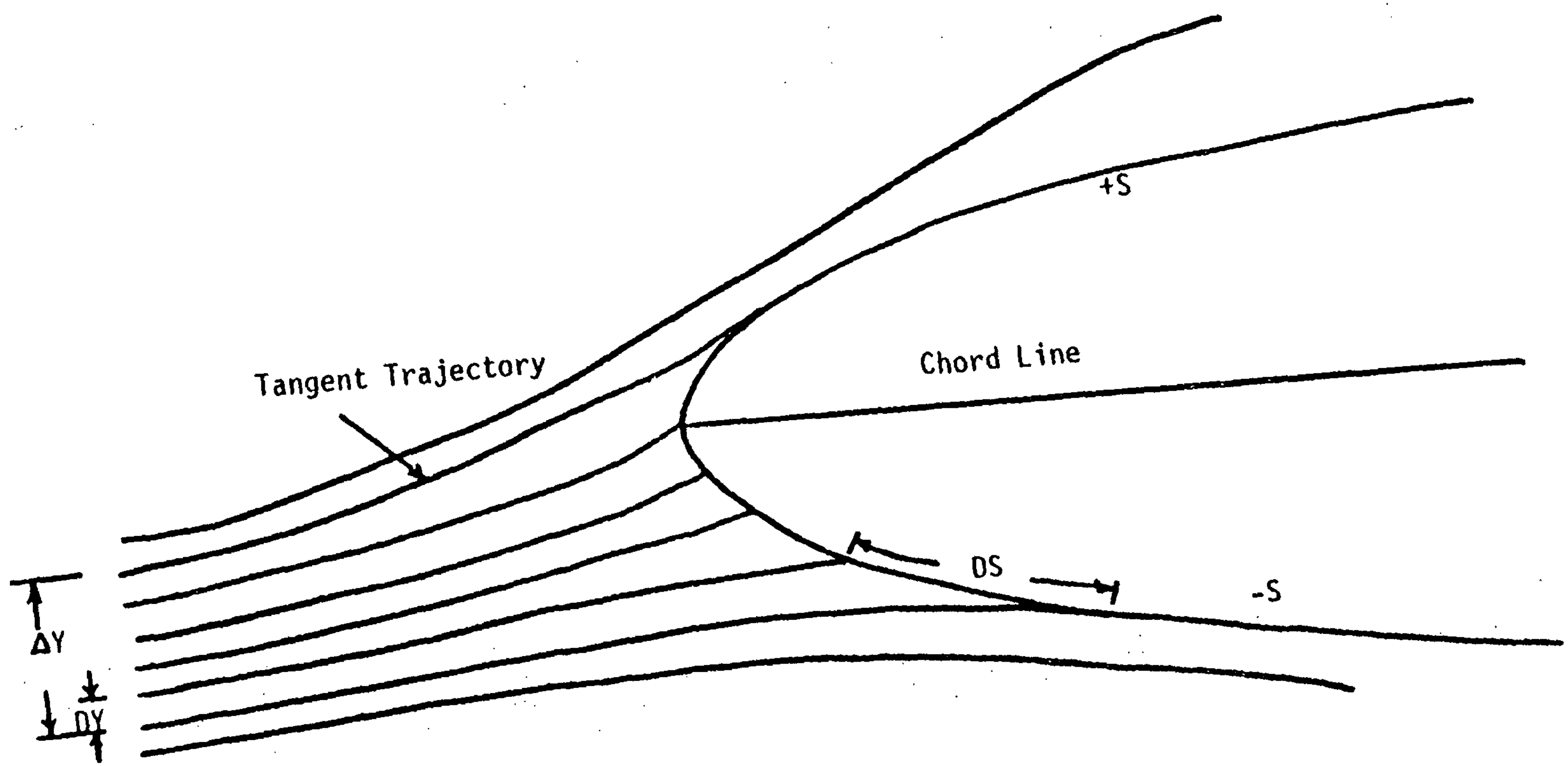

FIGURE 3. Determination of airfoil impingement efficiency

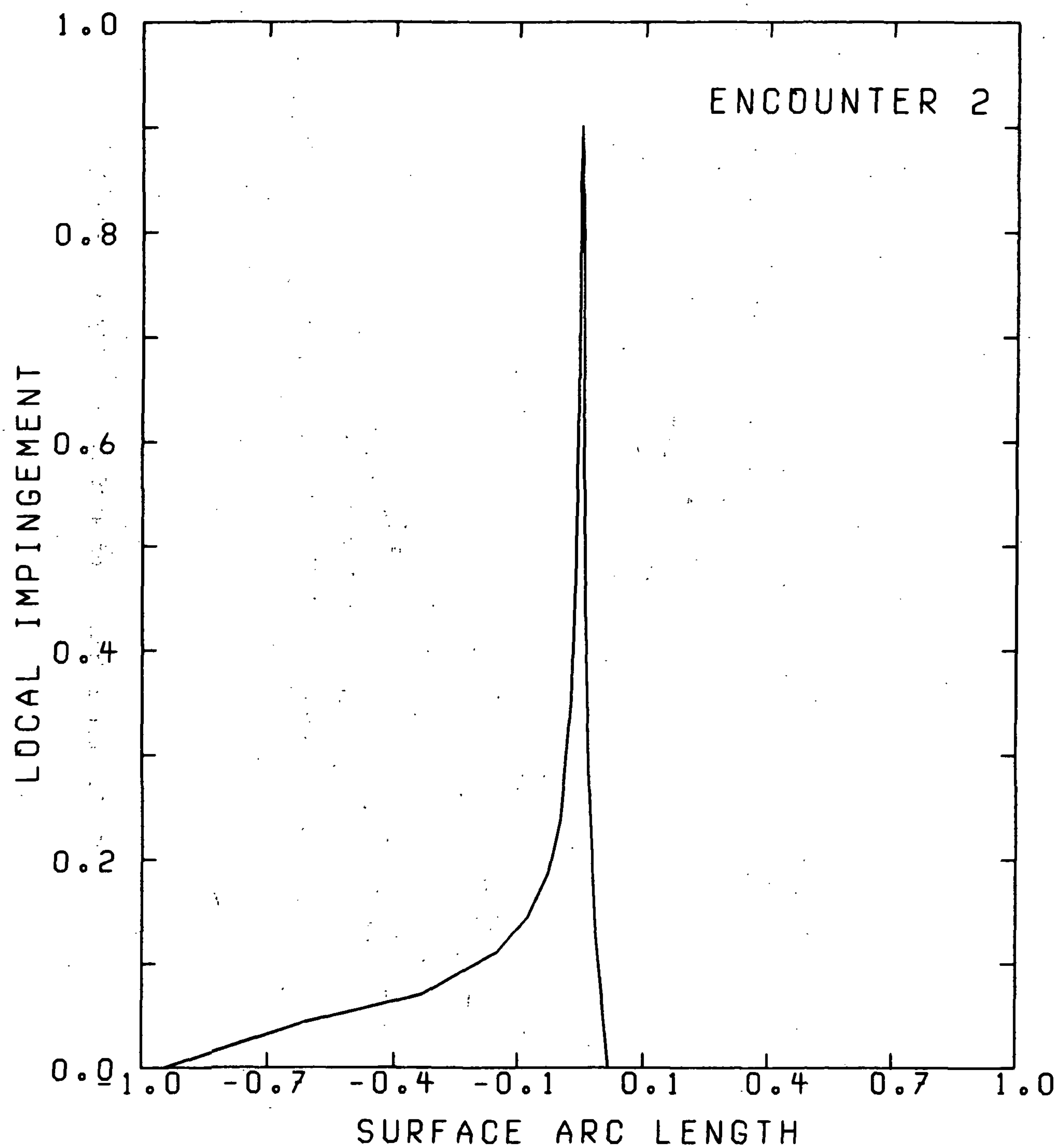

FIGURE 4. Variation of local impingement efficiency with airfoil surface arc length; r/R = 0.9, J = 1.18

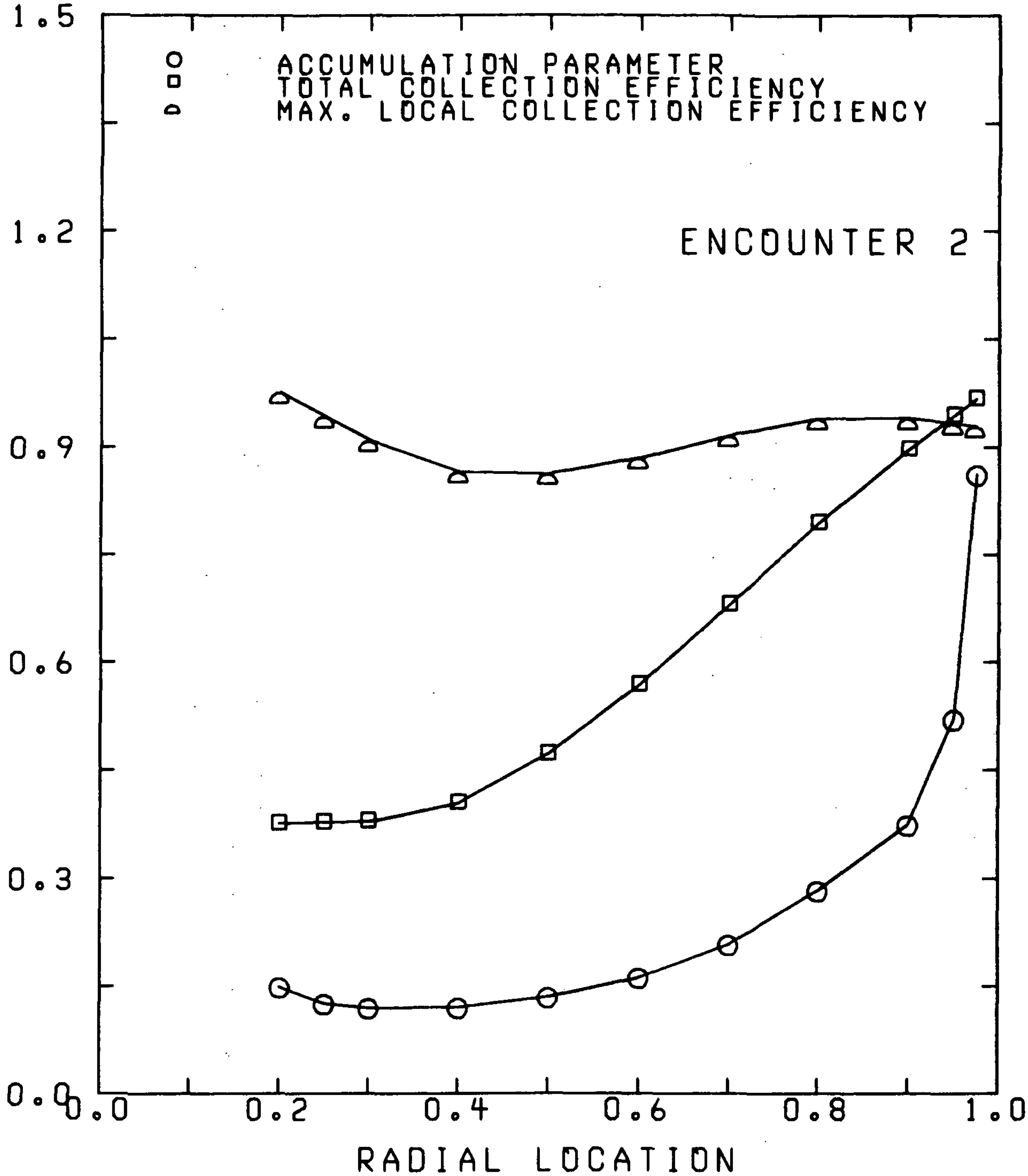

FIGURE 5. Radial variation of accumulation parameter, maximum local collection efficiency, and total collection efficiency for Encounter 2, J = 1.18

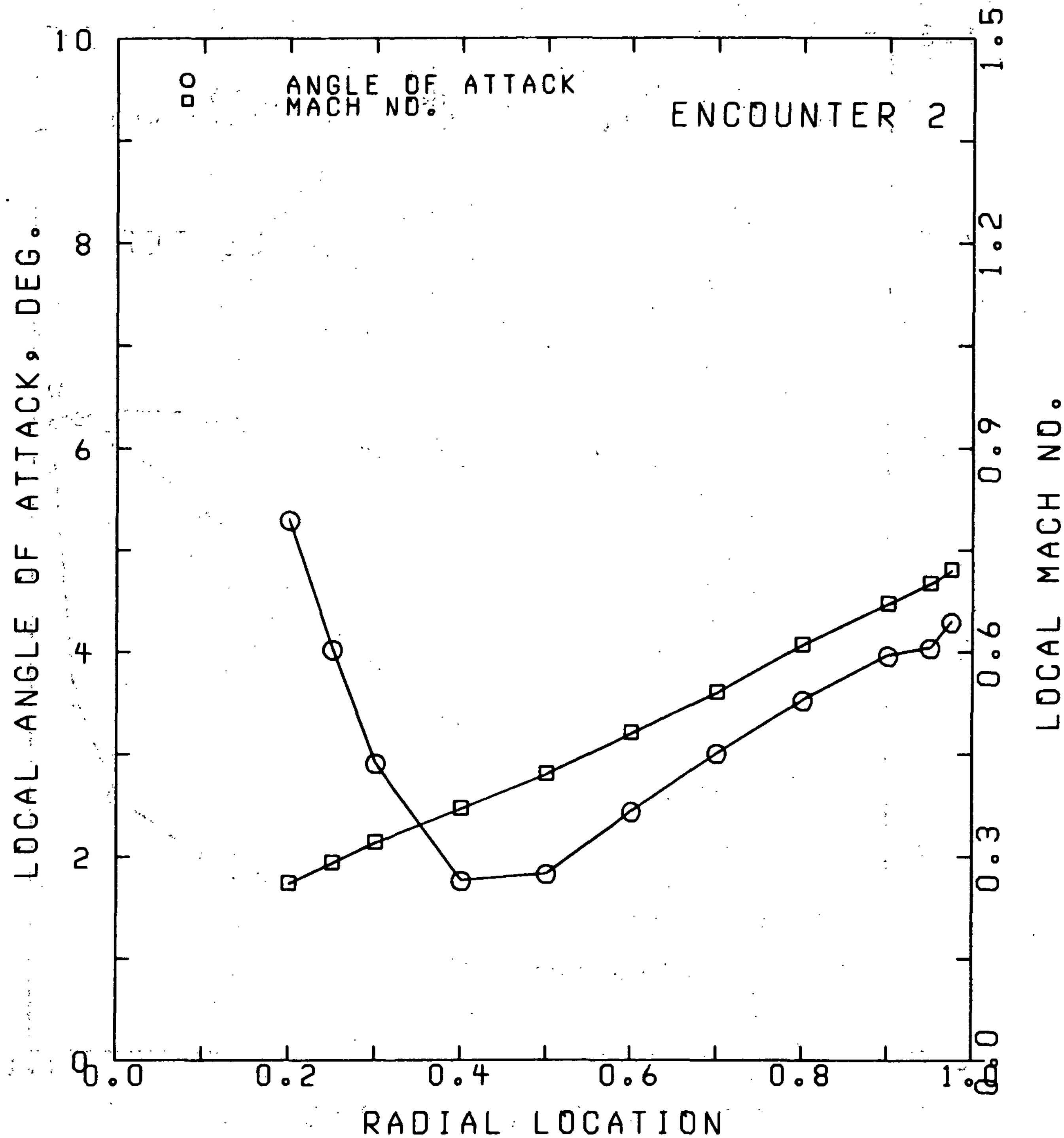

FIGURE 6. Radial variation of local angle of attack and Mach no. for Encounter 2, J = 1.18

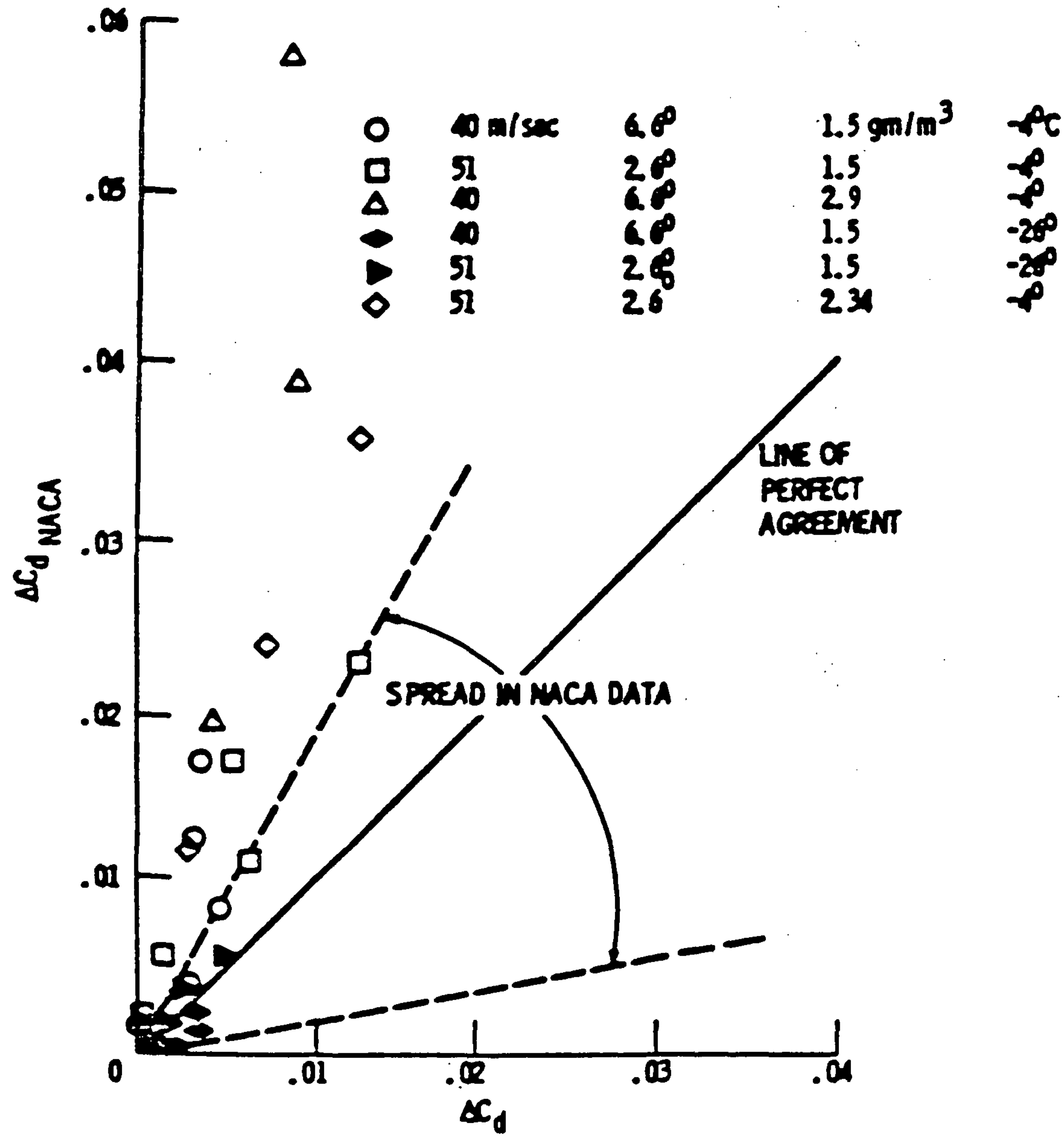

FIGURE 7. Comparison of experimental results with Gray's predicted ΔC_d values

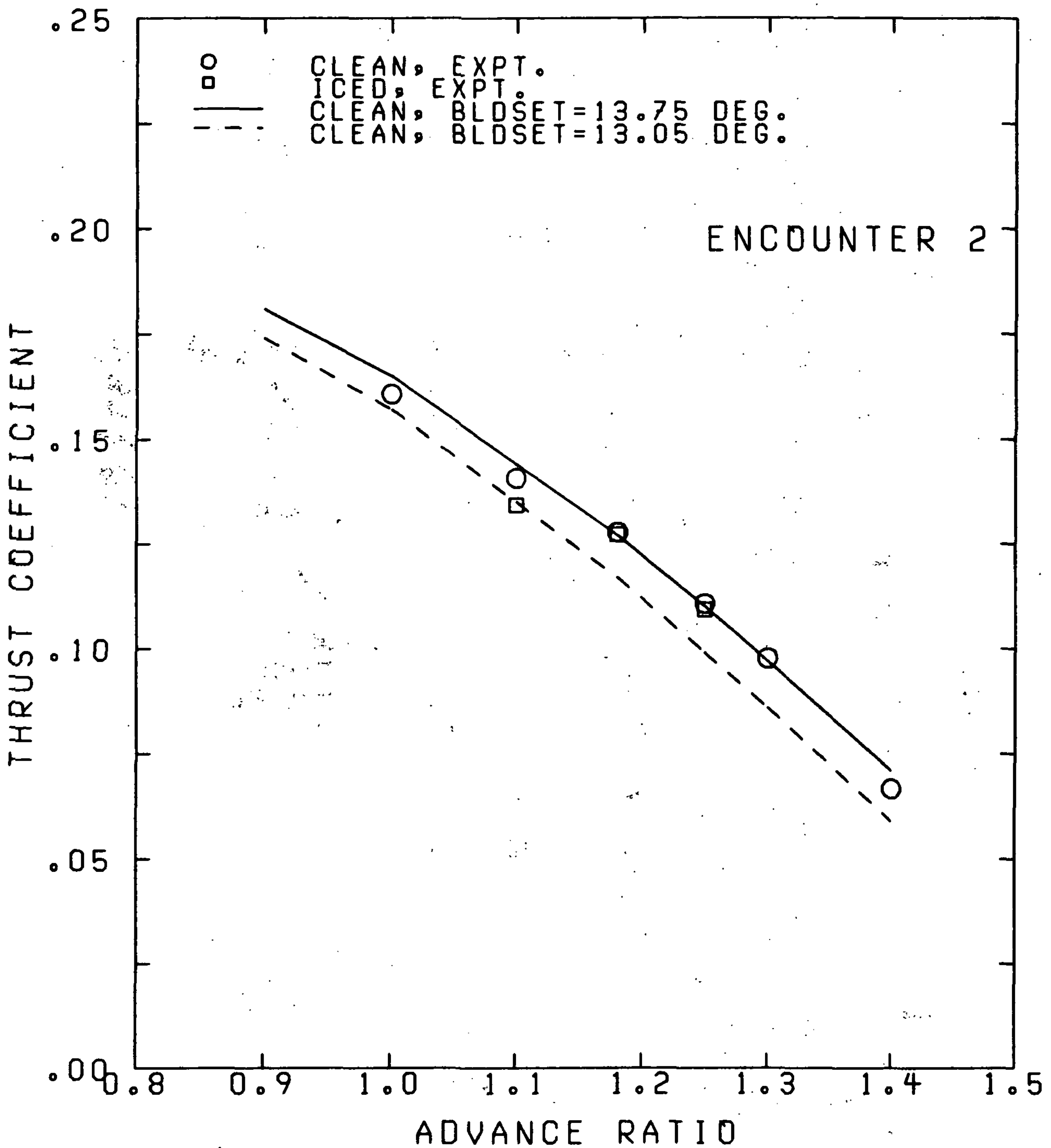

FIGURE 8. Effect of propeller blade setting on predicted thrust coefficient, Encounter 2

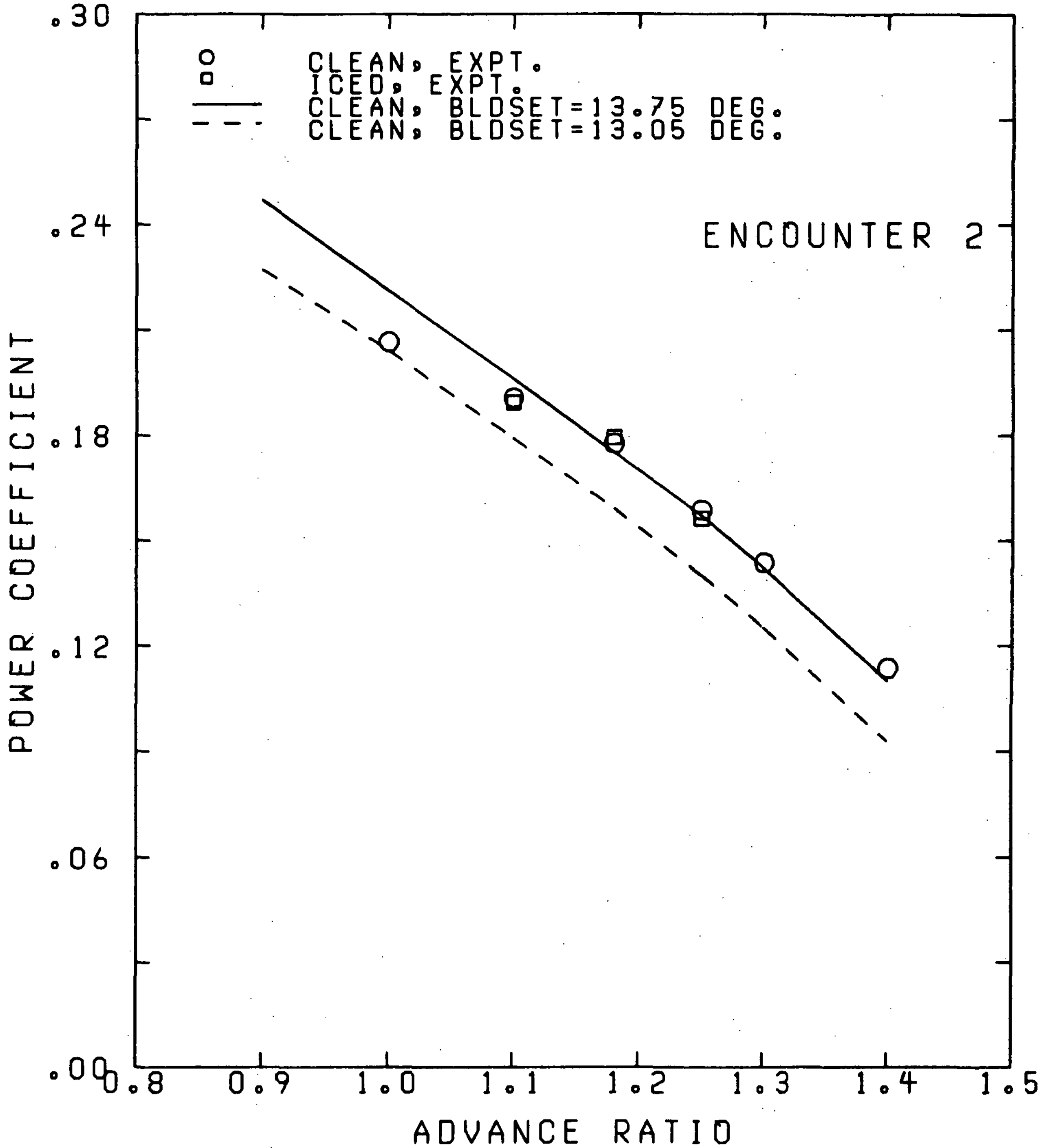

FIGURE 9. Effect of propeller blade setting on predicted power coefficient, Encounter 2

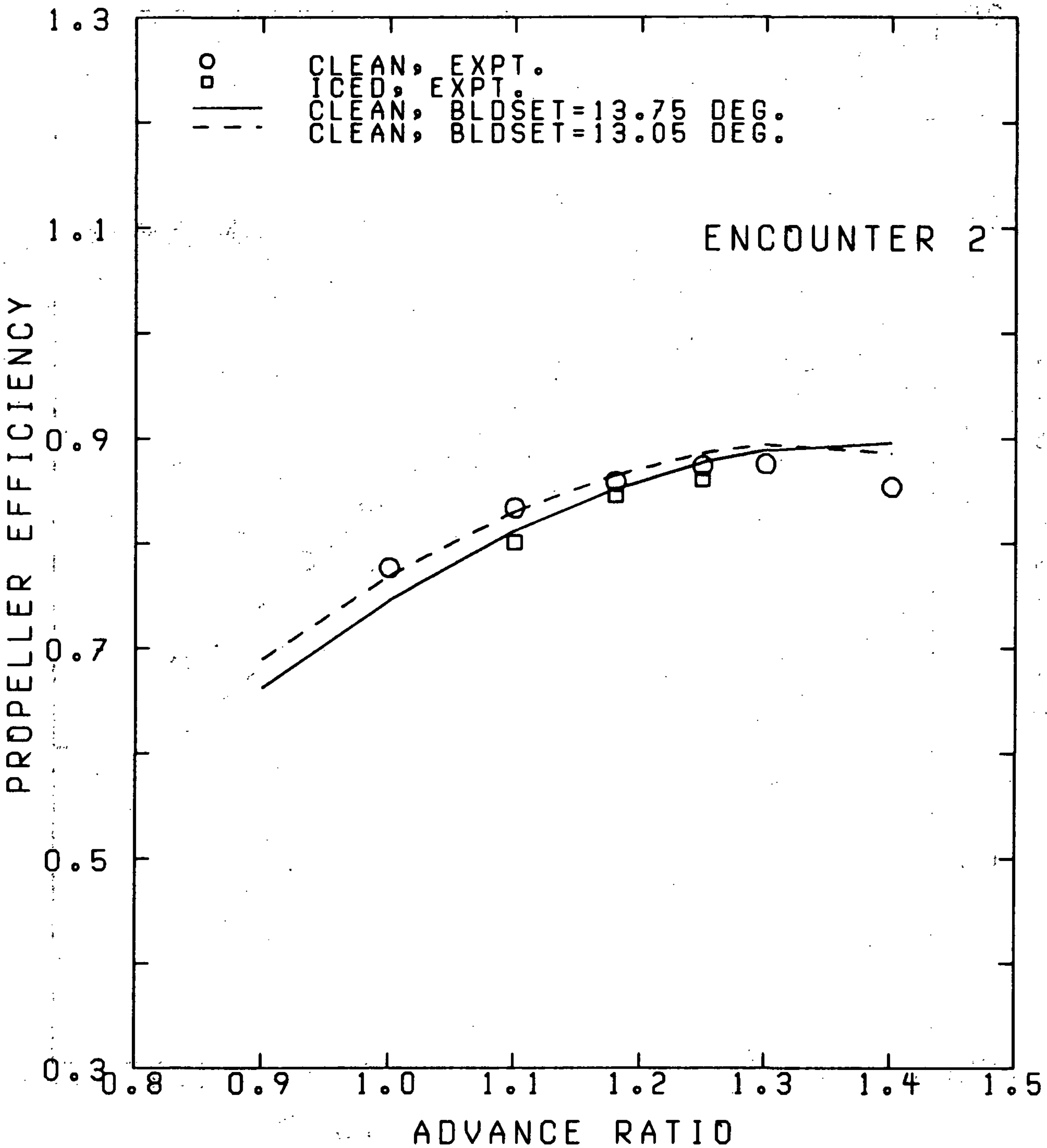

FIGURE 10. Effect of propeller blade setting on predicted propeller efficiency, Encounter 2

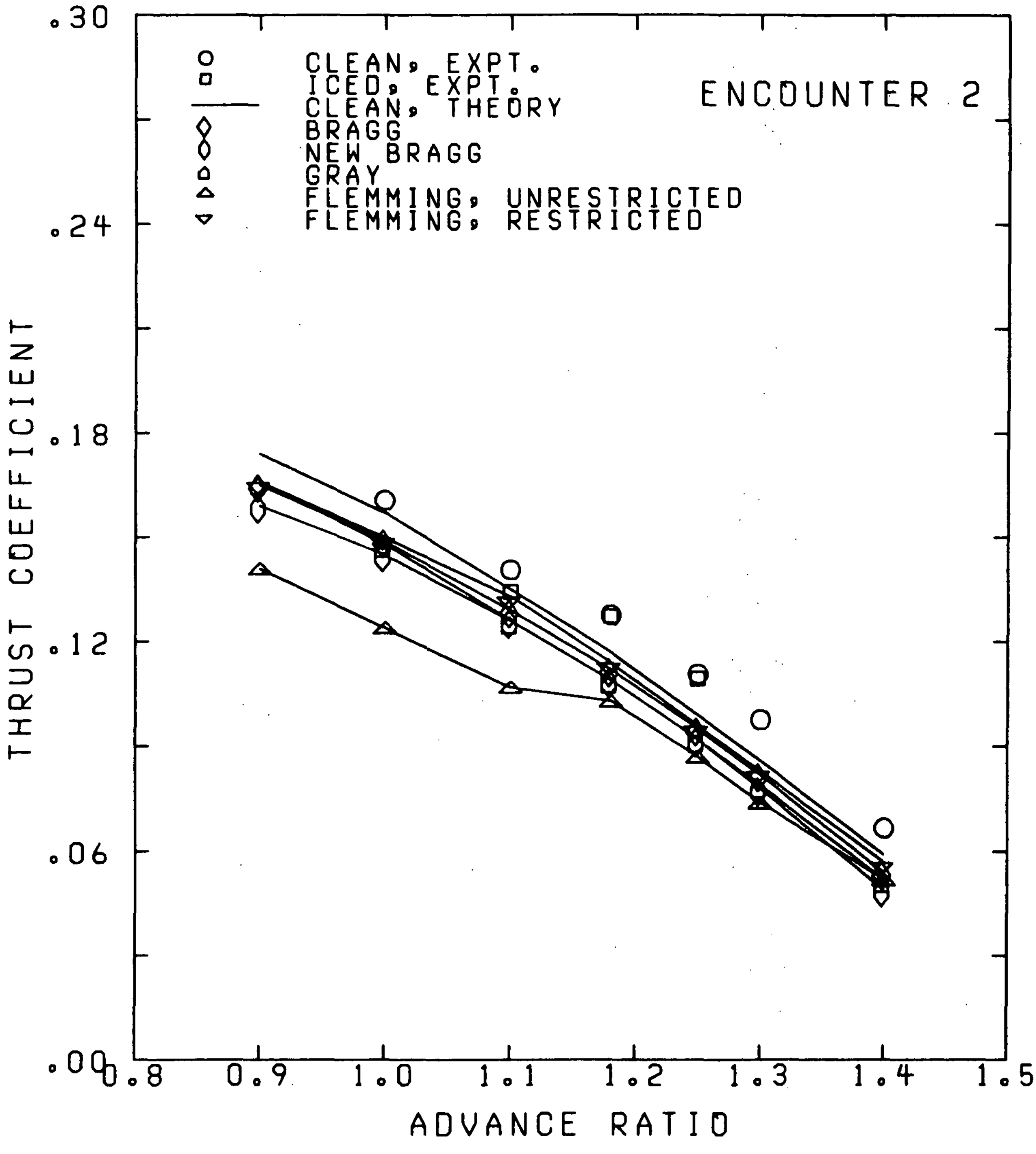

FIGURE 11. Variation of thrust coefficient with advance ratio, clean and iced (iced to r/R = 0.7), Encounter 2

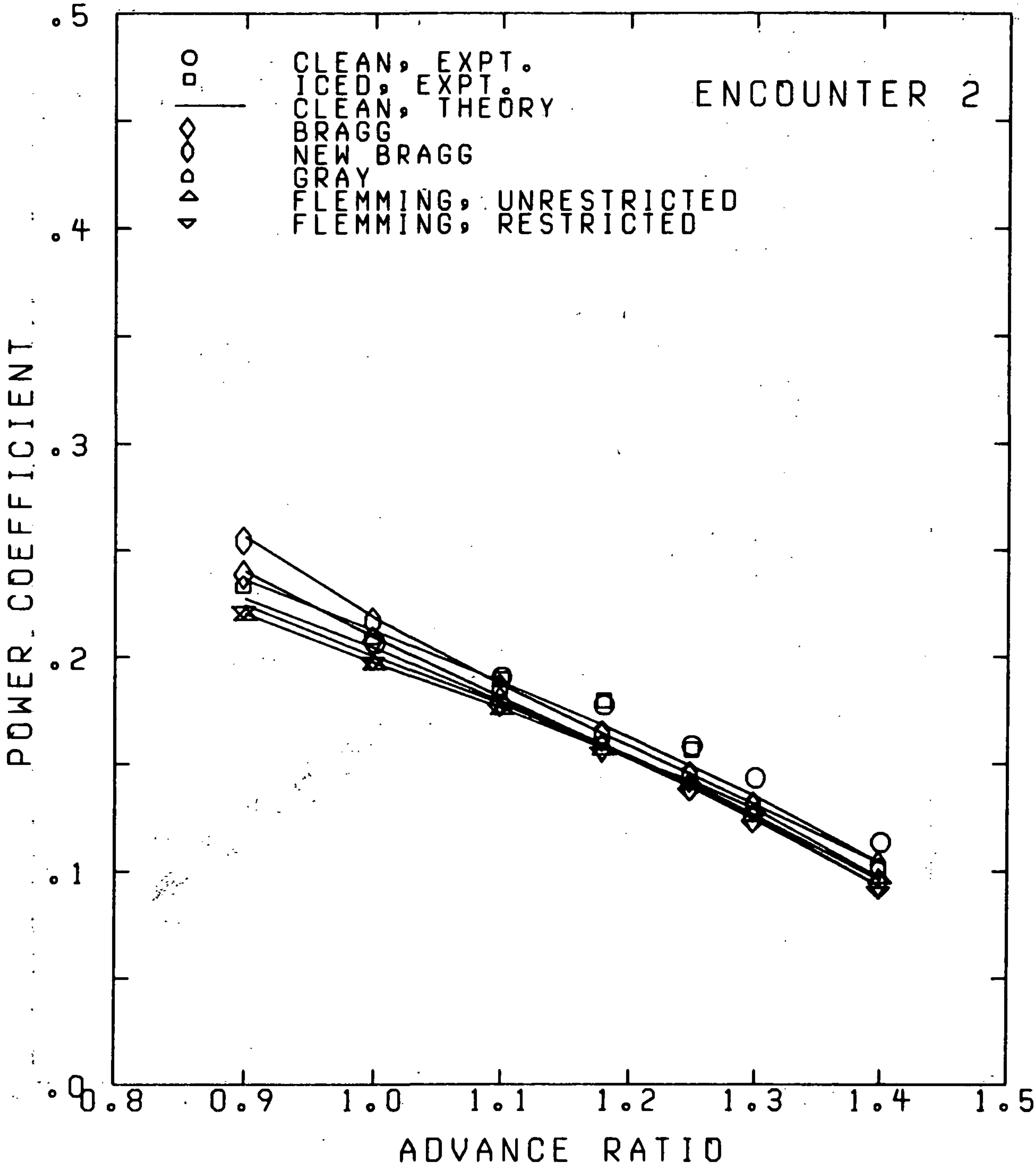

FIGURE 12. Variation of power coefficient with advance ratio, clean and iced (iced to r/R = 0.7), Encounter 2

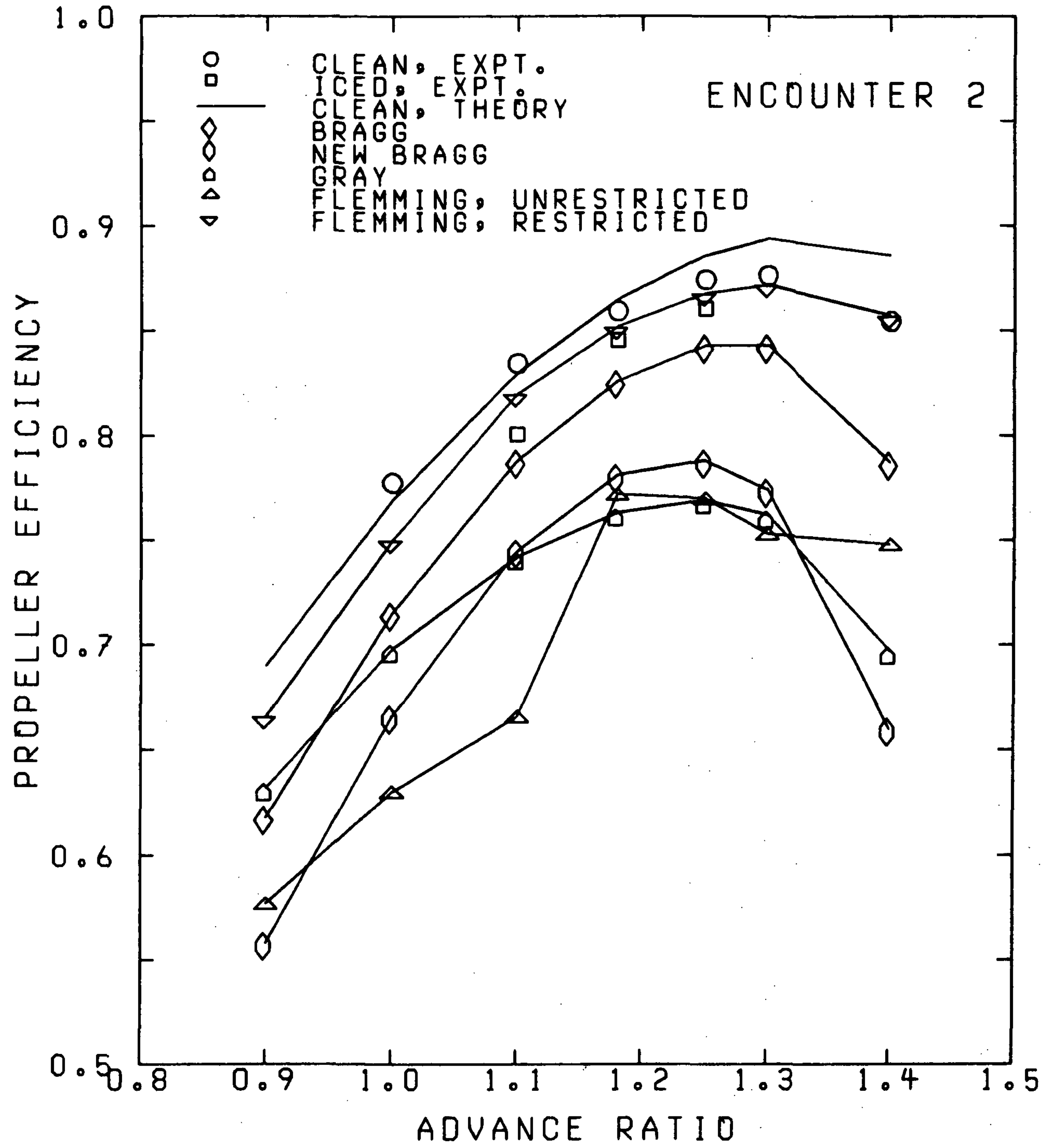

FIGURE 13. Variation of propeller efficiency with advance ratio, clean and iced (iced to r/R = 0.7), Encounter 2

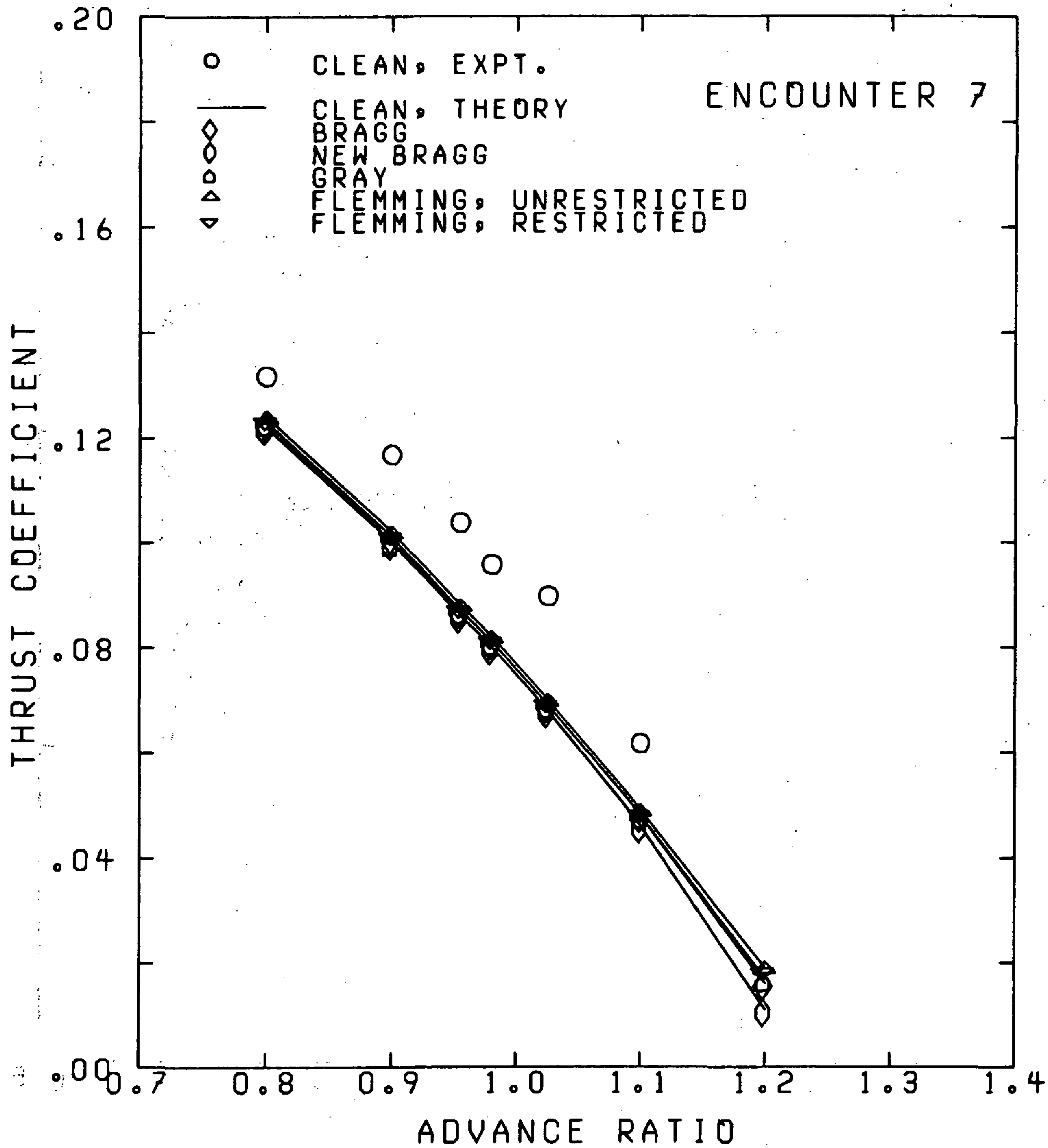

FIGURE 14. Variation of thrust coefficient with advance ratio, clean and iced (iced to r/R = 0.4), Encounter 7

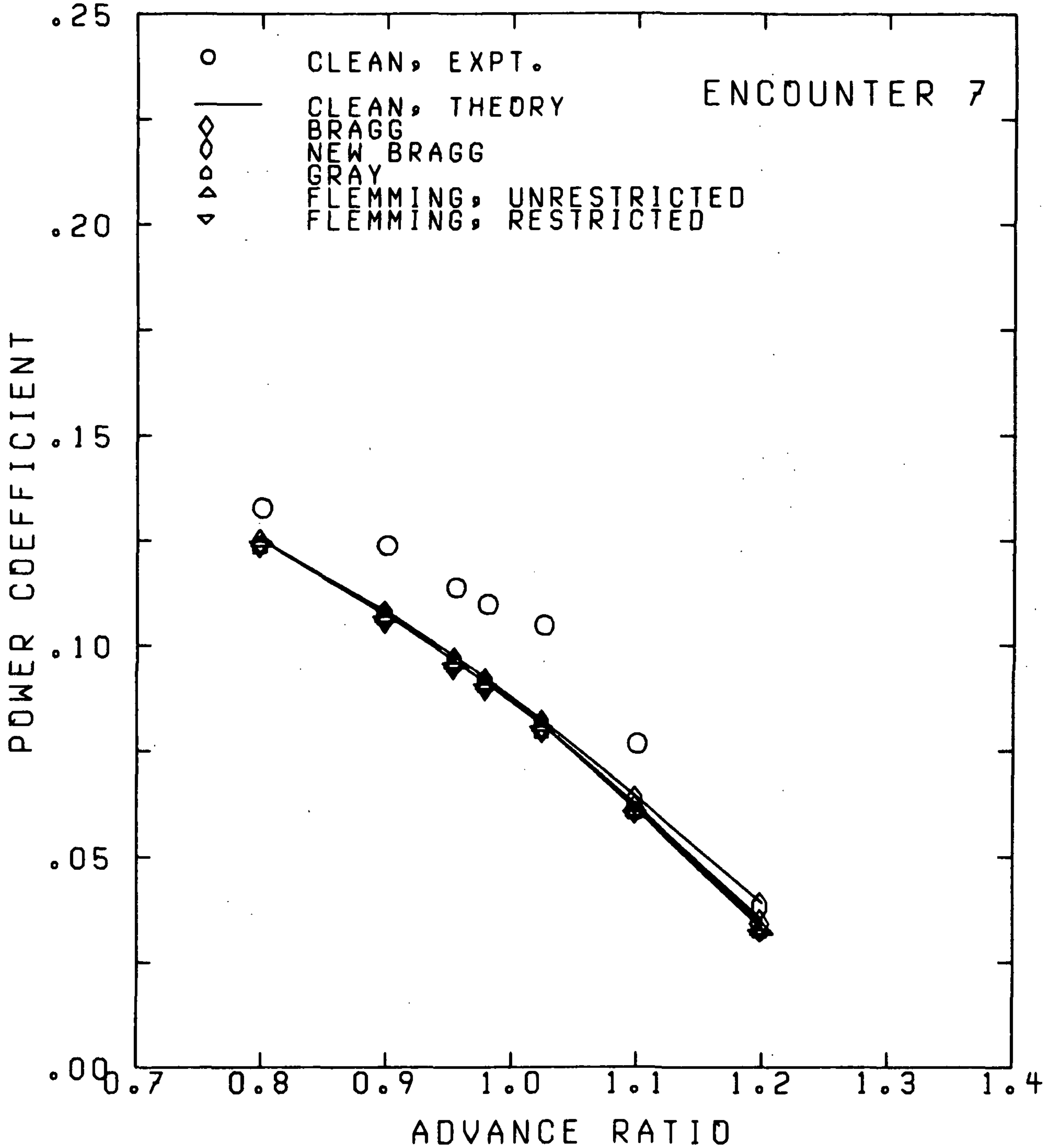

FIGURE 15. Variation of power coefficient with advance ratio, clean and iced (iced to r/R = 0.4), Encounter 7

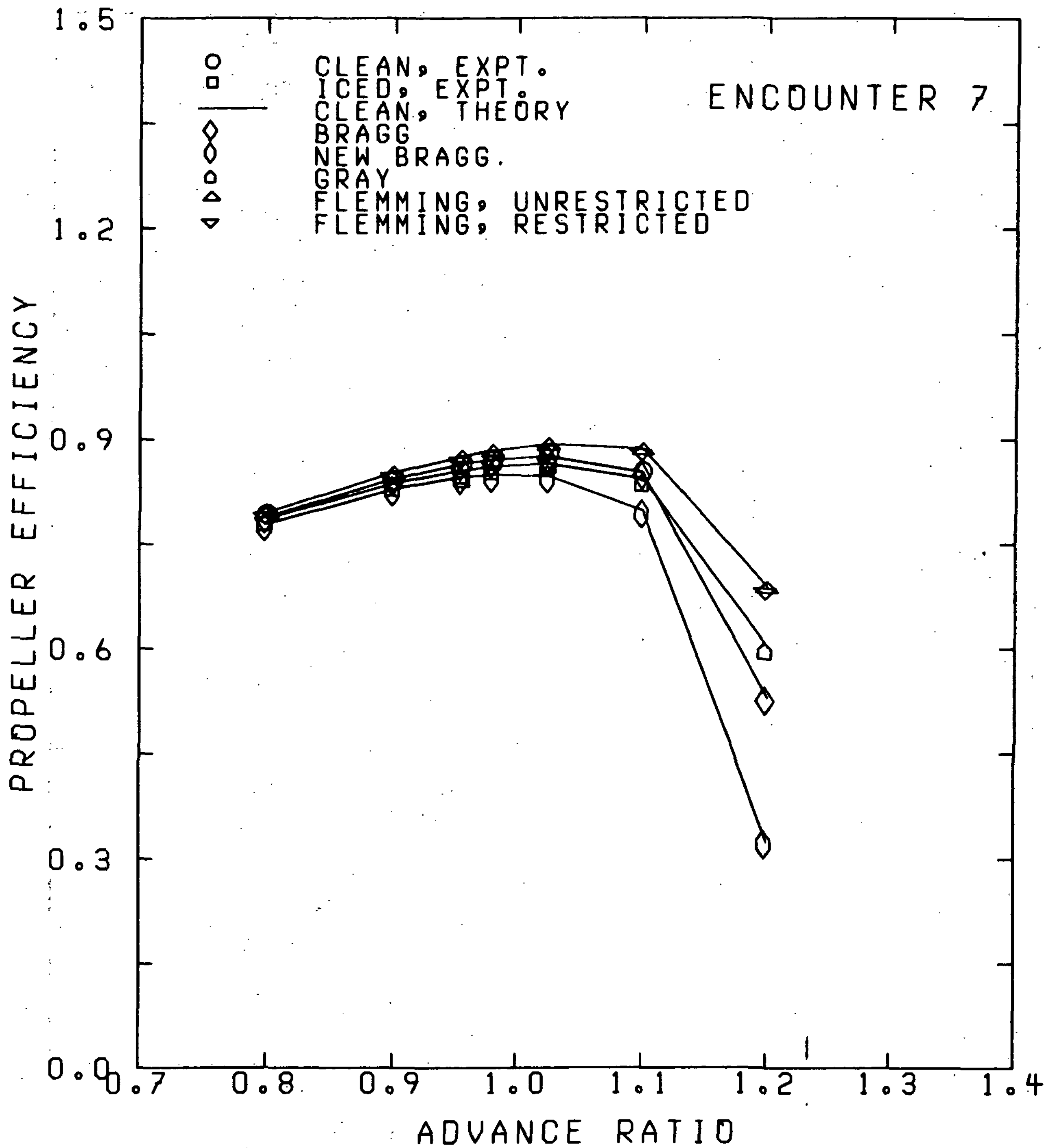

FIGURE 16. Variation of propeller efficiency with advance ratio, clean and iced (iced to r/R = 0.4), Encounter 7

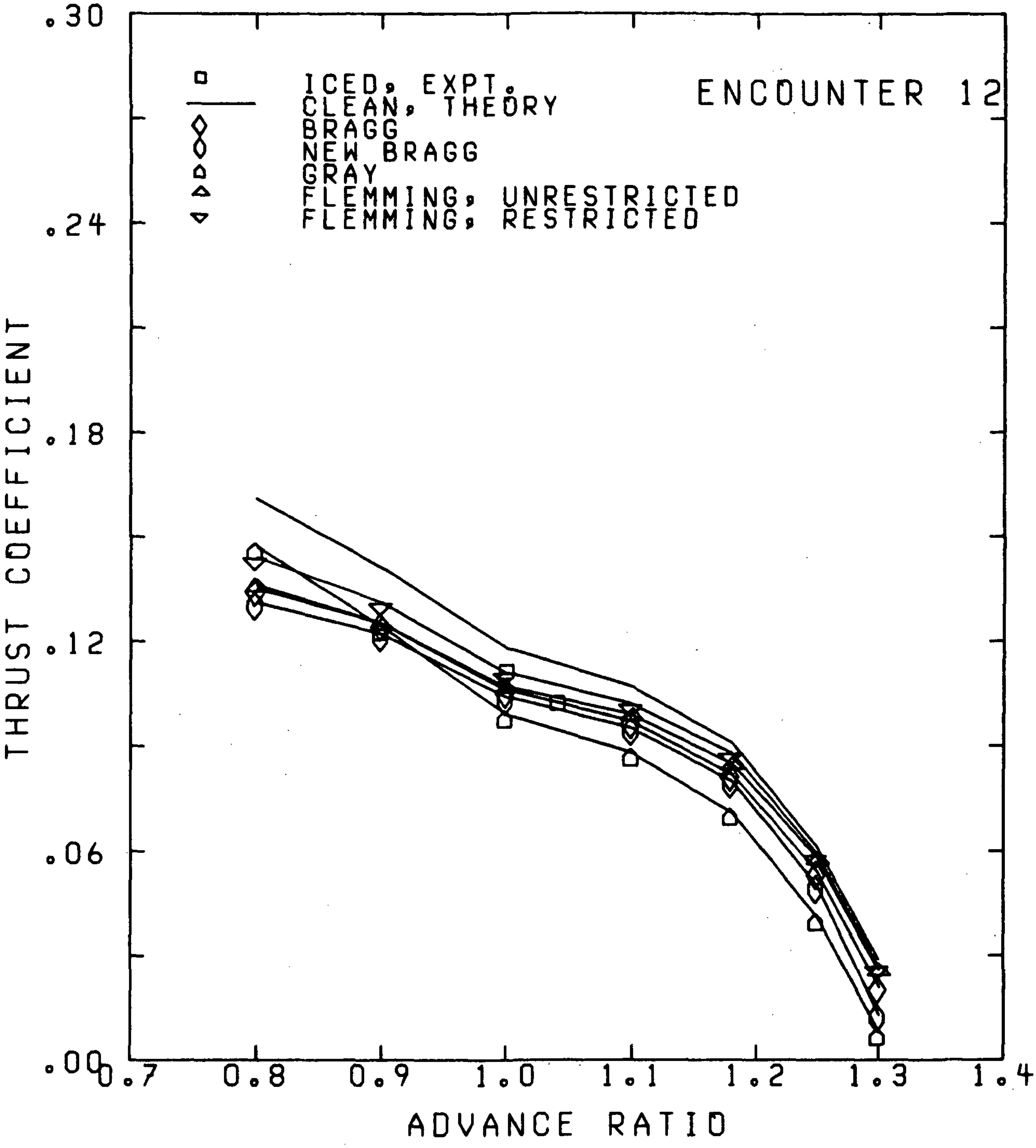

FIGURE 17. Variation of thrust coefficient with advance ratio, clean and iced (iced to r/R = 0.9), Encounter 12

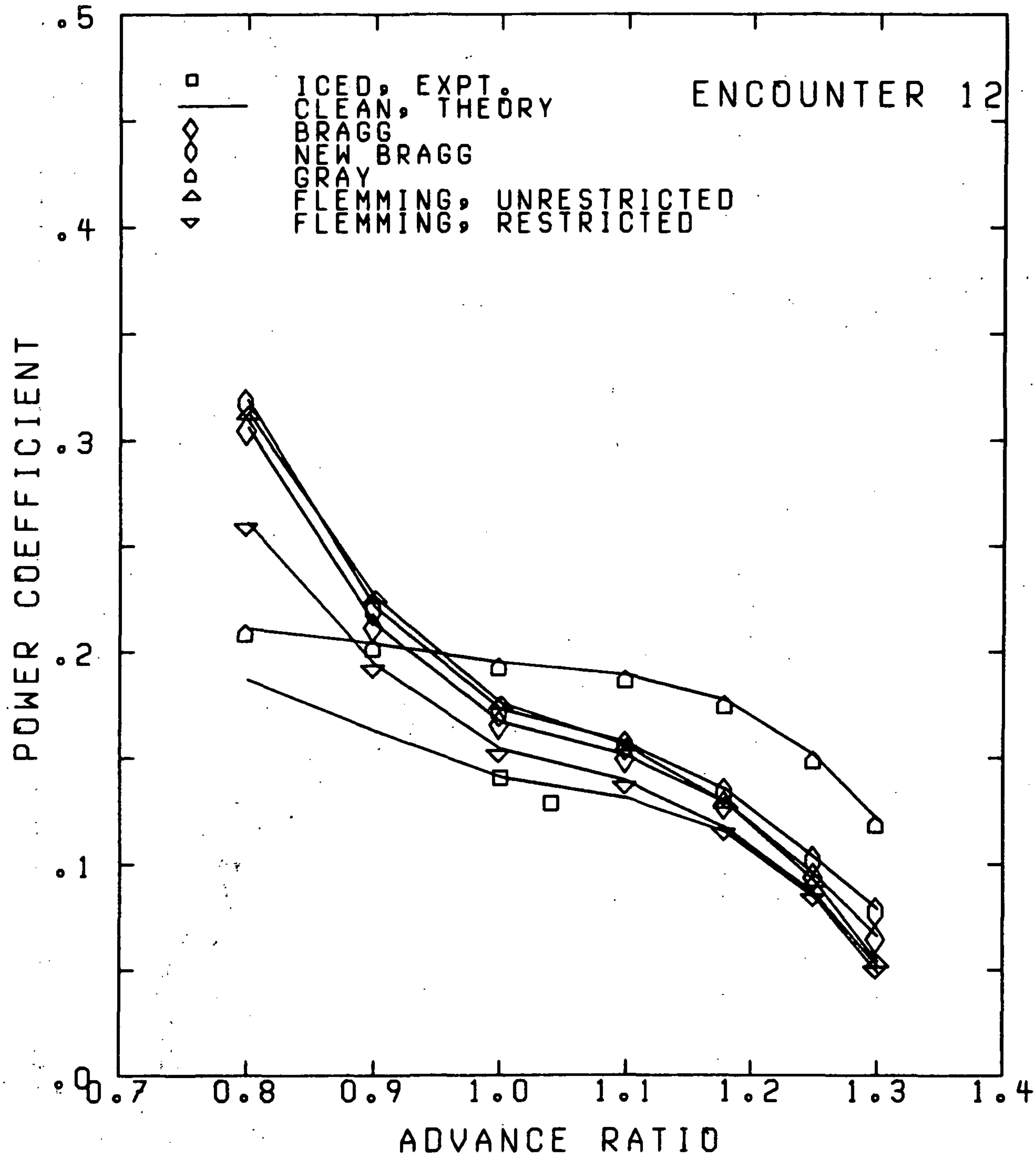

FIGURE 18. Variation of power coefficient with advance ratio, clean and iced (iced to r/R = 0.9), Encounter 12

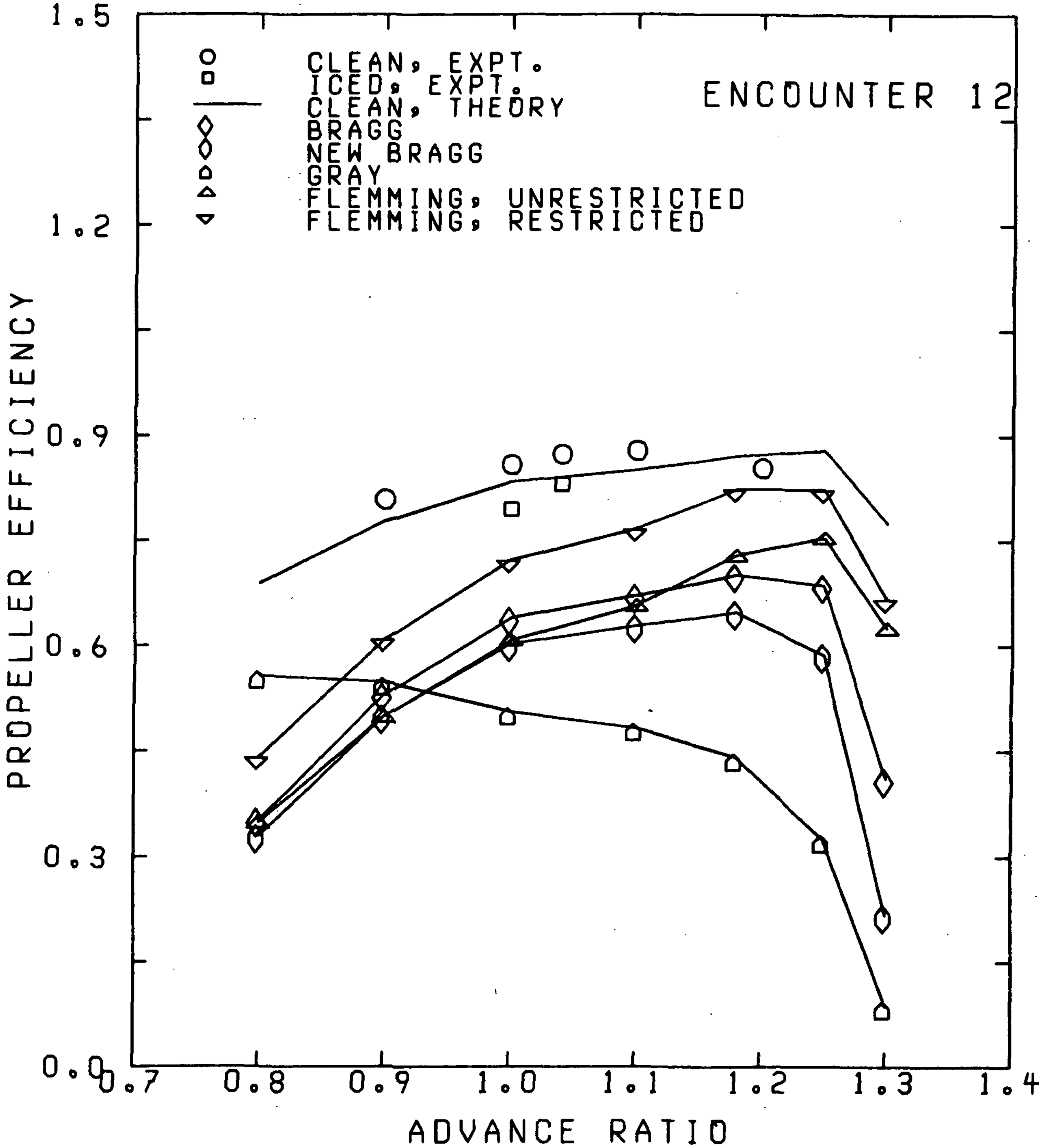

FIGURE 19. Variation of propeller efficiency with advance ratio, clean and iced (iced to r/R = 0.9), Encounter 12

Table 3. Flight and atmospheric parameters for each encounter.

Encounter	Propeller RPM	Propeller Blade Angle at 0.75R, deg.	Pressure Altitude ft.	Icing Time, min.	Air temp., °F	Avg. Liquid Water Content, g/m^3	Avg. Droplet Diameter, microns
2	1025	31.8	10000	10	1	0.41	18
3A	1025	25.8	7000	31	17	0.41	20
3B	1025	31.8	7000	31	17	0.41	20
4A	1025	25.8	9200	9	3	0.44	25
4B	1025	31.8	9200	9	3	0.44	25
5	1025	25.8	8200	19	9	0.27	17
6	1025	25.8	7500	20	10	0.58	15
7	1025	25.8	2000	60	26	0.10	19
8	1025	25.8	2500	30	20	0.04	9
12	1175	28.0	22700	33	-22	0.14	14

Table 4. Comparison of predicted and experimental propeller performance for Encounter 2.

J		CLEAN		ICED					
		Neel&Bright	ICEPERF	Neel&Bright	old,modifed Bragg	new Bragg	Gray	icing unrestricted Flemming	icing restricted Flemming
0.90	C_T		.174		.165	.159	.166	.138	.167
	C_p		.227		.240	.256	.236	.189	.220
	η		.690		.618	.558	.632	.659	.683
1.00	C_T	.161	.157		.149	.145	.148	.125	.151
	C_p	.207	.204		.209	.218	.212	.167	.198
	η	.778	.769		.715	.666	.698	.749	.766
1.10	C_T	.141	.135	.134	.129	.126	.127	.112	.134
	C_p	.191	.179	.189	.181	.187	.188	.150	.177
	η	.836	.830	.800	.788	.745	.742	.820	.829
1.18	C_T	.128	.117	.127	.112	.109	.109	.107	.115
	C_p	.178	.159	.179	.159	.164	.168	.147	.158
	η	.860	.865	.845	.826	.781	.763	.862	.864
1.25	C_T	.111	.099	.109	.095	.092	.092	.093	.098
	C_p	.159	.140	.156	.141	.145	.149	.131	.139
	η	.875	.886	.860	.843	.788	.769	.884	.885
1.30	C_T	.098	.086		.082	.078	.079	.081	.085
	C_p	.144	.125		.126	.131	.135	.188	.124
	η	.877	.894		.843	.774	.762	.892	.894
1.40	C_T	.067	.059		.054	.049	.052	.057	.059
	C_p	.114	.093		.096	.104	.104	.090	.093
	η	.855	.886		.787	.660	.697	.883	.885

Table 5. Comparison of predicted and experimental propeller performance for Encounter 7.

		CLEAN		ICED					
J		Neel&Bright	ICEPERF	Neel&Bright	old,modifed Bragg	new Bragg	Gray	icing unrestricted Flemming	icing restricted Flemming
0.80	C_T	.132	.124		.123	.122	.123	.124	.124
	C_p	.133	.125		.125	.125	.125	.125	.125
	η	.794	.796		.790	.779	.787	.796	.796
0.90	C_T	.117	.102		.101	.100	.100	.102	.102
	C_p	.124	.107		.107	.108	.108	.107	.107
	η	.843	.853		.844	.829	.837	.853	.853
0.955	C_T	.104	.088		.087	.086	.087	.088	.088
	C_p	.114	.096		.096	.097	.097	.096	.096
	η	.865	.876	.840	.865	.846	.855	.876	.876
0.98	C_T	.096	.082		.081	.080	.081	.082	.082
	C_p	.110	.091		.091	.092	.092	.091	.091
	η	.872	.884	.865	.871	.849	.861	.884	.884
1.025	C_T	.090	.070		.069	.068	.069	.070	.070
	C_p	.105	.081		.081	.082	.081	.081	.081
	η	.880	.893	.860	.876	.847	.865	.893	.893
1.10	C_T	.062	.049		.048	.046	.048	.049	.049
	C_p	.077	.061		.062	.064	.062	.061	.061
	η	.855	.886		.852	.797	.843	.886	.886
1.20	C_T		.019		.016	.011	.017	.019	.019
	C_p		.033		.035	.039	.034	.033	.033
	η		.688		.530	.603	.603	.688	.688

Table 6. Comparison of predicted and experimental propeller performance for Encounter 12.

J		CLEAN Neel&Bright	CLEAN ICEPERF	ICED Neel&Bright	ICED old, modifed Bragg	ICED new Bragg	ICED Gray	ICED icing unrestricted Flemming	ICED icing restricted Flemming
0.80	C_T		.161		.135	.131	.147	.152	.154
	C_P		.187		.306	.319	.211	.194	.190
	η		.688		.352	.329	.557	.628	.651
0.90	C_T		.141		.125	.122	.124	.135	.137
	C_P		.163		.213	.221	.204	.161	.160
	η	.810	.778		.530	.499	.548	.755	.768
1.00	C_T		.118	.111	.106	.104	.099	.114	.115
	C_P		.141	.140	.167	.173	.195	.138	.139
	η	.860	.834	.793	.639	.602	.506	.822	.831
1.04	C_T		.107	.102	.097	.095	.088	.104	.105
	C_P		.131	.128	.151	.157	.189	.129	.129
	η	.875	.851	.829	.671	.628	.483	.842	.849
1.10	C_T		.091		.082	.080	.071	.089	.090
	C_P		.115		.129	.135	.177	.113	.114
	η	.880	.871		.701	.648	.441	.866	.870
1.20	C_T		.061		.054	.050	.041	.061	.061
	C_P		.084		.095	.103	.151	.083	.084
	η	.855	.879		.686	.587	.325	.876	.878
1.30	C_T		.029		.021	.013	.008	.029	.029
	C_P		.049		.066	.079	.121	.048	.049
	η		.775		.411	.217	.088	.771	.772

Table 7. Experimental and predicted (Flemming correlations) radial extent for each encounter.

Encounter	2		3A		3B		4A		4B		6		6		7		8		12	
r/R	E	T	E	T	E	T	E	T	E	T	E	T	E	T	E	T	E	T	E	T
.20	✓		✓		✓		✓		✓		✓		✓		✓		✓		✓	
.25	✓		✓		✓		✓		✓		✓		✓		✓		✓		✓	
.30	✓		✓		✓		✓		✓		✓		✓		✓		✓		✓	
.40	✓	R	✓	G	✓	G	✓	R	✓	R	✓	R	✓	G	✓		✓	R	✓	R
.50	✓	R	✓	G	✓	G		R		R	✓	R	✓	G			✓	R	✓	R
.60	✓	G		G		G		G		G		G		G					✓	R
.70	✓	G				G		G		G		G		G					✓	R
.80		G						G		G		G		G					✓	R
.90		G						G		G									✓	R
.95		G						G		G										R
.975		G						G		G										R

E - experiment
✓ - iced

T - theory
G - glaze
R - rime

APPENDIX 1

PROGRAM FLOWCHART

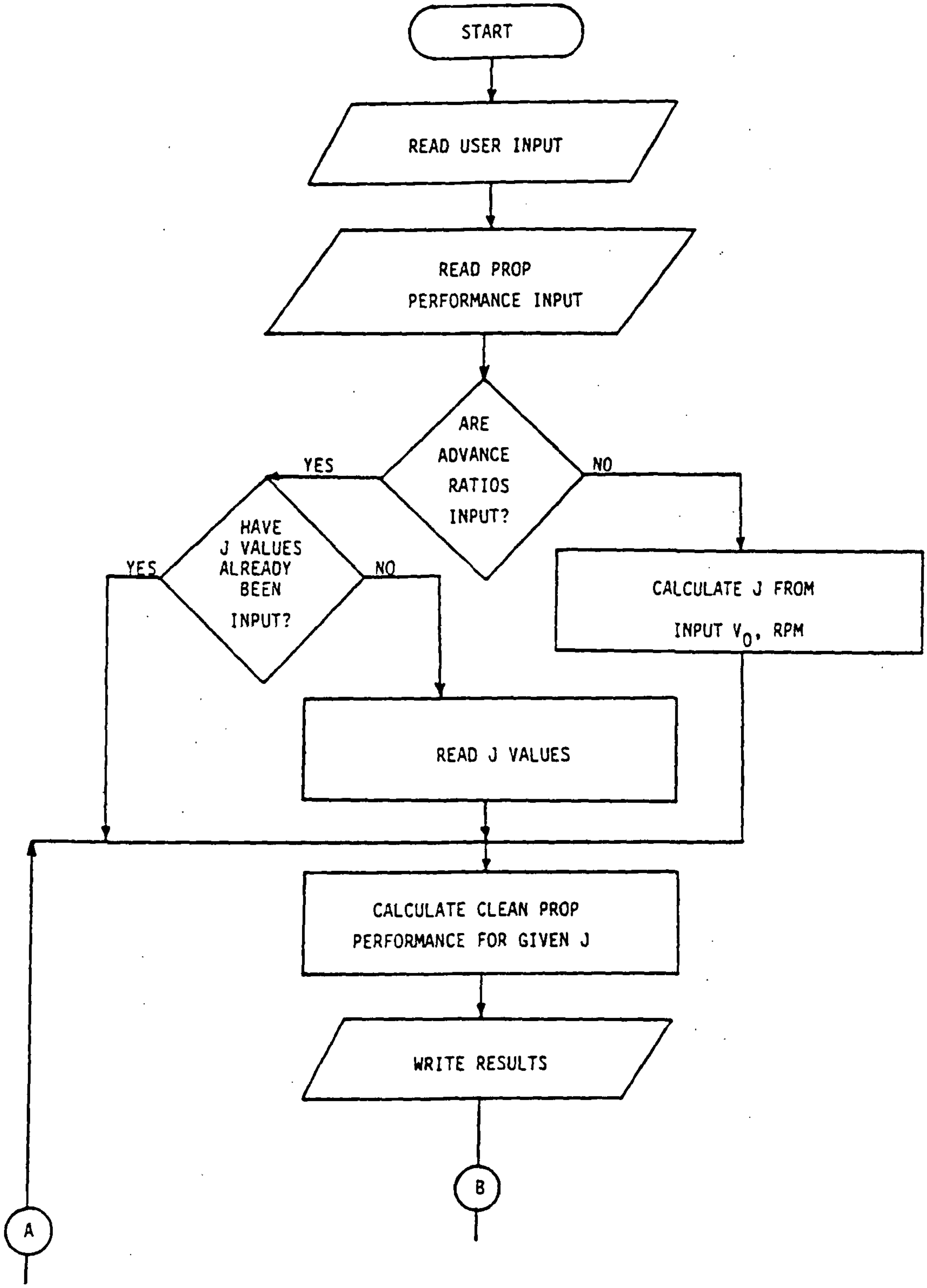

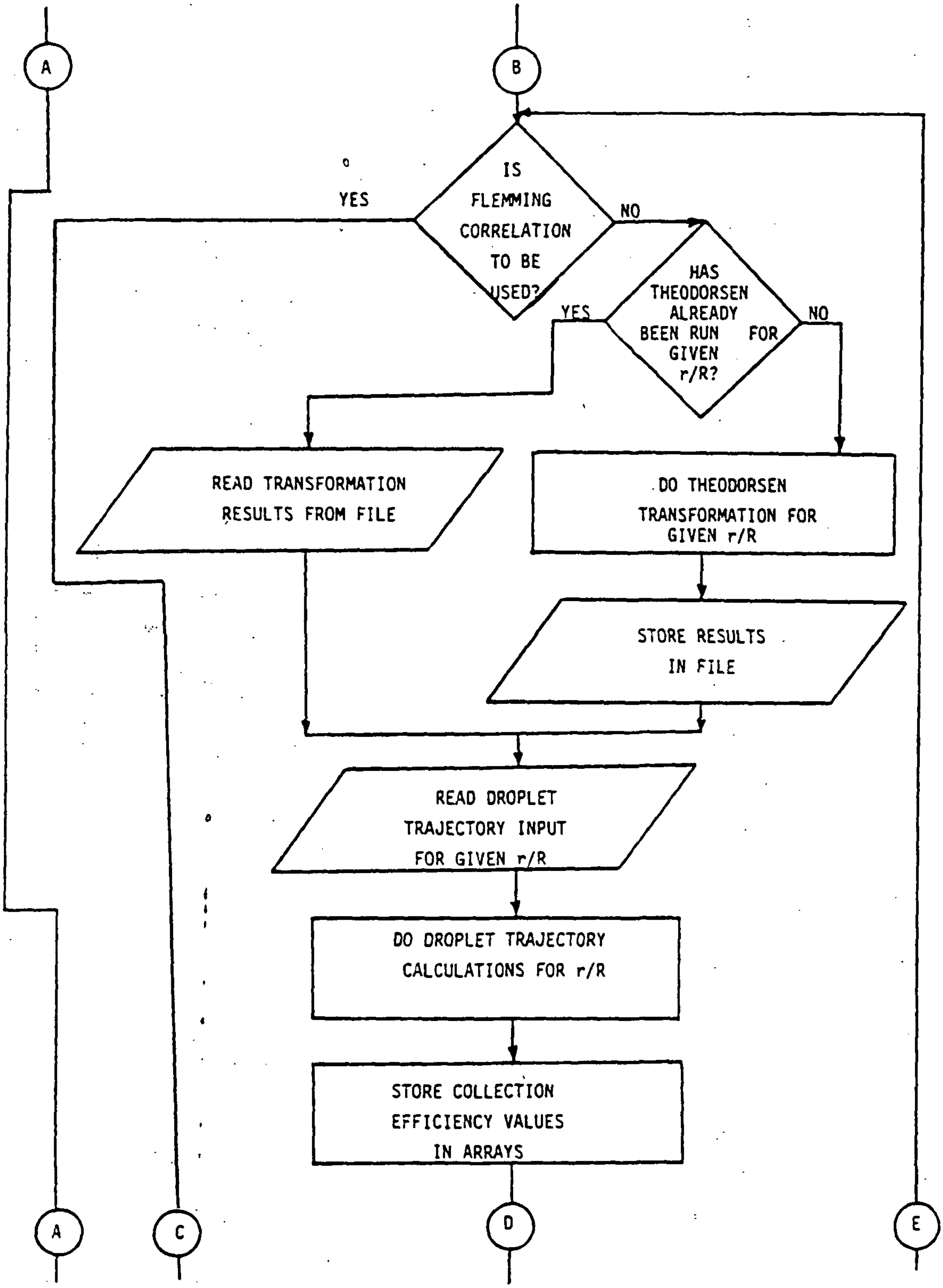

A
B
IS FLEMMING CORRELATION TO BE USED?
YES
NO
HAS THEODORSEN ALREADY BEEN RUN FOR GIVEN r/R?
YES
NO
READ TRANSFORMATION RESULTS FROM FILE
DO THEODORSEN TRANSFORMATION FOR GIVEN r/R
STORE RESULTS IN FILE
READ DROPLET TRAJECTORY INPUT FOR GIVEN r/R
DO DROPLET TRAJECTORY CALCULATIONS FOR r/R
STORE COLLECTION EFFICIENCY VALUES IN ARRAYS
A
C
D
E

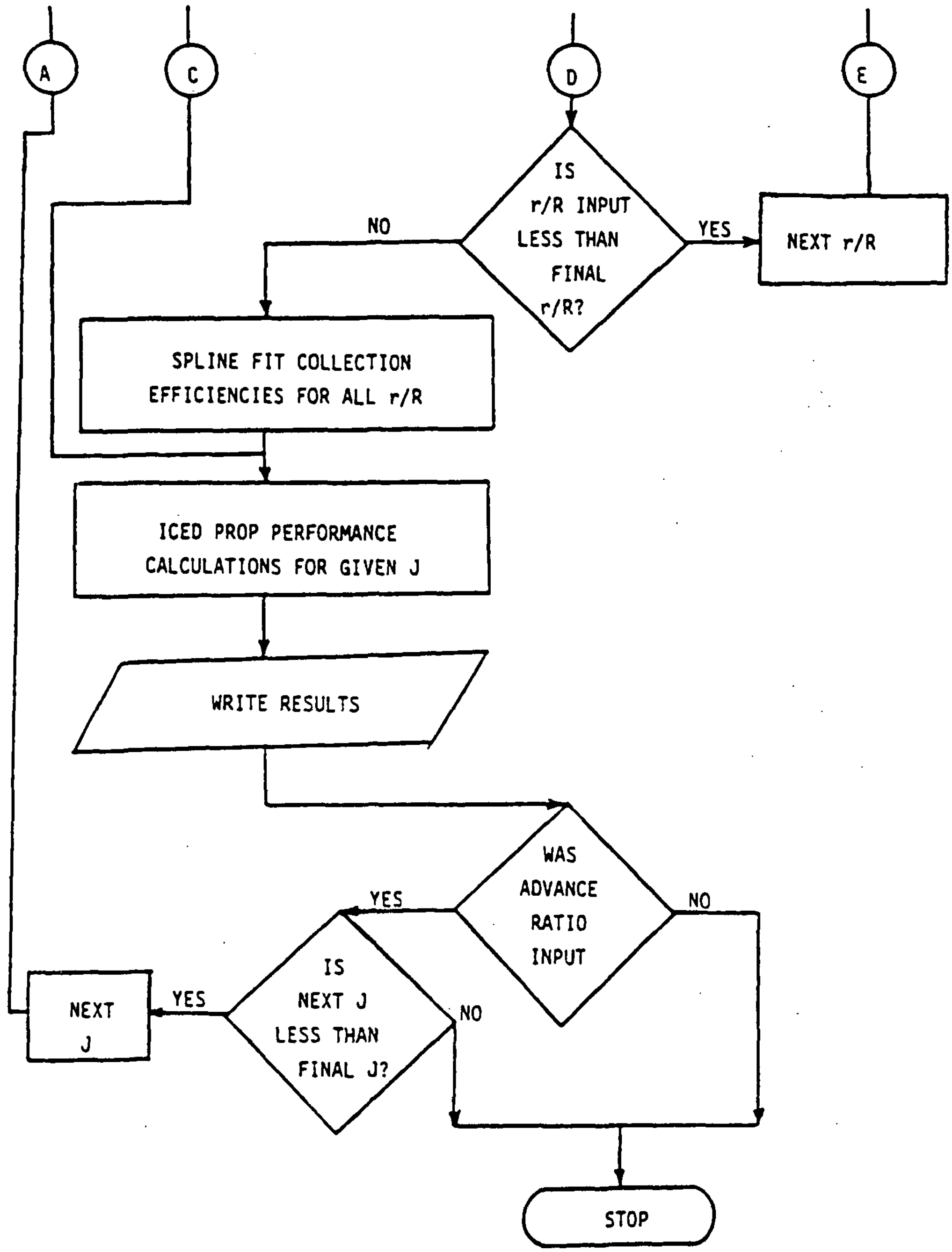
A
C
D
E
IS
r/R INPUT
LESS THAN
FINAL
r/R?
NO
YES
NEXT r/R
SPLINE FIT COLLECTION
EFFICIENCIES FOR ALL r/R
ICED PROP PERFORMANCE
CALCULATIONS FOR GIVEN J
WRITE RESULTS
WAS
ADVANCE
RATIO
INPUT
YES
NO
IS
NEXT J
LESS THAN
FINAL J?
YES
NO
NEXT
J
STOP

APPENDIX 2

USER'S GUIDE

ICEPERF has been designed such that user intervention in the run stream has been eliminated and the amount of user input is minimized. Still, with the wide scope of work and calculations which the code must perform, a substantial degree of input is required of the user. This information is provided through several files which are read at various points in the program and which are separated such that each contains input data relative to a particular phase of the program and to a particular radial location. As previously mentioned, the code handles four input radial locations, and a complete set of input data is required at each radial location.

The actual parameters in each file are described in the Comments section of the code listing which will follow. They are redescribed here to provide the user with a better idea of how to specify and use each variable.

Files 1 through 4 contain airfoil coordinates and other information related to the airfoil geometry at each radial location. These files are used in computing the flowfield about the airfoil. File 1 contains information for the most inboard radial station input, with files 2 through 4 containing input data for progressively more outboard stations.

Card 1 of files 1 through 4 contains the title for the Theodorsen transformation input. This title is printed at the beginning of the airfoil section geometry output for the particular radial location input. It may typically read similarly to, "CLARK-Y COORDINATES AT 30% STATION".

Card 2 contains five variables: LPT, ITAU, IZ1N, TAU, and XZ1N, input in the format (3I5,2F10.0).

LPT represents the number of harmonics which the user desires in the exponential transformation of the airfoil to the circle plane. A value of 50 to 60 is typically used for LPT to attain a satisfactory degree of accuracy.

ITAU is a flag which indicates whether or not the user wishes to input the trailing edge angle of the airfoil section. A value of 0 indicates that the trailing edge angle is not known or will not be input, and any value greater than 0 indicates that the user will input the section trailing edge angle.

IZ1N is a flag which indicates whether or not the user will input the nose singularity coordinates. An IZ1N value of 0 means that the nose singularity will not be input, and IZ1N should be set to any value greater than 0 to input the nose singularity coordinates.

TAU is the trailing edge angle in degrees, to be input if ITAU is greater than 0.

XZ1N and YZ1N are the x- and y-coordinates of the nose singularity, to be input if IZ1N is greater than 0.

Card 3 contains the variables NU and NL, which are the number of upper and lower surface coordinates to be input, respectively. This card has the format 2I5.

Cards 4 through the last contain the airfoil section coordinates, nondimensionalized with respect to chord. Eight values are listed on each line in format 8F10.0. Upper surface x-coordinates are all listed first, followed by upper surface y-coordinates, lower surface x-coordinates, and finally lower surface y-coordinates.

This then completes the input required to map the airfoil sections to the circle plane.

File 8 contains input parameters which are used to compute droplet impingement values for the airfoil. The same File 8 input data is used for each input radial location.

Card 1 of file 8 contains the title for that particular radial location, and would typically read similarly to "30% STATION TRAJECTORY INPUT." This title is printed at the beginning of the droplet trajectory section at each radial location.

Card 2 contains the variables IPRINT, MSPL, XFIRST, XLAST, and EPS.

IPRINT is a print option, with a value of 0 used for the shortened version of the trajectory summary output, and a value of 1 producing the complete printed output. The shortened version will print only the general input to the trajectory section, the tangent trajectories, and the impingement efficiencies. The trajectory tabulation and summary and surface impingement values are not printed when IPRINT equals 0.

MSPL is a variable which is used to select the method desired to calculate the impingement efficiency curve. Setting MSPL equal to 0 requests the program to select the best of three methods possible for calculating the curve. An MSPL value of 1 causes the program to use a simple cubic spline routine to calculate the curve. An MSPL value of 2 instructs the program to use a cubic spline but to piece in a linear fit where the cubic spline fails. An MSPL value of 3 causes a quadratic spline to be used, in which the coefficients are selected to optimize the fit of the curve. Setting MSPL equal to 0 has always produced satisfactory results in all cases run for this investigation.

XFIRST is the x-coordinate after which each step is checked for droplet impingement on the airfoil. A value of -0.05 is typically used for XFIRST.

XLAST is the x-coordinate at which droplet trajectory calculations are terminated. This value typically ranges from 0.5 to 1.0, and if the user lacks a good feel for the impingement characteristics to be expected for a given case, a value of 1.0 should be used for XLAST to ensure that no trajectories are terminated prematurely.

EPS is the maximum error allowed in the step integration process. A value of $1.\mathrm{x}10^{-5}$ is generally used for EPS.

Card 3 contains the variables XO, UDO, YO, VDO, and FR, in format 5F10.5.

XO is the initial droplet x-coordinate. This is the x-value of the point at which the trajectory investigation is begun, and it is typically given a value of -5.0, representing a starting point five chord lengths in front of the airfoil.

UDO is the initial droplet x-velocity with respect to freestream, and is commonly set equal to 1.

YO is the initial droplet y-coordinate. This is the starting point for the first trajectory calculation only, and its value will depend on the section angle of attack. For a positive angle of attack, it is suggested that to maximize the chance of initial droplet impingement a slightly negative value of YO be used, perhaps approximately -0.05.

VDO is the initial droplet y-velocity with respect to freestream, and is generally equal to 0 in the undisturbed flowfield five or more chordlengths in front of the airfoil.

FR represents Froude number. This parameter may be set equal to 0 to ignore the force of gravity on the droplet trajectories, and this is commonly done.

Card 4 contains four variables, DYO, CON, ERRY, and HGT, in the format 4F10.6.

DYO is the increment in YO used by the program to vary the beginning droplet y-coordinate. Values of DYO are commonly on the order of .001 to .01. The code has been set up to assign a value for DYO if the user inputs a value of 0 for this parameter. The internally assigned value will change with section angle of attack. If the user inputs a DYO value however, this value will be used regardless of the section angle of attack. When internally assigned, DYO is given a value of 0.003 for section angles of attack less than or equal to 4.6 degrees and is set equal to 0.005 for section angles of attack greater than 4.6 degrees.

CON is a multiplication constant for the impingement efficiency curve output. It is generally set equal to 1.

ERRY is the maximum error acceptable in total collection efficiency. A value of 2 (in percent) has commonly been used.

HGT is a reference height in the y-direction used to compute total collection efficiency. If this parameter is set equal to 0 the code will calculate and use for HGT the projected height of the airfoil section.

This then completes the droplet trajectory section input.

Files 12 through 15 contain binary flowfield information which is output by the flowfield computation section of the code when airfoil coordinates (files 1 through 4) are input. Since this flowfield information is independent of angle of attack and velocity, it is necessary to run the code with airfoil coordinates input only once for a particular geometry. In subsequent runs using the same geometry, the flowfield information calculated and stored in the initial run is read and used by the code, thereby eliminating the need for recalculation of propeller flowfield information in each run. The user must only set up the computer job control language (JCL) appropriately to exercise this option. For example, in the initial run of a particular geometry, units 12 through 15 must be set up to have the binary flowfield data written to them. In subsequent runs these files must be established as existing data files from which data is to be read. When previously computed airfoil flowfield information is used, it is not necessary to input airfoil coordinates, and the flowfield calculation section of the code will be bypassed.

File 16 contains input data for the propeller performance calculations. This file contains data for the entire propeller, so no duplicate files are required for different radial locations. Data for a maximum of 15 radial locations may be input.

Card 1 of this file contains the flight and atmospheric variables VO, TO, DD, W, TAUM, and ALTUDE in format 6F10.4.

VO is the freestream velocity in miles per hour.

TO is the freestream temperature in degrees Fahrenheit.

DD represents the volume mean droplet diameter of the icing cloud in microns.

W is cloud liquid water content in grams per cubic meter.

TAUM is the icing exposure time in minutes.

Finally, ALTUDE is the pressure altitude in feet at which the icing encounter occurred.

Card 2 contains the variables NUMBLD, NUMSTA, INCOMP and NUMADV in format 4I5.

NUMBLD represents the number of propeller blades.

NUMSTA is the number of radial locations to be input by the user (maximum is 15.)

INCOMP is a compressibility check flag which provides the user with the option of obtaining either a compressible or incompressible solution. If set equal to 0, a compressible solution is obtained and if set equal to 1, an incompressible solution is computed. Recall however that the flowfield around the various propeller sections was computed using a method which assumes imcompressible flow.

NUMADV is the number of advance ratios to be input. Set equal to 0 if advance ratio is to be calculated using input RPM and freestream velocity. NUMADV may have a maximum value of 10.

Card 3 contains the variables RADHUB, BLSET, RPM, CPDESI, DESIHP, and DIVIS in format 6F10.5.

RADHUB is the propeller hub radius in feet.

BLDSET represents the propeller blade setting in degrees. If either CPDESI or DESIHP are assigned values other than 0, the program will derive a BLDSET value based upon these input parameters.

RPM is the number of propeller revolutions per minute. If specified, RPM will be held constant. Otherwise RPM will be calculated based on the input freestream velocity and advance ratio. Either RPM or advance ratio must be specified in the input.

CPDESI is the design power coefficient. If set equal to 0, power coefficient will be calculated based upon the input value of BLDSET.

DESIHP is the design horsepower, and if it is input as 0, a value for DESIHP will be calculated based on the input BLDSET value.

DIVIS is a convergence aid variable for the design mode in which a BLDSET value must be computed. It is generally assigned a value between .001 and 1. When BLDSET is specified, the DIVIS variable is not employed.

Card 4 contains the variables CORTIP, RADIUS, STUBLT, CDINT, and CORHUB in format 5F10.5.

CORTIP is the propeller tip chord in feet.

RADIUS is the propeller radius in feet.

STUBLT is the propeller stub length in feet.

CDINT is a blade shank correction factor which takes into account interference from the blade shank. If a value for CDINT is unknown, a value of 0.567 should be used.

CORHUB represents the propeller hub chord in feet.

Card 5 is a title card which denotes the variables on the card to follow exactly as shown in the code input comments:

R/RAD= BLDANG= CHORD= T/C= ALPHAO= CLD=
VDIS= RC=

Cards 6 through NUMSTA contain values for these variables, in format 8F10.6.

XPR is the nondimensional radial location to be input.

BLDANG is the propeller blade angle in degrees of this section. Generally this is just the twist distribution built into the propeller.

CHORD is the propeller section chord in feet.

TC is the section thickness to chord ratio.

ALO is the angle of attack for zero lift, in degrees, referenced to the longest chordline.

CLD is the section design lift coefficient.

VDIS represents the velocity distribution seen by the section, taking into account nacelle effects. This parameter equals the local velocity divided by that of freestream.

Finally RC is the section leading edge radius of curvature, nondimensional with respect to section chord.

The final card(s), in format F10.6, with one value per card, are ADVRAT values.

ADVRAT is the propeller advance ratio, and as many as 10 values of ADVRAT may be input by the user, with performance calculations performed by the code for each advance ratio. If NUMADV is set equal to 0, such that advance ratio is to be calculated by the code given RPM and freestream velocity, no ADVRAT values should be input.

This completes the propeller performance section input.

File 17 contains input for options available to the user, including choice of aerodynamic coefficient correlation to be used as well as print options.

Card 1 is the title card for the run. This title is printed at the beginning of each section of calculations within the program and so should be general in nature, such as, "ENCOUNTER 2 FROM NEEL AND BRIGHT REPORT."

Card 2 contains the variables NCD, RADEXT, IREAD, IPRCOR, and NSECT in format I5,F10.5,3I5.

NCD is the aerodynamic coefficient correlation selector. A value of 1 for NCD calls for the use of Bragg's rime ice ΔC_d correlation. A value of 2 calls for the use of Gray's glaze ice ΔC_d correlation. A value of 3 calls for the use of Flemming's ΔC_l and ΔC_d correlations for rime and glaze ice.

RADEXT is the fractional radial extent of icing.

IREAD is a flag which determines whether or not the code will calculate the flowfield at the input radial locations. The option is to use previously calculated and stored flowfield data. For each radial location input, the code will write the flowfield information to a file if it has not been computed in a previous run. Set IREAD equal to 0 to calculate the flowfield, or set it equal to 1 to use the previously computed data. The user must also be sure that the corresponding JCL for each of these files is set up correctly, i.e., if IREAD equals 0 the JCL must be write-oriented, and if IREAD equals 1 the JCL for these files must be read-oriented.

IPRCOR is a flag which indicates whether or not the user wishes to have the airfoil coordinates at each of the four input radial locations printed. An IPRCOR value of 0 instructs the code to not print the coordinates, and an IPRCOR value of 1 causes the coordinates to be printed.

NSECT is a variable which indicates the number of radial locations to be input, with a maximum of four possible.

Cards 3 through 7 contains values for the variable RSTA in format F10.5.

RSTA is the nondimensional radial location at which flowfield calculations are to be performed. A maximum of four radial locations may be input. These radial locations must for the current version of the code be the same as any four of the radial locations input in the propeller performance section.

It may be shown that the curves of total and maximum local collection efficiencies are relatively smooth functions of radial location, so that four points should provide a reasonable representation of the variance of these impingement efficiencies with radial location. However, it is obvious that the fewer points one uses to fit these curves, the less accurate they will tend to be. It is recommended therefore that whenever possible, no less than the maximum of four stations should be input to maximize the available accuracy in the impingement efficiency calculations, which then affect the propeller performance computations for the iced configuration.

This then completes the required input to the code.

APPENDIX 3

SAMPLE CASE

The following output was produced for Encounter 2 at an advance ratio of 1.18. The iced calculations were performed using Bragg's older, modified correlation. This same format is output regardless of the user's choice of correlation. Use of the Bragg or Gray correlations will generate output similar in appearance to that shown here. When the Flemming correlations are used, no flowfield or droplet trajectory information is printed out.

The code requires approximately 570K of computer memory. Typical run times are roughly five minutes (CPU time) on an IBM 370 and 33 seconds on a CRAY-1S for one advance ratio using either the Bragg or Gray correlations. Use of the Flemming correlations significantly reduces run time because the flowfield and droplet trajectory calculation sections of the code are bypassed, resulting in typical run times for the Flemming runs of 8.4 seconds on the IBM 370 and 0.57 seconds on the CRAY-1S.

FILE 1 INPUT:

```
CLARK-Y COORDINATES, R/R=0.3
  59    0     0
  57   57
0.000000  0.000250  0.000500  0.000750  0.001000  0.001500  0.002000  0.002500
0.005000  0.010000  0.020000  0.030000  0.040000  0.050000  0.060000  0.070000
0.080000  0.090000  0.100000  0.125000  0.150000  0.175000  0.200000  0.225000
0.250000  0.275000  0.300000  0.325000  0.350000  0.375000  0.400000  0.425000
0.450000  0.475000  0.500000  0.525000  0.550000  0.575000  0.600000  0.625000
0.650000  0.675000  0.700000  0.725000  0.750000  0.775000  0.800000  0.825000
0.850000  0.875000  0.900000  0.925000  0.950000  0.970000  0.980000  0.990000
1.000000
0.001272  0.007136  0.009638  0.011586  0.013246  0.016067  0.018478  0.020627
0.029260  0.041940  0.060551  0.075131  0.087442  0.098169  0.107680  0.116229
0.123990  0.131069  0.137533  0.151363  0.162497  0.171463  0.178600  0.184143
0.188290  0.191189  0.192951  0.193672  0.193475  0.192473  0.190762  0.188433
0.185617  0.182448  0.179053  0.175523  0.171806  0.167809  0.163432  0.158580
0.153227  0.147360  0.140962  0.134007  0.126443  0.118201  0.109199  0.099345
0.088564  0.076780  0.063909  0.049868  0.034591  0.021461  0.014597  0.007544
0.000315
0.000000  0.000250  0.000500  0.000750  0.001000  0.001500  0.002000  0.002500
0.005000  0.010000  0.020000  0.030000  0.040000  0.050000  0.060000  0.070000
0.080000  0.090000  0.100000  0.125000  0.150000  0.175000  0.200000  0.225000
0.250000  0.275000  0.300000  0.325000  0.350000  0.375000  0.400000  0.425000
0.450000  0.475000  0.500000  0.525000  0.550000  0.575000  0.600000  0.625000
0.650000  0.675000  0.700000  0.725000  0.750000  0.775000  0.800000  0.825000
0.850000  0.875000  0.900000  0.925000  0.950000  0.970000  0.980000  0.990000
1.000000
 0.000000 -0.004326 -0.006566 -0.008255 -0.009658 -0.001970 -0.013878 -0.015529
-0.021733 -0.029779 -0.039746 -0.046309 -0.051161 -0.054975 -0.058087 -0.060673
-0.062842 -0.064683 -0.066269 -0.069416 -0.071678 -0.073275 -0.074348 -0.074994
-0.075285 -0.075273 -0.074999 -0.074496 -0.073794 -0.072921 -0.071898 -0.070747
-0.069492 -0.068158 -0.066768 -0.065338 -0.063856 -0.062303 -0.060656 -0.058893
-0.057005 -0.054983 -0.052817 -0.050492 -0.047984 -0.045260 -0.042280 -0.038996
-0.035354 -0.031285 -0.026701 -0.021487 -0.015489 -0.009987 -0.006954 -0.003702
-0.000218
```

Note: Format of files 2-4 identical to format of file 1. Files 2-4 will contain coordinates for additional input radial stations.

```
FILE 8 INPUT:

DROPLET TRAJECTORY INPUT
  1    0  -0.05    1.00      0.10D-05
 -5.        1.     -0.10     0.         0.
 0.0        1.       2.      0.


FILE 16 INPUT:

  ENCOUNTER 2 PERFORMANCE INPUT
      0.0       1.0      18.0       0.41       10.0     10000.
    4   11     0    1
   0.5015     13.05    1025.0       0.0        0.0        1.0
   0.2460      6.75       0.2     0.567      0.513
 R/RAD=    BLDANG=   CHORD=      T/C=    ALPHA0=        CLD=      VDIS=       R/C=
     .200       52.9      .513    .6175     -3.998        .790      .8550     0.0803
     .250       47.2      .675    .3900     -3.790        .742      .8975     0.0507
     .300       41.7      .775    .2790     -3.513        .693      .9250     0.0363
     .400       32.8      .902    .1715     -3.167        .608      .9500     0.0223
     .500       27.0      .929    .1250     -2.720        .525      .9650     0.0163
     .600       23.2      .878    .0975     -2.318        .448      .9775     0.0127
     .700       20.3      .772    .0798     -2.035        .382      .9890     0.0104
     .800       17.8      .632    .0725     -1.810        .342      .9985     0.0094
     .900       16.6      .528    .0710     -1.721        .330      .9993     0.0092
     .950       15.9      .398    .0695     -1.714        .326      .9995     0.0090
     .975       15.7      .246    .0676     -1.699        .321      .9999     0.0088
 0.90


FILE 17 INPUT:

NEEL & BRIGHT DATA, BRAGG CORRELATION
    1    0.7        1     0     4
       .001      250.
        0.3
        0.5
        0.7
        0.9
```

```
                         *** ICEPERF ***
               PROPELLER ICING ANALYSIS PROGRAM
                       BY T. L. MILLER
        TEXAS A&M UNIVERSITY & SVERDRUP TECHNOLOGY, INC.
                     LAST UPDATE  2/18/86

NEEL & BRIGHT DATA, BRAGG CORRELATION

ATMOSPHERIC AND FLIGHT CONDITIONS:

FREESTREAM VELOCITY=   0.00 MPH    TEMPERATURE=  1.00 DEG. F   DROPLET DIAMETER= 18.00 MICRONS
LIQUID WATER CONTENT=  0.41 G/M3      ICING TIME= 10.00 MIN.   PRESSURE ALTITUDE=10000.00 FT.
RADIAL ICING EXTENT=  0.70
```

PROPELLER PERFORMANCE AND DESIGN SECTION

* * * STRIP ANALYSIS METHOD * * *

ADVANCE RATIO=0.900

PROPELLER CHARACTERISTICS :

NUMBER OF BLADES	= 4
RADIUS OF PROPELLER	= 6.7500 (FEET)
RADIUS OF HUB	= 0.5015 (FEET)
NUMBER OF SECTIONS	= 11
CHORD AT PROPELLER TIP	= 0.2460 (FEET)

PROPELLER SECTION CHARACTERISTICS :

R/RAD=	BLDANG=	CHORD=	T/C=	ALPHA0=	CLD=	VDIS=	R/C=
0.2000	52.900	0.5130	0.6175	-3.998	0.7900	0.85500	0.0803
0.2500	47.200	0.6750	0.3900	-3.790	0.7420	0.89750	0.0507
0.3000	41.700	0.7750	0.2790	-3.513	0.6930	0.92500	0.0363
0.4000	32.800	0.9020	0.1715	-3.167	0.6080	0.95000	0.0223
0.5000	27.000	0.9290	0.1250	-2.720	0.5250	0.96500	0.0163
0.6000	23.200	0.8780	0.0975	-2.318	0.4480	0.97750	0.0127
0.7000	20.300	0.7720	0.0798	-2.035	0.3820	0.98900	0.0104
0.8000	17.800	0.6320	0.0725	-1.810	0.3420	0.99850	0.0094
0.9000	16.600	0.5280	0.0710	-1.721	0.3300	0.99930	0.0092
0.9500	15.900	0.3980	0.0695	-1.714	0.3260	0.99950	0.0090
0.9750	15.700	0.2460	0.0676	-1.699	0.3210	0.99990	0.0088

PROPELLER OPERATION CHARACTERISTICS :

FREE STREAM VELOCITY	= 207.5625 (FT/SEC)
FREE STREAM MACH NO.	= 0.19695
ALTITUDE FOR OPERATION	= 10000.000 (FEET)
PRESSURE AT ALTITUDE	= 1135.8375 (LB/FT**2)
TEMPERATURE AT ALTITUDE	= 461.000 (RANKINE)
DENSITY AT ALTITUDE	= 0.0014352 (LB*SEC**2/FT**4)
REQUIRED BLADE SETTING	= 13.050 (DEGREES)
REQUIRED HORSEPOWER	= 0.000
REQUIRED POWER COEFF.	= 0.000000

NOTE: IF ANY CHARACTERISTICS =0.0 ,THEN NOT SPECIFIED

PROPELLER PERFORMANCE CHARACTERISTICS :

R/RAD=	BETA=	PHI=	THETA=	ALPHA=	MACH=	REYN=
0.2000	65.950	50.767	4.288	10.895	0.21678	0.506
0.2500	60.250	45.804	5.161	9.285	0.24554	0.755
0.3000	54.750	41.454	5.360	7.935	0.27397	0.967
0.4000	45.850	34.231	5.252	6.367	0.33121	1.360
0.5000	40.050	28.938	4.977	6.135	0.39130	1.655
0.6000	36.250	25.019	4.850	6.381	0.45356	1.813
0.7000	33.350	22.036	4.817	6.497	0.51732	1.818
0.8000	30.850	19.675	4.584	6.590	0.58221	1.675
0.9000	29.650	17.645	4.846	7.159	0.64695	1.555
0.9500	28.950	16.773	5.210	6.967	0.67930	1.231
0.9750	28.750	16.372	5.738	6.640	0.69511	0.779

R/RAD=	VELI=	DELCT=	DELCQ=	CL=	CD=	CL/CD=
0.2000	17.129	0.01619	0.00402	1.1324	0.26156	4.329
0.2500	23.374	0.04346	0.00706	1.1322	0.02915	38.843
0.3000	27.092	0.06536	0.01090	1.0858	0.02292	47.371
0.4000	32.086	0.11656	0.01992	1.0015	0.01795	55.808
0.5000	35.911	0.17851	0.03138	0.9916	0.02077	47.750
0.6000	40.560	0.24532	0.04540	1.0311	0.03239	31.837
0.7000	45.950	0.29861	0.05920	1.0727	0.05014	21.393
0.8000	49.201	0.33154	0.07020	1.1297	0.07178	15.738
0.9000	57.810	0.39267	0.09551	1.2988	0.13426	9.674
0.9500	65.276	0.33629	0.08583	1.3358	0.14672	9.104
0.9750	73.606	0.21505	0.05573	1.3176	0.13584	9.700

PROPELLER PERFORMANCE OUTPUT :

PROPELLER ADVANCE RATIO	= 0.9000
PROPELLER R.P.M.	= 1025.000
TOTAL ACTIVITY FACTOR	= 275.820
BLADE ACTIVITY FACTOR	= 68.955
PROPELLER THRUST	= 2425.295 (LB)
PROPELLER TORQUE	= 6798.610 (FT*LB)
HORSEPOWER ABSORBED	= 1326.815
THRUST COEFFICIENT	= 0.17433
TORQUE COEFFICIENT	= 0.03620
POWER COEFFICIENT	= 0.22745
PROPELLER EFFICIENCY	= 0.68983
THRUST COEF. WITH CORRECTION	= 0.17381
POWER COEF. WITH CORRECTION	= 0.22746
PROP. EFF. WITH CORRECTION	= 0.68770

NOTE: ABOVE VALUES ARE FOR CLEAN CONFIGURATION

```
                                   *** ICEPERF ***
                         PROPELLER ICING ANALYSIS PROGRAM
                                  BY T. L. MILLER
                 TEXAS A&M UNIVERSITY & SVERDRUP TECHNOLOGY, INC.
                              LAST UPDATE  2/18/86

NEEL & BRIGHT DATA, BRAGG CORRELATION

 ADVANCE RATIO=0.900
 CLARK-Y COORDINATES, R/R=0.3

 CH,TAU,KAPA:          1.00000046      55.07143994       1.69404756
 XZ1T,YZ1T,XZ1N,YZ1N:          1.00000000      0.00031500       0.03288917       0.00133850
 XS1,YS1:         0.28544382      -0.00030209
 CENTROID: XZC,YZC:       -0.04789031       0.03876070
 R,PHIT:         0.31199614      -6.00207092
 EPSO (ANGLE OF ZERO-LIFT LINE) =      6.00207092 (DEG.)
 CL =       2.49596794 * PI * SIN(ALPHA + EPSO)

 FOURIER COEFFICIENTS C(J)=(A(J)+I * B(J)),J=1,LPT, LPT =  59

  (   0.00559617   -0.00045703)  (   0.00617019   -0.00186539)  (  -0.00014051   -0.00015992)
  (  -0.00004958    0.00009430)  (  -0.00000013   -0.00002260)  (  -0.00000165    0.00000234)
  (   0.00000058   -0.00000045)  (  -0.00000018    0.00000009)  (   0.00000002   -0.00000001)
  (  -0.00000001   -0.00000006)  (   0.00000000    0.00000000)  (  -0.00000000    0.00000000)
  (  -0.00000000    0.00000000)  (  -0.00000000   -0.00000000)  (   0.00000000    0.00000000)
  (  -0.00000000    0.00000000)  (  -0.00000000    0.00000000)  (  -0.00000000    0.00000000)
  (   0.00000000    0.00000000)  (  -0.00000000    0.00000000)  (   0.00000000    0.00000000)
  (  -0.00000000    0.00000000)  (   0.00000000    0.00000000)  (   0.00000000    0.00000000)
  (   0.00000000    0.00000000)  (   0.00000000    0.00000000)  (   0.00000000    0.00000000)
  (   0.00000000    0.00000000)  (   0.00000000    0.00000000)  (   0.00000000   -0.00000000)
  (   0.00000000   -0.00000000)  (   0.00000000   -0.00000000)  (   0.00000000   -0.00000000)
  (   0.00000000   -0.00000000)  (  -0.00000000   -0.00000000)  (   0.00000000   -0.00000000)
  (  -0.00000000   -0.00000000)  (   0.00000000    0.00000000)  (  -0.00000000   -0.00000000)
  (  -0.00000000    0.00000000)  (  -0.00000000   -0.00000000)  (  -0.00000000    0.00000000)
  (  -0.00000000   -0.00000000)  (  -0.00000000    0.00000000)  (   0.00000000   -0.00000000)
  (  -0.00000000    0.00000000)  (   0.00000000   -0.00000000)  (  -0.00000000    0.00000000)
  (   0.00000000   -0.00000000)  (  -0.00000000    0.00000000)  (   0.00000000   -0.00000000)
  (  -0.00000000   -0.00000000)  (   0.00000000    0.00000000)  (  -0.00000000   -0.00000000)
  (   0.00000000    0.00000000)  (  -0.00000000   -0.00000000)  (  -0.00000000    0.00000000)
  (  -0.00000000   -0.00000000)  (  -0.00000000    0.00000000)  (
```

```
                                   *** ICEPERF ***
                          PROPELLER ICING ANALYSIS PROGRAM
                                BY T. L. MILLER
                  TEXAS A&M UNIVERSITY & SVERDRUP TECHNOLOGY, INC.
                             LAST UPDATE  2/18/86

NEEL & BRIGHT DATA, BRAGG CORRELATION
R/R= 0.30

 ADVANCE RATIO=0.900


TRAJECTORY CALCULATION GENERAL INPUT:
  DROPLET TRAJECTORY INPUT
IPRINT= 1              MSPL= 0                XFIRST= -0.050000      XLAST=  1.000000
EPS= 0.100D-05         ALPHA= 7.94
X0=  -5.00000          UD0=   1.00000         Y0=  -0.10000          VD0=   0.00000
RU=  72.59059          AK=   0.41660          FR=   0.00000
DY0=  0.005000         CON=  1.000000         ERRY=  2.000000        HGT=  0.000000

RUN        X0             Y0              XF           YF           UDF          VDF          TF           THF
  1 -0.500000D 01 -0.100000D 00    PARTICLE PASSES BODY
  1 -0.500000D 01 -0.110000D 00    PARTICLE PASSES BODY
  1 -0.500000D 01 -0.120000D 00    PARTICLE PASSES BODY
  1 -0.500000D 01 -0.130000D 00    PARTICLE PASSES BODY
  1 -0.500000D 01 -0.140000D 00    PARTICLE PASSES BODY
  1 -0.500000D 01 -0.150000D 00    PARTICLE PASSES BODY
  1 -0.500000D 01 -0.160000D 00    PARTICLE PASSES BODY
  1 -0.500000D 01 -0.170000D 00    PARTICLE PASSES BODY
  1 -0.500000D 01 -0.180000D 00    PARTICLE PASSES BODY
  1 -0.500000D 01 -0.190000D 00    PARTICLE PASSES BODY
  1 -0.500000D 01 -0.200000D 00    PARTICLE PASSES BODY
  1 -0.500000D 01 -0.210000D 00    PARTICLE PASSES BODY
  1 -0.500000D 01 -0.220000D 00    PARTICLE PASSES BODY
  1 -0.500000D 01 -0.230000D 00    PARTICLE PASSES BODY
  1 -0.500000D 01 -0.240000D 00    PARTICLE PASSES BODY
  1 -0.500000D 01 -0.250000D 00    PARTICLE PASSES BODY
  1 -0.500000D 01 -0.260000D 00    PARTICLE PASSES BODY
  1 -0.500000D 01 -0.270000D 00    PARTICLE PASSES BODY
  1 -0.500000D 01 -0.280000D 00    PARTICLE PASSES BODY
  1 -0.500000D 01 -0.290000D 00    PARTICLE PASSES BODY
```

```
 1 -0.500000D 01 -0.300000D 00    PARTICLE PASSES BODY
 1 -0.500000D 01 -0.310000D 00    PARTICLE PASSES BODY
 1 -0.500000D 01 -0.320000D 00    PARTICLE PASSES BODY
 1 -0.500000D 01 -0.330000D 00  0.120252D-01  0.342223D-01  0.643150D 00  0.598574D 00  0.514319D 01  0.314691D 00  0.352150
 2 -0.500000D 01 -0.325000D 00  0.218180D-01  0.494295D-01  0.694866D 00  0.663553D 00  0.515379D 01  0.178095D 00  0.532974
 3 -0.500000D 01 -0.320000D 00    PARTICLE PASSES BODY
 4 -0.500000D 01 -0.335000D 00  0.623667D-02  0.223435D-01  0.607062D 00  0.544637D 00  0.513738D 01  0.444232D 00  0.219988
 5 -0.500000D 01 -0.340000D 00  0.252468D-02  0.120048D-01  0.580040D 00  0.493547D 00  0.513400D 01  0.593563D 00  0.110086
 6 -0.500000D 01 -0.345000D 00  0.406250D-03  0.278862D-02  0.560370D 00  0.445239D 00  0.513257D 01  0.747179D 00  0.154613
 7 -0.500000D 01 -0.350000D 00 -0.392564D-03 -0.561155D-02  0.546291D 00  0.399196D 00  0.513283D 01  0.921640D 00 -0.689862
 8 -0.500000D 01 -0.355000D 00  0.152572D-03 -0.132629D-01  0.535236D 00  0.356017D 00  0.513495D 01  0.881111D 00 -0.301733
 9 -0.500000D 01 -0.360000D 00  0.142342D-02 -0.206477D-01  0.531670D 00  0.312942D 00  0.513787D 01  0.131501D 01 -0.377028
10 -0.500000D 01 -0.365000D 00  0.389112D-02 -0.275296D-01  0.530434D 00  0.272538D 00  0.514253D 01  0.152044D 01 -0.450103
11 -0.500000D 01 -0.370000D 00  0.756452D-02 -0.340306D-01  0.531951D 00  0.234017D 00  0.514892D 01  0.170293D 01 -0.524468
12 -0.500000D 01 -0.375000D 00  0.123109D-01 -0.403069D-01  0.537530D 00  0.198029D 00  0.515679D 01  0.199432D 01 -0.603329
13 -0.500000D 01 -0.380000D 00  0.185491D-01 -0.463010D-01  0.544363D 00  0.163518D 00  0.516688D 01  0.212094D 01 -0.689070
14 -0.500000D 01 -0.385000D 00  0.262342D-01 -0.521608D-01  0.553849D 00  0.131146D 00  0.517904D 01  0.228734D 01 -0.785556
15 -0.500000D 01 -0.390000D 00  0.355471D-01 -0.579602D-01  0.565768D 00  0.101013D 00  0.519349D 01  0.244261D 01 -0.895254
16 -0.500000D 01 -0.395000D 00  0.468023D-01 -0.637380D-01  0.579423D 00  0.730697D-01  0.521066D 01  0.258524D 01 -0.102178
17 -0.500000D 01 -0.400000D 00  0.605195D-01 -0.695886D-01  0.594981D 00  0.467310D-01  0.523127D 01  0.269357D 01 -0.117093
18 -0.500000D 01 -0.405000D 00  0.774070D-01 -0.755935D-01  0.612353D 00  0.217144D-01  0.525627D 01  0.279269D 01 -0.135018
19 -0.500000D 01 -0.410000D 00  0.985654D-01 -0.819193D-01  0.632155D 00 -0.209964D-02  0.528709D 01  0.287737D 01 -0.157103
20 -0.500000D 01 -0.415000D 00  0.125754D 00 -0.888062D-01  0.655118D 00 -0.245265D-01  0.532596D 01  0.294651D 01 -0.185151
21 -0.500000D 01 -0.420000D 00  0.163213D 00 -0.967340D-01  0.682837D 00 -0.457049D-01  0.537841D 01  0.301848D 01 -0.223442
22 -0.500000D 01 -0.425000D 00  0.223893D 00 -0.107108D 00  0.720056D 00 -0.661645D-01  0.546120D 01  0.308162D 01 -0.285006
23 -0.500000D 01 -0.430000D 00    PARTICLE PASSES BODY
 1 -0.500000D 01 -0.427374D 00  0.284342D 00 -0.115397D 00  0.750325D 00 -0.769022D-01  0.554158D 01  0.312061D 01 -0.346023
 2 -0.500000D 01 -0.428013D 00    PARTICLE PASSES BODY
 1 -0.500000D 01 -0.321740D 00    PARTICLE PASSES BODY
 1 -0.500000D 01 -0.323370D 00  0.284491D-01  0.575564D-01  0.724290D 00  0.699940D 00  0.516167D 01  0.116724D 00  0.637638
```

TRAJECTORY SUMMARY

SF	YO
-0.358337D 00	-0.427694D 00
-0.285006D 00	-0.425000D 00
-0.223442D 00	-0.420000D 00
-0.185151D 00	-0.415000D 00
-0.157103D 00	-0.410000D 00
-0.135018D 00	-0.405000D 00
-0.117093D 00	-0.400000D 00
-0.102178D 00	-0.395000D 00
-0.895254D-01	-0.390000D 00
-0.785556D-01	-0.385000D 00
-0.689070D-01	-0.380000D 00
-0.603329D-01	-0.375000D 00
-0.524468D-01	-0.370000D 00
-0.450103D-01	-0.365000D 00
-0.377028D-01	-0.360000D 00
-0.301733D-01	-0.355000D 00
-0.689862D-02	-0.350000D 00
0.154613D-02	-0.345000D 00
0.110086D-01	-0.340000D 00
0.219988D-01	-0.335000D 00
0.352150D-01	-0.330000D 00
0.532974D-01	-0.325000D 00
0.836704D-01	-0.322555D 00

TANGENT TRAJECTORIES:

YO(UPPER)=-0.322555D 00   SF(UPPER)= 0.836704D-01

YO(LOWER)=-0.427694D 00   SF(LOWER)=-0.358337D 00

YO(UPPER) -YO(LOWER)= 0.105139D 00

AIRFOIL PROJECTED HEIGHT= 0.304492D 00

COLLECTION EFFICIENCY, E= 0.345291D 00

MAXIMUM ERROR IN E =   0.107891D 01 PERCENT

MAXIMUM IMPINGEMENT= 0.724981D 00

YO(MAX)=-0.359074D 00   SF(MAX)=-0.364195D-01

SURFACE IMPINGEMENT VALUES

YO	S	DYODS	CON*DYODS
-0.427694D 00	-0.358337D 00	0.000000	0.000000
-0.427487D 00	-0.340004D 00	0.219049D-01	0.219049D-01
-0.426917D 00	-0.321672D 00	0.395663D-01	0.395663D-01
-0.426062D 00	-0.303339D 00	0.529842D-01	0.529842D-01
-0.425000D 00	-0.285006D 00	0.621585D-01	0.621585D-01
-0.423627D 00	-0.264485D 00	0.724582D-01	0.724582D-01
-0.421993D 00	-0.243964D 00	0.875683D-01	0.875683D-01
-0.420000D 00	-0.223442D 00	0.107489D 00	0.107489D 00
-0.418536D 00	-0.210679D 00	0.122128D 00	0.122128D 00
-0.416876D 00	-0.197915D 00	0.138277D 00	0.138277D 00
-0.415000D 00	-0.185151D 00	0.155933D 00	0.155933D 00
-0.413477D 00	-0.175802D 00	0.170120D 00	0.170120D 00
-0.411815D 00	-0.166453D 00	0.185710D 00	0.185710D 00
-0.410000D 00	-0.157103D 00	0.202702D 00	0.202702D 00
-0.408454D 00	-0.149742D 00	0.217566D 00	0.217566D 00
-0.406792D 00	-0.142380D 00	0.234294D 00	0.234294D 00
-0.405000D 00	-0.135018D 00	0.252884D 00	0.252884D 00
-0.403440D 00	-0.129043D 00	0.269491D 00	0.269491D 00
-0.401776D 00	-0.123068D 00	0.287621D 00	0.287621D 00
-0.400000D 00	-0.117093D 00	0.307275D 00	0.307275D 00
-0.398429D 00	-0.112121D 00	0.325090D 00	0.325090D 00
-0.396765D 00	-0.107150D 00	0.344561D 00	0.344561D 00
-0.395000D 00	-0.102178D 00	0.365688D 00	0.365688D 00
-0.393821D 00	-0.990149D-01	0.379947D 00	0.379947D 00
-0.392596D 00	-0.958518D-01	0.394787D 00	0.394787D 00
-0.391323D 00	-0.926886D-01	0.410207D 00	0.410207D 00
-0.390000D 00	-0.895254D-01	0.426207D 00	0.426207D 00
-0.388811D 00	-0.867830D-01	0.440582D 00	0.440582D 00
-0.387583D 00	-0.840405D-01	0.455460D 00	0.455460D 00
-0.386313D 00	-0.812981D-01	0.470842D 00	0.470842D 00

-0.385000D 00	-0.785556D-01	0.486727D 00	0.486727D 00
-0.383808D 00	-0.761435D-01	0.501501D 00	0.501501D 00
-0.382580D 00	-0.737313D-01	0.517436D 00	0.517436D 00
-0.381311D 00	-0.713192D-01	0.534533D 00	0.534533D 00
-0.380000D 00	-0.689070D-01	0.552791D 00	0.552791D 00
-0.378389D 00	-0.660490D-01	0.574071D 00	0.574071D 00
-0.376720D 00	-0.631909D-01	0.593268D 00	0.593268D 00
-0.375000D 00	-0.603329D-01	0.610381D 00	0.610381D 00
-0.373376D 00	-0.577042D-01	0.625655D 00	0.625655D 00
-0.371710D 00	-0.550755D-01	0.641916D 00	0.641916D 00
-0.370000D 00	-0.524468D-01	0.659162D 00	0.659162D 00
-0.367513D 00	-0.487286D-01	0.675332D 00	0.675332D 00
-0.365000D 00	-0.450103D-01	0.673662D 00	0.673662D 00
-0.362538D 00	-0.413566D-01	0.678983D 00	0.678983D 00
-0.360000D 00	-0.377028D-01	0.715760D 00	0.715760D 00
-0.359613D 00	-0.371650D-01	0.721869D 00	0.721869D 00
-0.359224D 00	-0.366272D-01	0.724740D 00	0.724740D 00
-0.359074D 00	-0.364195D-01	0.724981D 00	0.724981D 00
-0.358834D 00	-0.360893D-01	0.724371D 00	0.724371D 00
-0.358445D 00	-0.355515D-01	0.720763D 00	0.720763D 00
-0.358060D 00	-0.350137D-01	0.713916D 00	0.713916D 00
-0.357678D 00	-0.344759D-01	0.703830D 00	0.703830D 00
-0.357303D 00	-0.339381D-01	0.690505D 00	0.690505D 00
-0.356936D 00	-0.334002D-01	0.673941D 00	0.673941D 00
-0.356579D 00	-0.328624D-01	0.654138D 00	0.654138D 00
-0.356233D 00	-0.323246D-01	0.631096D 00	0.631096D 00
-0.355900D 00	-0.317868D-01	0.604815D 00	0.604815D 00
-0.355583D 00	-0.312489D-01	0.575295D 00	0.575295D 00
-0.355282D 00	-0.307111D-01	0.542535D 00	0.542535D 00
-0.355000D 00	-0.301733D-01	0.506537D 00	0.506537D 00
-0.353047D 00	-0.243546D-01	0.197477D 00	0.197477D 00
-0.352322D 00	-0.185360D-01	0.842618D-01	0.842618D-01
-0.351686D 00	-0.127173D-01	0.166893D 00	0.166893D 00
-0.350000D 00	-0.689862D-02	0.445370D 00	0.445370D 00
-0.349640D 00	-0.613091D-02	0.491897D 00	0.491897D 00
-0.349246D 00	-0.536321D-02	0.532155D 00	0.532155D 00
-0.348824D 00	-0.459550D-02	0.566144D 00	0.566144D 00
-0.348379D 00	-0.382780D-02	0.593864D 00	0.593864D 00
-0.347914D 00	-0.306010D-02	0.615315D 00	0.615315D 00
-0.347435D 00	-0.229239D-02	0.630498D 00	0.630498D 00
-0.346948D 00	-0.152469D-02	0.639411D 00	0.639411D 00
-0.346455D 00	-0.756983D-03	0.642055D 00	0.642055D 00
-0.345963D 00	0.107212D-04	0.638430D 00	0.638430D 00
-0.345477D 00	0.778425D-03	0.628537D 00	0.628537D 00
-0.345000D 00	0.154613D-02	0.612374D 00	0.612374D 00
-0.344293D 00	0.272894D-02	0.584281D 00	0.584281D 00
-0.343616D 00	0.391175D-02	0.559465D 00	0.559465D 00
-0.342968D 00	0.509456D-02	0.537926D 00	0.537926D 00
-0.342343D 00	0.627737D-02	0.519664D 00	0.519664D 00
-0.341737D 00	0.746018D-02	0.504679D 00	0.504679D 00
-0.341147D 00	0.864299D-02	0.492970D 00	0.492970D 00
-0.340570D 00	0.982580D-02	0.484539D 00	0.484539D 00
-0.340000D 00	0.110086D-01	0.479384D 00	0.479384D 00
-0.338267D 00	0.146720D-01	0.465794D 00	0.465794D 00
-0.336594D 00	0.183354D-01	0.446805D 00	0.446805D 00
-0.335000D 00	0.219988D-01	0.422416D 00	0.422416D 00
-0.333909D 00	0.246421D-01	0.403444D 00	0.403444D 00
-0.332866D 00	0.272853D-01	0.385617D 00	0.385617D 00
-0.331869D 00	0.299285D-01	0.368935D 00	0.368935D 00
-0.330915D 00	0.325718D-01	0.353398D 00	0.353398D 00

-0.330000D 00	0.352150D-01	0.339006D 00	0.339006D 00
-0.329330D 00	0.372241D-01	0.327938D 00	0.327938D 00
-0.328683D 00	0.392333D-01	0.315742D 00	0.315742D 00
-0.328062D 00	0.412425D-01	0.302418D 00	0.302418D 00
-0.327468D 00	0.432516D-01	0.287966D 00	0.287966D 00
-0.326905D 00	0.452608D-01	0.272387D 00	0.272387D 00
-0.326375D 00	0.472700D-01	0.255680D 00	0.255680D 00
-0.325879D 00	0.492791D-01	0.237844D 00	0.237844D 00
-0.325420D 00	0.512883D-01	0.218882D 00	0.218882D 00
-0.325000D 00	0.532974D-01	0.198791D 00	0.198791D 00
-0.324563D 00	0.556338D-01	0.175444D 00	0.175444D 00
-0.324179D 00	0.579702D-01	0.153439D 00	0.153439D 00
-0.323845D 00	0.603066D-01	0.132777D 00	0.132777D 00
-0.323558D 00	0.626430D-01	0.113458D 00	0.113458D 00
-0.323314D 00	0.649793D-01	0.954808D-01	0.954808D-01
-0.323110D 00	0.673157D-01	0.788466D-01	0.788466D-01
-0.322944D 00	0.696521D-01	0.635550D-01	0.635550D-01
-0.322812D 00	0.719885D-01	0.496060D-01	0.496060D-01
-0.322711D 00	0.743249D-01	0.369996D-01	0.369996D-01
-0.322638D 00	0.766613D-01	0.257358D-01	0.257358D-01
-0.322590D 00	0.789976D-01	0.158146D-01	0.158146D-01
-0.322564D 00	0.813340D-01	0.723599D-02	0.723599D-02
-0.322555D 00	0.836704D-01	0.000000	0.000000

```
                              *** ICEPERF ***
                      PROPELLER ICING ANALYSIS PROGRAM
                             BY T. L. MILLER
            TEXAS A&M UNIVERSITY & SVERDRUP TECHNOLOGY, INC.
                          LAST UPDATE  2/18/86

NEEL & BRIGHT DATA, BRAGG CORRELATION

 ADVANCE RATIO=0.900
  CLARK-Y COORDINATES, R/R=0.5

 CH,TAU,KAPA:          1.00000008      27.85186919       1.84526739
 XZIT,YZIT,XZIN,YZIN:          1.00000000       0.00013400        0.00612858        0.00056825
 XSI,YSI:          0.26930282       -0.00011767
 CENTROID: XZC,YZC:         -0.01915888        0.01501550
 R,PHIT:          0.27684003       -2.28655759
 EPSO (ANGLE OF ZERO-LIFT LINE) =       2.28655759 (DEG.)
 CL =        2.21472008 * PI * SIN(ALPHA + EPSO)

 FOURIER COEFFICIENTS C(J)=(A(J)+I * B(J)),J=1,LPT, LPT =  59

  (    0.00400902    -0.00035540)  (    0.00305262    -0.00090512)  (   -0.00012852    -0.00000548)
  (    0.00000165     0.00000115)  (   -0.00000476    -0.00000421)  (   -0.00000033     0.00000058)
  (   -0.00000017    -0.00000014)  (   -0.00000003     0.00000007)  (   -0.00000000     0.00000000)
  (    0.00000000     0.00000000)  (    0.00000000    -0.00000000)  (    0.00000000    -0.00000000)
  (    0.00000000    -0.00000000)  (   -0.00000000    -0.00000000)  (   -0.00000000    -0.00000000)
  (   -0.00000000    -0.00000000)  (   -0.00000000    -0.00000000)  (   -0.00000000     0.00000000)
  (   -0.00000000     0.00000000)  (    0.00000000     0.00000000)  (    0.00000000     0.00000000)
  (    0.00000000     0.00000000)  (    0.00000000    -0.00000000)  (    0.00000000    -0.00000000)
  (    0.00000000    -0.00000000)  (   -0.00000000    -0.00000000)  (   -0.00000000    -0.00000000)
  (   -0.00000000     0.00000000)  (   -0.00000000     0.00000000)  (   -0.00000000     0.00000000)
  (   -0.00000000     0.00000000)  (   -0.00000000     0.00000000)  (    0.00000000     0.00000000)
  (    0.00000000     0.00000000)  (    0.00000000    -0.00000000)  (   -0.00000000    -0.00000000)
  (   -0.00000000    -0.00000000)  (   -0.00000000    -0.00000000)  (   -0.00000000    -0.00000000)
  (    0.00000000    -0.00000000)  (    0.00000000    -0.00000000)  (    0.00000000    -0.00000000)
  (    0.00000000    -0.00000000)  (   -0.00000000    -0.00000000)  (   -0.00000000    -0.00000000)
  (   -0.00000000    -0.00000000)  (   -0.00000000     0.00000000)  (   -0.00000000     0.00000000)
  (   -0.00000000     0.00000000)  (    0.00000000     0.00000000)  (    0.00000000     0.00000000)
  (    0.00000000    -0.00000000)  (    0.00000000    -0.00000000)  (    0.00000000    -0.00000000)
  (    0.00000000    -0.00000000)  (   -0.00000000    -0.00000000)  (   -0.00000000     0.00000000)
  (    0.00000000     0.00000000)  (    0.00000000     0.00000000)  (
```

*** ICEPERF ***

PROPELLER ICING ANALYSIS PROGRAM

BY T. L. MILLER

TEXAS A&M UNIVERSITY & SVERDRUP TECHNOLOGY, INC.

LAST UPDATE 2/18/86

NEEL & BRIGHT DATA, BRAGG CORRELATION

R/R= 0.50

ADVANCE RATIO=0.900

TRAJECTORY CALCULATION GENERAL INPUT:

DROPLET TRAJECTORY INPUT

IPRINT= 1	MSPL= 0	XFIRST= -0.050000	XLAST= 1.000000
EPS= 0.100D-05	ALPHA= 6.13		
X0= -5.00000	UD0= 1.00000	Y0= -0.10000	VD0= 0.00000
RU= 103.55089	AK= 0.49577	FR= 0.00000	
DY0= 0.005000	CON= 1.000000	ERRY= 2.000000	HGT= 0.000000

RUN	X0	Y0	XF	YF	UDF	VDF	TF	THF	
1	-0.500000D 01	-0.100000D 00	PARTICLE PASSES BODY						
1	-0.500000D 01	-0.110000D 00	PARTICLE PASSES BODY						
1	-0.500000D 01	-0.120000D 00	PARTICLE PASSES BODY						
1	-0.500000D 01	-0.130000D 00	PARTICLE PASSES BODY						
1	-0.500000D 01	-0.140000D 00	PARTICLE PASSES BODY						
1	-0.500000D 01	-0.150000D 00	PARTICLE PASSES BODY						
1	-0.500000D 01	-0.160000D 00	PARTICLE PASSES BODY						
1	-0.500000D 01	-0.170000D 00	PARTICLE PASSES BODY						
1	-0.500000D 01	-0.180000D 00	0.165225D-01	0.201007D-01	0.923138D 00	0.481579D 00	0.505823D 01	0.983452D-01	0.
2	-0.500000D 01	-0.175000D 00	PARTICLE PASSES BODY						
3	-0.500000D 01	-0.185000D 00	0.294911D-02	0.782276D-02	0.818617D 00	0.418675D 00	0.504493D 01	0.506008D 00	0.
4	-0.500000D 01	-0.190000D 00	0.513985D-04	0.476609D-03	0.764265D 00	0.355646D 00	0.504301D 01	0.103954D 01	-0.
5	-0.500000D 01	-0.195000D 00	0.982255D-03	-0.541017D-02	0.736328D 00	0.300225D 00	0.504550D 01	0.158806D 01	-0.
6	-0.500000D 01	-0.200000D 00	0.453509D-02	-0.105530D-01	0.720212D 00	0.252712D 00	0.505117D 01	0.196823D 01	-0.
7	-0.500000D 01	-0.205000D 00	0.103561D-01	-0.152561D-01	0.713055D 00	0.210543D 00	0.505967D 01	0.224658D 01	-0.
8	-0.500000D 01	-0.210000D 00	0.185831D-01	-0.196347D-01	0.711849D 00	0.173737D 00	0.507121D 01	0.245437D 01	-0.
9	-0.500000D 01	-0.215000D 00	0.291164D-01	-0.238529D-01	0.714784D 00	0.142552D 00	0.508565D 01	0.260168D 01	-0.
10	-0.500000D 01	-0.220000D 00	0.422634D-01	-0.279689D-01	0.719402D 00	0.115096D 00	0.510338D 01	0.270812D 01	-0.
11	-0.500000D 01	-0.225000D 00	0.583996D-01	-0.320628D-01	0.725149D 00	0.897408D-01	0.512487D 01	0.278620D 01	-0.
12	-0.500000D 01	-0.230000D 00	0.781119D-01	-0.362361D-01	0.732465D 00	0.654726D-01	0.515084D 01	0.285621D 01	-0.

```
13 -0.500000D 01 -0.235000D 00   0.102398D 00 -0.406099D-01   0.742207D 00  0.420336D-01   0.518249D 01   0.291840D 01 -0.115758
14 -0.500000D 01 -0.240000D 00   0.132494D 00 -0.453318D-01   0.754937D 00  0.203714D-01   0.522119D 01   0.296524D 01 -0.146222
15 -0.500000D 01 -0.245000D 00   0.170606D 00 -0.505752D-01   0.770208D 00  0.167822D-02   0.526948D 01   0.300861D 01 -0.184694
16 -0.500000D 01 -0.250000D 00   0.219766D 00 -0.565535D-01   0.786486D 00 -0.144847D-01   0.533079D 01   0.304458D 01 -0.234216
17 -0.500000D 01 -0.255000D 00   0.288160D 00 -0.638930D-01   0.805300D 00 -0.317577D-01   0.541476D 01   0.307944D 01 -0.303003
18 -0.500000D 01 -0.260000D 00   0.411290D 00 -0.753815D-01   0.838068D 00 -0.508738D-01   0.556245D 01   0.311513D 01 -0.426669
19 -0.500000D 01 -0.265000D 00   0.901177D 00 -0.113994D 00   0.917261D 00 -0.661301D-01   0.611785D 01   0.277442D 01 -0.919188
20 -0.500000D 01 -0.270000D 00     PARTICLE PASSES BODY
 1 -0.500000D 01 -0.267500D 00   0.908230D 00 -0.116568D 00   0.919679D 00 -0.646097D-01   0.612440D 01   0.295457D 01 -0.926707
 2 -0.500000D 01 -0.268798D 00     PARTICLE PASSES BODY
 1 -0.500000D 01 -0.179397D 00     PARTICLE PASSES BODY


   TRAJECTORY SUMMARY

     SF            YO
 -0.934513D 00 -0.268149D 00
 -0.919188D 00 -0.265000D 00
 -0.426669D 00 -0.260000D 00
 -0.303003D 00 -0.255000D 00
 -0.234216D 00 -0.250000D 00
 -0.184694D 00 -0.245000D 00
 -0.146222D 00 -0.240000D 00
 -0.115758D 00 -0.235000D 00
 -0.910804D-01 -0.230000D 00
 -0.709302D-01 -0.225000D 00
 -0.542819D-01 -0.220000D 00
 -0.405043D-01 -0.215000D 00
 -0.291562D-01 -0.210000D 00
 -0.198472D-01 -0.205000D 00
 -0.123654D-01 -0.200000D 00
 -0.608873D-02 -0.195000D 00
 -0.626276D-04 -0.190000D 00
  0.791436D-02 -0.185000D 00
  0.263176D-01 -0.180000D 00
  0.307572D-01 -0.179698D 00


TANGENT TRAJECTORIES:

YO(UPPER)=-0.179698D 00     SF(UPPER)= 0.307572D-01

YO(LOWER)=-0.268149D 00     SF(LOWER)=-0.934513D 00

YO(UPPER) -YO(LOWER)= 0.884504D-01

AIRFOIL PROJECTED HEIGHT= 0.172892D 00

COLLECTION EFFICIENCY, E= 0.511592D 00

MAXIMUM ERROR IN E =    0.107449D 01 PERCENT


MAXIMUM IMPINGEMENT= 0.851848D 00

YO(MAX)=-0.193761D 00       SF(MAX)=-0.462977D-02
```

SURFACE IMPINGEMENT VALUES

Y0	S	DYODS	CON*DYODS
-0.268149D 00	-0.934513D 00	0.000000	0.000000
-0.266594D 00	-0.926851D 00	0.305681D 00	0.305681D 00
-0.265000D 00	-0.919188D 00	0.101519D-01	0.101519D-01
-0.262500D 00	-0.672929D 00	0.101519D-01	0.101519D-01
-0.260000D 00	-0.426669D 00	0.101519D-01	0.101519D-01
-0.258300D 00	-0.364836D 00	0.426282D-01	0.426282D-01
-0.255000D 00	-0.303003D 00	0.619248D-01	0.619248D-01
-0.252717D 00	-0.268610D 00	0.717643D-01	0.717643D-01
-0.250000D 00	-0.234216D 00	0.871470D-01	0.871470D-01
-0.247676D 00	-0.209455D 00	0.100778D 00	0.100778D 00
-0.245000D 00	-0.184694D 00	0.115530D 00	0.115530D 00
-0.242651D 00	-0.165458D 00	0.129330D 00	0.129330D 00
-0.240000D 00	-0.146222D 00	0.146940D 00	0.146940D 00
-0.237637D 00	-0.130990D 00	0.163692D 00	0.163692D 00
-0.235000D 00	-0.115758D 00	0.183047D 00	0.183047D 00
-0.232629D 00	-0.103419D 00	0.201906D 00	0.201906D 00
-0.230000D 00	-0.910804D-01	0.225020D 00	0.225020D 00
-0.227623D 00	-0.810053D-01	0.247511D 00	0.247511D 00
-0.225000D 00	-0.709302D-01	0.273757D 00	0.273757D 00
-0.223436D 00	-0.653808D-01	0.290361D 00	0.290361D 00
-0.221773D 00	-0.598313D-01	0.309189D 00	0.309189D 00
-0.220000D 00	-0.542819D-01	0.330242D 00	0.330242D 00
-0.218838D 00	-0.508375D-01	0.344965D 00	0.344965D 00
-0.217621D 00	-0.473931D-01	0.361620D 00	0.361620D 00
-0.216344D 00	-0.439487D-01	0.380208D 00	0.380208D 00
-0.215000D 00	-0.405043D-01	0.400727D 00	0.400727D 00
-0.213837D 00	-0.376673D-01	0.419264D 00	0.419264D 00
-0.212619D 00	-0.348303D-01	0.439479D 00	0.439479D 00
-0.211342D 00	-0.319932D-01	0.461375D 00	0.461375D 00
-0.210000D 00	-0.291562D-01	0.484949D 00	0.484949D 00
-0.209237D 00	-0.276047D-01	0.499310D 00	0.499310D 00
-0.208450D 00	-0.260532D-01	0.515690D 00	0.515690D 00
-0.207635D 00	-0.245017D-01	0.534089D 00	0.534089D 00
-0.206791D 00	-0.229502D-01	0.554507D 00	0.554507D 00
-0.205914D 00	-0.213987D-01	0.576945D 00	0.576945D 00
-0.205000D 00	-0.198472D-01	0.601401D 00	0.601401D 00
-0.204430D 00	-0.189120D-01	0.617009D 00	0.617009D 00
-0.203846D 00	-0.179768D-01	0.633131D 00	0.633131D 00
-0.203246D 00	-0.170415D-01	0.649767D 00	0.649767D 00
-0.202630D 00	-0.161063D-01	0.666916D 00	0.666916D 00
-0.201998D 00	-0.151711D-01	0.684579D 00	0.684579D 00
-0.201350D 00	-0.142358D-01	0.702756D 00	0.702756D 00
-0.200684D 00	-0.133006D-01	0.721447D 00	0.721447D 00
-0.200000D 00	-0.123654D-01	0.740652D 00	0.740652D 00
-0.199054D 00	-0.111101D-01	0.765652D 00	0.765652D 00
-0.198079D 00	-0.985473D-02	0.788406D 00	0.788406D 00
-0.197076D 00	-0.859940D-02	0.808915D 00	0.808915D 00
-0.196049D 00	-0.734406D-02	0.827177D 00	0.827177D 00
-0.195000D 00	-0.608873D-02	0.843193D 00	0.843193D 00
-0.193761D 00	-0.462977D-02	0.851848D 00	0.851848D 00
-0.193721D 00	-0.458221D-02	0.851838D 00	0.851838D 00
-0.192443D 00	-0.307568D-02	0.842028D 00	0.842028D 00
-0.191193D 00	-0.156915D-02	0.813760D 00	0.813760D 00

-0.190000D 00	-0.626276D-04	0.767037D 00	0.767037D 00
-0.189597D 00	0.469171D-03	0.747392D 00	0.747392D 00
-0.189205D 00	0.100097D-02	0.727957D 00	0.727957D 00
-0.188823D 00	0.153277D-02	0.708733D 00	0.708733D 00
-0.188451D 00	0.206457D-02	0.689719D 00	0.689719D 00
-0.188089D 00	0.259637D-02	0.670916D 00	0.670916D 00
-0.187738D 00	0.312817D-02	0.652323D 00	0.652323D 00
-0.187396D 00	0.365997D-02	0.633941D 00	0.633941D 00
-0.187063D 00	0.419176D-02	0.615770D 00	0.615770D 00
-0.186741D 00	0.472356D-02	0.597809D 00	0.597809D 00
-0.186427D 00	0.525536D-02	0.580058D 00	0.580058D 00
-0.186124D 00	0.578716D-02	0.562519D 00	0.562519D 00
-0.185829D 00	0.631896D-02	0.545189D 00	0.545189D 00
-0.185544D 00	0.685076D-02	0.528071D 00	0.528071D 00
-0.185267D 00	0.738256D-02	0.511162D 00	0.511162D 00
-0.185000D 00	0.791436D-02	0.494465D 00	0.494465D 00
-0.184579D 00	0.879070D-02	0.467560D 00	0.467560D 00
-0.184180D 00	0.966705D-02	0.441530D 00	0.441530D 00
-0.183804D 00	0.105434D-01	0.416376D 00	0.416376D 00
-0.183450D 00	0.114197D-01	0.392097D 00	0.392097D 00
-0.183117D 00	0.122961D-01	0.368692D 00	0.368692D 00
-0.182804D 00	0.131724D-01	0.346163D 00	0.346163D 00
-0.182510D 00	0.140488D-01	0.324509D 00	0.324509D 00
-0.182235D 00	0.149251D-01	0.303730D 00	0.303730D 00
-0.181977D 00	0.158015D-01	0.283826D 00	0.283826D 00
-0.181737D 00	0.166778D-01	0.264798D 00	0.264798D 00
-0.181513D 00	0.175541D-01	0.246644D 00	0.246644D 00
-0.181304D 00	0.184305D-01	0.229365D 00	0.229365D 00
-0.181111D 00	0.193068D-01	0.212962D 00	0.212962D 00
-0.180931D 00	0.201832D-01	0.197434D 00	0.197434D 00
-0.180764D 00	0.210595D-01	0.182780D 00	0.182780D 00
-0.180610D 00	0.219359D-01	0.169002D 00	0.169002D 00
-0.180468D 00	0.228122D-01	0.156099D 00	0.156099D 00
-0.180336D 00	0.236886D-01	0.144072D 00	0.144072D 00
-0.180215D 00	0.245649D-01	0.132919D 00	0.132919D 00
-0.180103D 00	0.254412D-01	0.122641D 00	0.122641D 00
-0.180000D 00	0.263176D-01	0.113239D 00	0.113239D 00
-0.179919D 00	0.270575D-01	0.103785D 00	0.103785D 00
-0.179847D 00	0.277975D-01	0.905638D-01	0.905638D-01
-0.179786D 00	0.285374D-01	0.735746D-01	0.735746D-01
-0.179739D 00	0.292773D-01	0.528176D-01	0.528176D-01
-0.179709D 00	0.300173D-01	0.282927D-01	0.282927D-01
-0.179698D 00	0.307572D-01	0.000000	0.000000

```
                                        *** ICEPERF ***

                               PROPELLER ICING ANALYSIS PROGRAM

                                     BY T. L. MILLER

                       TEXAS A&M UNIVERSITY & SVERDRUP TECHNOLOGY, INC.

                                  LAST UPDATE  2/18/86

NEEL & BRIGHT DATA, BRAGG CORRELATION

 ADVANCE RATIO=0.900
  CLARK-Y COORDINATES, R/R=0.7

 CH,TAU,KAPA:         1.00000007      22.24798747       1.87640007
 XZ1T,YZ1T,XZ1N,YZ1N:         1.00000000       0.00064100       0.00323626       0.00029700
 XS1,YS1:          0.26560534       0.00009166
 CENTROID: XZC,YZC:        -0.01390164       0.01057204
 R,PHIT:          0.26929263      -1.69807032
 EPSO (ANGLE OF ZERO-LIFT LINE) =     1.69807032 (DEG.)
 CL =      2.15434094 * PI * SIN(ALPHA + EPSO)

 FOURIER COEFFICIENTS C(J)=(A(J)+I * B(J)),J=1,LPT, LPT =  59

  (   0.00348270  -0.00014161)  (   0.00250826  -0.00056992)  (  -0.00009754   0.00004682)
  (   0.00000829  -0.00000011)  (  -0.00000278  -0.00000180)  (   0.00000019   0.00000015)
  (  -0.00000010  -0.00000009)  (  -0.00000001   0.00000001)  (  -0.00000001  -0.00000000)
  (  -0.00000000   0.00000000)  (   0.00000000  -0.00000000)  (  -0.00000000   0.00000000)
  (  -0.00000000  -0.00000000)  (  -0.00000000   0.00000000)  (  -0.00000000  -0.00000000)
  (  -0.00000000  -0.00000000)  (   0.00000000  -0.00000000)  (   0.00000000  -0.00000000)
  (   0.00000000  -0.00000000)  (   0.00000000  -0.00000000)  (   0.00000000  -0.00000000)
  (   0.00000000   0.00000000)  (   0.00000000   0.00000000)  (  -0.00000000   0.00000000)
  (  -0.00000000   0.00000000)  (  -0.00000000   0.00000000)  (  -0.00000000   0.00000000)
  (  -0.00000000   0.00000000)  (  -0.00000000   0.00000000)  (  -0.00000000   0.00000000)
  (  -0.00000000   0.00000000)  (  -0.00000000   0.00000000)  (  -0.00000000  -0.00000000)
  (  -0.00000000  -0.00000000)  (   0.00000000  -0.00000000)  (   0.00000000  -0.00000000)
  (   0.00000000  -0.00000000)  (   0.00000000  -0.00000000)  (   0.00000000  -0.00000000)
  (   0.00000000  -0.00000000)  (   0.00000000  -0.00000000)  (  -0.00000000  -0.00000000)
  (   0.00000000  -0.00000000)  (  -0.00000000  -0.00000000)  (   0.00000000  -0.00000000)
  (   0.00000000   0.00000000)  (   0.00000000   0.00000000)  (   0.00000000   0.00000000)
  (   0.00000000   0.00000000)  (   0.00000000   0.00000000)  (   0.00000000   0.00000000)
  (   0.00000000   0.00000000)  (   0.00000000   0.00000000)  (   0.00000000   0.00000000)
  (   0.00000000   0.00000000)  (   0.00000000   0.00000000)  (   0.00000000   0.00000000)
  (   0.00000000   0.00000000)  (   0.00000000   0.00000000)  (
```

```
                              *** ICEPERF ***
                      PROPELLER ICING ANALYSIS PROGRAM
                             BY T. L. MILLER
             TEXAS A&M UNIVERSITY & SVERDRUP TECHNOLOGY, INC.
                           LAST UPDATE  2/18/86

NEEL & BRIGHT DATA, BRAGG CORRELATION
R/R= 0.70

 ADVANCE RATIO=0.900

TRAJECTORY CALCULATION GENERAL INPUT:
  DROPLET TRAJECTORY INPUT
IPRINT= 1             MSPL= 0              XFIRST= -0.050000      XLAST=  1.000000
EPS= 0.100D-05        ALPHA= 6.50
X0=  -5.00000         UD0=   1.00000       Y0=  -0.10000          VD0=   0.00000
RU= 136.83643         AK=   0.78836        FR=   0.00000
DY0=  0.005000        CON=  1.000000       ERRY=  2.000000        HGT=  0.000000
```

RUN	X0	Y0	XF	YF	UDF	VDF	TF	THF	SF
1	-0.500000D 01	-0.100000D 00	PARTICLE PASSES BODY						
1	-0.500000D 01	-0.110000D 00	PARTICLE PASSES BODY						
1	-0.500000D 01	-0.120000D 00	PARTICLE PASSES BODY						
1	-0.500000D 01	-0.130000D 00	PARTICLE PASSES BODY						
1	-0.500000D 01	-0.140000D 00	PARTICLE PASSES BODY						
1	-0.500000D 01	-0.150000D 00	PARTICLE PASSES BODY						
1	-0.500000D 01	-0.160000D 00	0.395142D-02	0.672000D-02	0.917861D 00	0.387286D 00	0.502927D 01	0.353175D 00	0.770230
2	-0.500000D 01	-0.155000D 00	PARTICLE PASSES BODY						
3	-0.500000D 01	-0.165000D 00	-0.767751D-05	-0.379466D-03	0.840807D 00	0.328953D 00	0.502628D 01	0.119193D 01	-0.655167
4	-0.500000D 01	-0.170000D 00	0.215016D-02	-0.546253D-02	0.805844D 00	0.278647D 00	0.502999D 01	0.194360D 01	-0.630359
5	-0.500000D 01	-0.175000D 00	0.758520D-02	-0.977294D-02	0.787477D 00	0.238100D 00	0.503754D 01	0.234088D 01	-0.132635
6	-0.500000D 01	-0.180000D 00	0.156614D-01	-0.136550D-01	0.778167D 00	0.204913D 00	0.504825D 01	0.252141D 01	-0.222159
7	-0.500000D 01	-0.185000D 00	0.263264D-01	-0.172346D-01	0.772969D 00	0.176929D 00	0.506211D 01	0.263583D 01	-0.334493
8	-0.500000D 01	-0.190000D 00	0.392371D-01	-0.206864D-01	0.770621D 00	0.152876D 00	0.507872D 01	0.270346D 01	-0.468109
9	-0.500000D 01	-0.195000D 00	0.543547D-01	-0.240896D-01	0.770014D 00	0.131443D 00	0.509801D 01	0.276653D 01	-0.623074
10	-0.500000D 01	-0.200000D 00	0.718136D-01	-0.274931D-01	0.770743D 00	0.111766D 00	0.512014D 01	0.281403D 01	-0.800953
11	-0.500000D 01	-0.205000D 00	0.918152D-01	-0.309521D-01	0.772779D 00	0.934618D-01	0.514536D 01	0.285913D 01	-0.100394
12	-0.500000D 01	-0.210000D 00	0.114481D 00	-0.345249D-01	0.775999D 00	0.764613D-01	0.517377D 01	0.289057D 01	-0.123340
13	-0.500000D 01	-0.215000D 00	0.140150D 00	-0.382615D-01	0.780280D 00	0.606345D-01	0.520575D 01	0.292382D 01	-0.149279
14	-0.500000D 01	-0.220000D 00	0.169214D 00	-0.422026D-01	0.785413D 00	0.457558D-01	0.524173D 01	0.295363D 01	-0.178609

```
15 -0.500000D 01 -0.225000D 00   0.202344D 00 -0.464169D-01   0.791434D 00  0.316028D-01   0.528249D 01   0.297762D 01 -0.2
16 -0.500000D 01 -0.230000D 00   0.2[illegible]0353D 00 -0.509704D-01   0.798396D 00  0.179864D-01   0.532892D 01   0.300547D 01 -0.2
17 -0.500000D 01 -0.235000D 00   0.284640D 00 -0.559866D-01   0.806521D 00  0.495333D-02   0.538262D 01   0.302426D 01 -0.2
18 -0.500000D 01 -0.240000D 00   0.336960D 00 -0.616067D-01   0.815778D 00 -0.738753D-02   0.544554D 01   0.304699D 01 -0.3
19 -0.500000D 01 -0.245000D 00   0.399787D 00 -0.680356D-01   0.826074D 00 -0.192435D-01   0.552039D 01   0.306717D 01 -0.4
20 -0.500000D 01 -0.250000D 00   0.477440D 00 -0.756851D-01   0.838078D 00 -0.312845D-01   0.561196D 01   0.307979D 01 -0.4
21 -0.500000D 01 -0.255000D 00   0.574715D 00 -0.851269D-01   0.853002D 00 -0.428321D-01   0.572515D 01   0.309622D 01 -0.5
22 -0.500000D 01 -0.260000D 00   0.712963D 00 -0.978877D-01   0.872241D 00 -0.540055D-01   0.588349D 01   0.311628D 01 -0.7
23 -0.500000D 01 -0.265000D 00     PARTICLE PASSES BODY
 1 -0.500000D 01 -0.263155D 00     PARTICLE PASSES BODY
 1 -0.500000D 01 -0.261577D 00   0.791960D 00 -0.104494D 00   0.884202D 00 -0.585643D-01   0.597284D 01   0.312908D 01 -0.8
 1 -0.500000D 01 -0.158947D 00   0.677432D-02  0.896522D-02   0.943449D 00  0.397954D 00   0.503195D 01   0.234852D 00   0.1
 2 -0.500000D 01 -0.157903D 00   0.128097D-01  0.124957D-01   0.981758D 00  0.411923D 00   0.503785D 01   0.886584D-01   0.1
 3 -0.500000D 01 -0.157586D 00     PARTICLE PASSES BODY


   TRAJECTORY SUMMARY

    SF             Y0
 -0.863958D 00 -0.262366D 00
 -0.725231D 00 -0.260000D 00
 -0.586394D 00 -0.255000D 00
 -0.488663D 00 -0.250000D 00
 -0.410634D 00 -0.245000D 00
 -0.347479D 00 -0.240000D 00
 -0.294857D 00 -0.235000D 00
 -0.250287D 00 -0.230000D 00
 -0.212006D 00 -0.225000D 00
 -0.178609D 00 -0.220000D 00
 -0.149279D 00 -0.215000D 00
 -0.123340D 00 -0.210000D 00
 -0.100394D 00 -0.205000D 00
 -0.800953D-01 -0.200000D 00
 -0.623074D-01 -0.195000D 00
 -0.468109D-01 -0.190000D 00
 -0.334493D-01 -0.185000D 00
 -0.222159D-01 -0.180000D 00
 -0.132635D-01 -0.175000D 00
 -0.630359D-02 -0.170000D 00
 -0.655167D-03 -0.165000D 00
  0.770230D-02 -0.160000D 00
  0.225365D-01 -0.157744D 00


TANGENT TRAJECTORIES:

Y0(UPPER)=-0.157744D 00      SF(UPPER)= 0.225365D-01

Y0(LOWER)=-0.262366D 00      SF(LOWER)=-0.863958D 00

Y0(UPPER) -Y0(LOWER)= 0.104622D 00

AIRFOIL PROJECTED HEIGHT= 0.147522D 00

COLLECTION EFFICIENCY, E= 0.709193D 00

MAXIMUM ERROR IN E =    0.905288D 00 PERCENT
```

MAXIMUM IMPINGEMENT= 0.910784D 00

YO(MAX)=-0.167716D 00 SF(MAX)=-0.373804D-02

SURFACE IMPINGEMENT VALUES

YO	S	DYODS	CON*DYODS
-0.262366D 00	-0.863958D 00	0.000000	0.000000
-0.261680D 00	-0.794594D 00	0.184155D-01	0.184155D-01
-0.260000D 00	-0.725231D 00	0.286787D-01	0.286787D-01
-0.257774D 00	-0.655813D 00	0.357278D-01	0.357278D-01
-0.255000D 00	-0.586394D 00	0.444913D-01	0.444913D-01
-0.252662D 00	-0.537528D 00	0.511862D-01	0.511862D-01
-0.250000D 00	-0.488663D 00	0.577265D-01	0.577265D-01
-0.247636D 00	-0.449648D 00	0.637806D-01	0.637806D-01
-0.245000D 00	-0.410634D 00	0.716230D-01	0.716230D-01
-0.242623D 00	-0.379056D 00	0.790517D-01	0.790517D-01
-0.240000D 00	-0.347479D 00	0.871954D-01	0.871954D-01
-0.237608D 00	-0.321168D 00	0.948328D-01	0.948328D-01
-0.235000D 00	-0.294857D 00	0.103578D 00	0.103578D 00
-0.232600D 00	-0.272572D 00	0.112001D 00	0.112001D 00
-0.230000D 00	-0.250287D 00	0.121517D 00	0.121517D 00
-0.227589D 00	-0.231147D 00	0.130500D 00	0.130500D 00
-0.225000D 00	-0.212006D 00	0.140168D 00	0.140168D 00
-0.222583D 00	-0.195308D 00	0.149511D 00	0.149511D 00
-0.220000D 00	-0.178609D 00	0.160074D 00	0.160074D 00
-0.217578D 00	-0.163944D 00	0.170325D 00	0.170325D 00
-0.215000D 00	-0.149279D 00	0.181456D 00	0.181456D 00
-0.212577D 00	-0.136310D 00	0.192491D 00	0.192491D 00
-0.210000D 00	-0.123340D 00	0.205133D 00	0.205133D 00
-0.207576D 00	-0.111867D 00	0.217684D 00	0.217684D 00
-0.205000D 00	-0.100394D 00	0.231550D 00	0.231550D 00
-0.202580D 00	-0.902446D-01	0.245840D 00	0.245840D 00
-0.200000D 00	-0.800953D-01	0.263015D 00	0.263015D 00
-0.197584D 00	-0.712013D-01	0.280650D 00	0.280650D 00
-0.195000D 00	-0.623074D-01	0.300926D 00	0.300926D 00
-0.192590D 00	-0.545591D-01	0.321926D 00	0.321926D 00
-0.190000D 00	-0.468109D-01	0.347294D 00	0.347294D 00
-0.188416D 00	-0.423570D-01	0.364184D 00	0.364184D 00
-0.186753D 00	-0.379032D-01	0.383177D 00	0.383177D 00
-0.185000D 00	-0.334493D-01	0.404272D 00	0.404272D 00
-0.184078D 00	-0.312026D-01	0.416992D 00	0.416992D 00
-0.183124D 00	-0.289559D-01	0.432807D 00	0.432807D 00
-0.182131D 00	-0.267092D-01	0.451718D 00	0.451718D 00
-0.181092D 00	-0.244625D-01	0.473724D 00	0.473724D 00
-0.180000D 00	-0.222159D-01	0.498825D 00	0.498825D 00
-0.179242D 00	-0.207238D-01	0.517073D 00	0.517073D 00
-0.178456D 00	-0.192317D-01	0.536418D 00	0.536418D 00
-0.177641D 00	-0.177397D-01	0.556862D 00	0.556862D 00
-0.176794D 00	-0.162476D-01	0.578403D 00	0.578403D 00
-0.175914D 00	-0.147555D-01	0.601043D 00	0.601043D 00
-0.175000D 00	-0.132635D-01	0.624781D 00	0.624781D 00
-0.174635D 00	-0.126835D-01	0.634992D 00	0.634992D 00

-0.174263D 00	-0.121035D-01	0.646744D 00	0.646744D 00
-0.173884D 00	-0.115235D-01	0.660036D 00	0.660036D 00
-0.173497D 00	-0.109435D-01	0.674870D 00	0.674870D 00
-0.173101D 00	-0.103635D-01	0.691244D 00	0.691244D 00
-0.172695D 00	-0.978352D-02	0.709160D 00	0.709160D 00
-0.172278D 00	-0.920353D-02	0.728616D 00	0.728616D 00
-0.171850D 00	-0.862354D-02	0.749613D 00	0.749613D 00
-0.171408D 00	-0.804355D-02	0.772151D 00	0.772151D 00
-0.170954D 00	-0.746356D-02	0.796229D 00	0.796229D 00
-0.170484D 00	-0.688358D-02	0.821849D 00	0.821849D 00
-0.170000D 00	-0.630359D-02	0.849009D 00	0.849009D 00
-0.167716D 00	-0.373804D-02	0.910784D 00	0.910784D 00
-0.167481D 00	-0.347938D-02	0.910156D 00	0.910156D 00
-0.165000D 00	-0.655167D-03	0.821584D 00	0.821584D 00
-0.164705D 00	-0.291798D-03	0.800661D 00	0.800661D 00
-0.164418D 00	0.715700D-04	0.779948D 00	0.779948D 00
-0.164138D 00	0.434938D-03	0.759445D 00	0.759445D 00
-0.163866D 00	0.798307D-03	0.739152D 00	0.739152D 00
-0.163601D 00	0.116167D-02	0.719069D 00	0.719069D 00
-0.163344D 00	0.152504D-02	0.699196D 00	0.699196D 00
-0.163093D 00	0.188841D-02	0.679532D 00	0.679532D 00
-0.162850D 00	0.225178D-02	0.660078D 00	0.660078D 00
-0.162613D 00	0.261515D-02	0.640834D 00	0.640834D 00
-0.162384D 00	0.297852D-02	0.621800D 00	0.621800D 00
-0.162161D 00	0.334188D-02	0.602976D 00	0.602976D 00
-0.161946D 00	0.370525D-02	0.584361D 00	0.584361D 00
-0.161737D 00	0.406862D-02	0.565956D 00	0.565956D 00
-0.161534D 00	0.443199D-02	0.547762D 00	0.547762D 00
-0.161339D 00	0.479536D-02	0.529776D 00	0.529776D 00
-0.161149D 00	0.515873D-02	0.512001D 00	0.512001D 00
-0.160967D 00	0.552209D-02	0.494436D 00	0.494436D 00
-0.160790D 00	0.588546D-02	0.477080D 00	0.477080D 00
-0.160620D 00	0.624883D-02	0.459935D 00	0.459935D 00
-0.160456D 00	0.661220D-02	0.442999D 00	0.442999D 00
-0.160298D 00	0.697557D-02	0.426273D 00	0.426273D 00
-0.160146D 00	0.733894D-02	0.409756D 00	0.409756D 00
-0.160000D 00	0.770230D-02	0.393450D 00	0.393450D 00
-0.159733D 00	0.840869D-02	0.362562D 00	0.362562D 00
-0.159487D 00	0.911508D-02	0.332889D 00	0.332889D 00
-0.159262D 00	0.982147D-02	0.304431D 00	0.304431D 00
-0.159057D 00	0.105279D-01	0.277189D 00	0.277189D 00
-0.158871D 00	0.112343D-01	0.251161D 00	0.251161D 00
-0.158702D 00	0.119406D-01	0.226349D 00	0.226349D 00
-0.158550D 00	0.126470D-01	0.202753D 00	0.202753D 00
-0.158415D 00	0.133534D-01	0.180371D 00	0.180371D 00
-0.158295D 00	0.140598D-01	0.159205D 00	0.159205D 00
-0.158190D 00	0.147662D-01	0.139254D 00	0.139254D 00
-0.158098D 00	0.154726D-01	0.120518D 00	0.120518D 00
-0.158019D 00	0.161790D-01	0.102998D 00	0.102998D 00
-0.157953D 00	0.168854D-01	0.866927D-01	0.866927D-01
-0.157897D 00	0.175918D-01	0.716028D-01	0.716028D-01
-0.157851D 00	0.182981D-01	0.577280D-01	0.577280D-01
-0.157815D 00	0.190045D-01	0.450686D-01	0.450686D-01
-0.157787D 00	0.197109D-01	0.336244D-01	0.336244D-01
-0.157767D 00	0.204173D-01	0.233954D-01	0.233954D-01
-0.157754D 00	0.211237D-01	0.143817D-01	0.143817D-01
-0.157746D 00	0.218301D-01	0.658322D-02	0.658322D-02
-0.157744D 00	0.225365D-01	0.000000	0.000000

```
                                        *** ICEPERF ***
                              PROPELLER ICING ANALYSIS PROGRAM
                                      BY T. L. MILLER
                       TEXAS A&M UNIVERSITY & SVERDRUP TECHNOLOGY, INC.
                                    LAST UPDATE  2/18/86

NEEL & BRIGHT DATA, BRAGG CORRELATION

 ADVANCE RATIO=0.900
  CLARK-Y COORDINATES, R/R=0.9

 CH,TAU,KAPA:          1.00000003      20.06805440      1.88851081
 XZ1T,YZ1T,XZ1N,YZ1N:          1.00000000       0.00056100       0.00247764       0.00034925
 XS1,YS1:            0.26410290        0.00005606
 CENTROID: XZC,YZC:           -0.01214905        0.00909377
 R,PHIT:             0.26693882      -1.48101880
 EPSO (ANGLE OF ZERO-LIFT LINE) =      1.48101880 (DEG.)
 CL =       2.13551047 * PI * SIN(ALPHA + EPSO)

 FOURIER COEFFICIENTS C(J)=(A(J)+I * B(J)),J=1,LPT, LPT =  59

  (    0.00319609   -0.00011571)  (    0.00223965   -0.00048661)  (   -0.00008504    0.00004382)
  (    0.00000823   -0.00000094)  (   -0.00000258   -0.00000138)  (    0.00000020    0.00000009)
  (   -0.00000010   -0.00000006)  (   -0.00000001    0.00000001)  (   -0.00000001   -0.00000000)
  (   -0.00000000    0.00000000)  (   -0.00000000   -0.00000000)  (   -0.00000000    0.00000000)
  (   -0.00000000   -0.00000000)  (   -0.00000000    0.00000000)  (   -0.00000000   -0.00000000)
  (   -0.00000000   -0.00000000)  (    0.00000000   -0.00000000)  (    0.00000000   -0.00000000)
  (    0.00000000   -0.00000000)  (    0.00000000    0.00000000)  (    0.00000000   -0.00000000)
  (    0.00000000    0.00000000)  (    0.00000000    0.00000000)  (   -0.00000000    0.00000000)
  (   -0.00000000    0.00000000)  (   -0.00000000    0.00000000)  (   -0.00000000    0.00000000)
  (   -0.00000000    0.00000000)  (   -0.00000000    0.00000000)  (   -0.00000000    0.00000000)
  (   -0.00000000    0.00000000)  (   -0.00000000    0.00000000)  (   -0.00000000   -0.00000000)
  (   -0.00000000   -0.00000000)  (    0.00000000   -0.00000000)  (    0.00000000   -0.00000000)
  (    0.00000000   -0.00000000)  (    0.00000000   -0.00000000)  (    0.00000000   -0.00000000)
  (    0.00000000   -0.00000000)  (    0.00000000   -0.00000000)  (    0.00000000   -0.00000000)
  (    0.00000000   -0.00000000)  (   -0.00000000   -0.00000000)  (    0.00000000    0.00000000)
  (   -0.00000000    0.00000000)  (    0.00000000    0.00000000)  (   -0.00000000    0.00000000)
  (    0.00000000    0.00000000)  (    0.00000000    0.00000000)  (    0.00000000    0.00000000)
  (    0.00000000    0.00000000)  (    0.00000000    0.00000000)  (    0.00000000    0.00000000)
  (    0.00000000    0.00000000)  (    0.00000000    0.00000000)  (    0.00000000    0.00000000)
  (    0.00000000   -0.00000000)  (    0.00000000   -0.00000000)  (
```

*** ICEPERF ***

PROPELLER ICING ANALYSIS PROGRAM

BY T. L. MILLER

TEXAS A&M UNIVERSITY & SVERDRUP TECHNOLOGY, INC.

LAST UPDATE 2/18/86

NEEL & BRIGHT DATA, BRAGG CORRELATION

R/R= 0.90

ADVANCE RATIO=0.900

TRAJECTORY CALCULATION GENERAL INPUT:

DROPLET TRAJECTORY INPUT

IPRINT= 1	MSPL= 0	XFIRST= -0.050000	XLAST= 1.000000
EPS= 0.100D-05	ALPHA= 7.16		
X0= -5.00000	UD0= 1.00000	Y0= -0.10000	VD0= 0.00000
RU= 171.13921	AK= 1.4163	FR= 0.00000	
DY0= 0.005000	CON= 1.000000	ERRY= 2.000000	HGT= 0.000000

RUN	X0	Y0	XF	YF	UDF	VDF	TF	THF	S
1	-0.500000D 01	-0.100000D 00	PARTICLE PASSES BODY						
1	-0.500000D 01	-0.110000D 00	PARTICLE PASSES BODY						
1	-0.500000D 01	-0.120000D 00	PARTICLE PASSES BODY						
1	-0.500000D 01	-0.130000D 00	PARTICLE PASSES BODY						
1	-0.500000D 01	-0.140000D 00	0.343632D-02	0.545572D-02	0.956821D 00	0.318727D 00	0.502020D 01	0.383854D 00	0.6292
2	-0.500000D 01	-0.135000D 00	PARTICLE PASSES BODY						
3	-0.500000D 01	-0.145000D 00	0.543436D-04	-0.937688D-03	0.890987D 00	0.277513D 00	0.501771D 01	0.140770D 01	-0.1269
4	-0.500000D 01	-0.150000D 00	0.311181D-02	-0.563856D-02	0.860117D 00	0.241086D 00	0.502209D 01	0.215652D 01	-0.6994
5	-0.500000D 01	-0.155000D 00	0.966685D-02	-0.965968D-02	0.843371D 00	0.212100D 00	0.503041D 01	0.242179D 01	-0.1469
6	-0.500000D 01	-0.160000D 00	0.188403D-01	-0.133183D-01	0.833833D 00	0.188802D 00	0.504175D 01	0.257597D 01	-0.2456
7	-0.500000D 01	-0.165000D 00	0.301774D-01	-0.167720D-01	0.827725D 00	0.169518D 00	0.505561D 01	0.266964D 01	-0.3641
8	-0.500000D 01	-0.170000D 00	0.434795D-01	-0.201007D-01	0.823429D 00	0.152756D 00	0.507177D 01	0.272954D 01	-0.5013
9	-0.500000D 01	-0.175000D 00	0.585800D-01	-0.233723D-01	0.820465D 00	0.137701D 00	0.509006D 01	0.277336D 01	-0.6558
10	-0.500000D 01	-0.180000D 00	0.753760D-01	-0.266329D-01	0.818549D 00	0.123930D 00	0.511033D 01	0.280961D 01	-0.8269
11	-0.500000D 01	-0.185000D 00	0.938872D-01	-0.299108D-01	0.817536D 00	0.111180D 00	0.513262D 01	0.283852D 01	-0.1014
12	-0.500000D 01	-0.190000D 00	0.114038D 00	-0.332375D-01	0.817254D 00	0.993545D-01	0.515683D 01	0.286409D 01	-0.1219
13	-0.500000D 01	-0.195000D 00	0.135894D 00	-0.366357D-01	0.817600D 00	0.883141D-01	0.518302D 01	0.288282D 01	-0.1440
14	-0.500000D 01	-0.200000D 00	0.159498D 00	-0.401205D-01	0.818401D 00	0.779071D-01	0.521123D 01	0.290358D 01	-0.1678
15	-0.500000D 01	-0.205000D 00	0.184939D 00	-0.437090D-01	0.819592D 00	0.679832D-01	0.524156D 01	0.292282D 01	-0.1935
16	-0.500000D 01	-0.210000D 00	0.212337D 00	-0.474181D-01	0.821160D 00	0.584282D-01	0.527414D 01	0.294130D 01	-0.2212

```
17 -0.500000D 01 -0.215000D 00   0.241905D 00 -0.512757D-01   0.823166D 00   0.491985D-01   0.530922D 01   0.295685D 01 -0.251052
18 -0.500000D 01 -0.220000D 00   0.273817D 00 -0.553021D-01   0.825612D 00   0.403097D-01   0.534696D 01   0.296800D 01 -0.283218
19 -0.500000D 01 -0.225000D 00   0.308182D 00 -0.595089D-01   0.828427D 00   0.317968D-01   0.538748D 01   0.298529D 01 -0.317840
20 -0.500000D 01 -0.230000D 00   0.345409D 00 -0.639402D-01   0.831599D 00   0.236648D-01   0.543123D 01   0.299656D 01 -0.355329
21 -0.500000D 01 -0.235000D 00   0.385597D 00 -0.686100D-01   0.835012D 00   0.157944D-01   0.547829D 01   0.300864D 01 -0.395788
22 -0.500000D 01 -0.240000D 00   0.429066D 00 -0.735534D-01   0.838696D 00   0.801240D-02   0.552901D 01   0.302212D 01 -0.439537
23 -0.500000D 01 -0.245000D 00   0.476354D 00 -0.788462D-01   0.842854D 00   0.220513D-03   0.558397D 01   0.303240D 01 -0.487120
24 -0.500000D 01 -0.250000D 00   0.527684D 00 -0.845378D-01   0.847647D 00 -0.742625D-02   0.564336D 01   0.303981D 01 -0.538765
25 -0.500000D 01 -0.255000D 00   0.583554D 00 -0.906676D-01   0.853032D 00 -0.146760D-01   0.570768D 01   0.304866D 01 -0.594970
26 -0.500000D 01 -0.260000D 00   0.645449D 00 -0.973299D-01   0.858858D 00 -0.215542D-01   0.577856D 01   0.306129D 01 -0.657223
27 -0.500000D 01 -0.265000D 00   0.715498D 00 -0.104640D 00   0.865436D 00 -0.287335D-01   0.585834D 01   0.307179D 01 -0.727652
28 -0.500000D 01 -0.270000D 00   0.801274D 00 -0.113058D 00   0.874627D 00 -0.362348D-01   0.595541D 01   0.309084D 01 -0.813841
29 -0.500000D 01 -0.275000D 00     PARTICLE PASSES BODY
 1 -0.500000D 01 -0.272500D 00   0.858780D 00 -0.118096D 00   0.880565D 00 -0.392328D-01   0.602015D 01   0.310485D 01 -0.871567
 1 -0.500000D 01 -0.139063D 00   0.583722D-02  0.718171D-02   0.975329D 00   0.324676D 00   0.502245D 01   0.205648D 00  0.925369
 2 -0.500000D 01 -0.138522D 00   0.770372D-02  0.832385D-02   0.986767D 00   0.327388D 00   0.502421D 01   0.197489D 00  0.114375
 3 -0.500000D 01 -0.136761D 00     PARTICLE PASSES BODY
```

*** FOR GIVEN ERRY A LARGE EXTRAPOLATION IS REQUIRED FOR SF CALCULATION ***

TRAJECTORY SUMMARY

```
     SF              YO
-0.914862D 00 -0.273750D 00
-0.813841D 00 -0.270000D 00
-0.727652D 00 -0.265000D 00
-0.657223D 00 -0.260000D 00
-0.594970D 00 -0.255000D 00
-0.538765D 00 -0.250000D 00
-0.487120D 00 -0.245000D 00
-0.439537D 00 -0.240000D 00
-0.395788D 00 -0.235000D 00
-0.355329D 00 -0.230000D 00
-0.317840D 00 -0.225000D 00
-0.283218D 00 -0.220000D 00
-0.251052D 00 -0.215000D 00
-0.221234D 00 -0.210000D 00
-0.193587D 00 -0.205000D 00
-0.167894D 00 -0.200000D 00
-0.144033D 00 -0.195000D 00
-0.121915D 00 -0.190000D 00
-0.101491D 00 -0.185000D 00
-0.826920D-01 -0.180000D 00
-0.655822D-01 -0.175000D 00
-0.501312D-01 -0.170000D 00
-0.364185D-01 -0.165000D 00
-0.245659D-01 -0.160000D 00
-0.146903D-01 -0.155000D 00
-0.699455D-02 -0.150000D 00
-0.126994D-02 -0.145000D 00
 0.629283D-02 -0.140000D 00
 0.167705D-01 -0.137641D 00
```

TANGENT TRAJECTORIES:

```
YO(UPPER)=-0.137641D 00     SF(UPPER)= 0.167705D-01
YO(LOWER)=-0.273750D 00     SF(LOWER)=-0.914862D 00
YO(UPPER) -YO(LOWER)= 0.136109D 00
AIRFOIL PROJECTED HEIGHT= 0.150303D 00
COLLECTION EFFICIENCY, E= 0.905560D 00
MAXIMUM ERROR IN E =    0.156528D 01 PERCENT

MAXIMUM IMPINGEMENT= 0.898764D 00
YO(MAX)=-0.147235D 00       SF(MAX)=-0.381145D-02
```

SURFACE IMPINGEMENT VALUES

YO	S	DYODS	CON*DYODS
-0.273750D 00	-0.914862D 00	0.000000	0.000000
-0.273191D 00	-0.881188D 00	0.310810D-01	0.310810D-01
-0.271799D 00	-0.847514D 00	0.494944D-01	0.494944D-01
-0.270000D 00	-0.813841D 00	0.552402D-01	0.552402D-01
-0.267598D 00	-0.770746D 00	0.571311D-01	0.571311D-01
-0.265000D 00	-0.727652D 00	0.643087D-01	0.643087D-01
-0.262606D 00	-0.692437D 00	0.713285D-01	0.713285D-01
-0.260000D 00	-0.657223D 00	0.763377D-01	0.763377D-01
-0.257565D 00	-0.626096D 00	0.802071D-01	0.802071D-01
-0.255000D 00	-0.594970D 00	0.847371D-01	0.847371D-01
-0.252558D 00	-0.566867D 00	0.890017D-01	0.890017D-01
-0.250000D 00	-0.538765D 00	0.930189D-01	0.930189D-01
-0.247550D 00	-0.512943D 00	0.967611D-01	0.967611D-01
-0.245000D 00	-0.487120D 00	0.100832D 00	0.100832D 00
-0.242553D 00	-0.463329D 00	0.104993D 00	0.104993D 00
-0.240000D 00	-0.439537D 00	0.109668D 00	0.109668D 00
-0.237551D 00	-0.417662D 00	0.114267D 00	0.114267D 00
-0.235000D 00	-0.395788D 00	0.118993D 00	0.118993D 00
-0.232547D 00	-0.375558D 00	0.123543D 00	0.123543D 00
-0.230000D 00	-0.355329D 00	0.128333D 00	0.128333D 00
-0.227549D 00	-0.336584D 00	0.133249D 00	0.133249D 00
-0.225000D 00	-0.317840D 00	0.138895D 00	0.138895D 00
-0.222548D 00	-0.300529D 00	0.144426D 00	0.144426D 00
-0.220000D 00	-0.283218D 00	0.149916D 00	0.149916D 00
-0.217546D 00	-0.267135D 00	0.155332D 00	0.155332D 00
-0.215000D 00	-0.251052D 00	0.161420D 00	0.161420D 00
-0.212548D 00	-0.236143D 00	0.167606D 00	0.167606D 00
-0.210000D 00	-0.221234D 00	0.174253D 00	0.174253D 00
-0.207546D 00	-0.207410D 00	0.180794D 00	0.180794D 00
-0.205000D 00	-0.193587D 00	0.187664D 00	0.187664D 00
-0.202546D 00	-0.180740D 00	0.194504D 00	0.194504D 00
-0.200000D 00	-0.167894D 00	0.201950D 00	0.201950D 00
-0.197547D 00	-0.155963D 00	0.209451D 00	0.209451D 00
-0.195000D 00	-0.144033D 00	0.217565D 00	0.217565D 00

-0.192549D 00	-0.132974D 00	0.225885D 00	0.225885D 00
-0.190000D 00	-0.121915D 00	0.235235D 00	0.235235D 00
-0.187550D 00	-0.111703D 00	0.244696D 00	0.244696D 00
-0.185000D 00	-0.101491D 00	0.254859D 00	0.254859D 00
-0.182556D 00	-0.920916D-01	0.265611D 00	0.265611D 00
-0.180000D 00	-0.826920D-01	0.278507D 00	0.278507D 00
-0.177561D 00	-0.741371D-01	0.291977D 00	0.291977D 00
-0.175000D 00	-0.655822D-01	0.306958D 00	0.306958D 00
-0.172569D 00	-0.578567D-01	0.322996D 00	0.322996D 00
-0.170000D 00	-0.501312D-01	0.342686D 00	0.342686D 00
-0.167580D 00	-0.432748D-01	0.363914D 00	0.363914D 00
-0.165000D 00	-0.364185D-01	0.389407D 00	0.389407D 00
-0.163827D 00	-0.334553D-01	0.402952D 00	0.402952D 00
-0.162609D 00	-0.304922D-01	0.419709D 00	0.419709D 00
-0.161336D 00	-0.275290D-01	0.439676D 00	0.439676D 00
-0.160000D 00	-0.245659D-01	0.462855D 00	0.462855D 00
-0.158831D 00	-0.220970D-01	0.483908D 00	0.483908D 00
-0.157610D 00	-0.196281D-01	0.505764D 00	0.505764D 00
-0.156333D 00	-0.171592D-01	0.528423D 00	0.528423D 00
-0.155000D 00	-0.146903D-01	0.551886D 00	0.551886D 00
-0.154671D 00	-0.140984D-01	0.558685D 00	0.558685D 00
-0.154338D 00	-0.135064D-01	0.567636D 00	0.567636D 00
-0.153999D 00	-0.129144D-01	0.578739D 00	0.578739D 00
-0.153652D 00	-0.123224D-01	0.591994D 00	0.591994D 00
-0.153298D 00	-0.117304D-01	0.607402D 00	0.607402D 00
-0.152933D 00	-0.111384D-01	0.624963D 00	0.624963D 00
-0.152557D 00	-0.105465D-01	0.644676D 00	0.644676D 00
-0.152169D 00	-0.995447D-02	0.666541D 00	0.666541D 00
-0.151768D 00	-0.936249D-02	0.690558D 00	0.690558D 00
-0.151351D 00	-0.877050D-02	0.716728D 00	0.716728D 00
-0.150919D 00	-0.817852D-02	0.745050D 00	0.745050D 00
-0.150469D 00	-0.758654D-02	0.775525D 00	0.775525D 00
-0.150000D 00	-0.699455D-02	0.808152D 00	0.808152D 00
-0.147523D 00	-0.413224D-02	0.897843D 00	0.897843D 00
-0.147235D 00	-0.381145D-02	0.898764D 00	0.898764D 00
-0.145000D 00	-0.126994D-02	0.840998D 00	0.840998D 00
-0.144685D 00	-0.891797D-03	0.823749D 00	0.823749D 00
-0.144377D 00	-0.513659D-03	0.806380D 00	0.806380D 00
-0.144075D 00	-0.135521D-03	0.788892D 00	0.788892D 00
-0.143780D 00	0.242618D-03	0.771284D 00	0.771284D 00
-0.143492D 00	0.620756D-03	0.753557D 00	0.753557D 00
-0.143211D 00	0.998894D-03	0.735710D 00	0.735710D 00
-0.142936D 00	0.137703D-02	0.717744D 00	0.717744D 00
-0.142668D 00	0.175517D-02	0.699658D 00	0.699658D 00
-0.142407D 00	0.213331D-02	0.681452D 00	0.681452D 00
-0.142152D 00	0.251145D-02	0.663127D 00	0.663127D 00
-0.141905D 00	0.288959D-02	0.644682D 00	0.644682D 00
-0.141665D 00	0.326772D-02	0.626117D 00	0.626117D 00
-0.141432D 00	0.364586D-02	0.607433D 00	0.607433D 00
-0.141205D 00	0.402400D-02	0.588630D 00	0.588630D 00
-0.140986D 00	0.440214D-02	0.569707D 00	0.569707D 00
-0.140775D 00	0.478028D-02	0.550664D 00	0.550664D 00
-0.140570D 00	0.515842D-02	0.531501D 00	0.531501D 00
-0.140373D 00	0.553655D-02	0.512220D 00	0.512220D 00
-0.140183D 00	0.591469D-02	0.492818D 00	0.492818D 00
-0.140000D 00	0.629283D-02	0.473297D 00	0.473297D 00
-0.139806D 00	0.671194D-02	0.451705D 00	0.451705D 00
-0.139621D 00	0.713104D-02	0.430336D 00	0.430336D 00
-0.139445D 00	0.755015D-02	0.409187D 00	0.409187D 00
-0.139278D 00	0.796926D-02	0.388261D 00	0.388261D 00

-0.139120D 00	0.838836D-02	0.367556D 00	0.367556D 00
-0.138970D 00	0.880747D-02	0.347073D 00	0.347073D 00
-0.138829D 00	0.922657D-02	0.326811D 00	0.326811D 00
-0.138696D 00	0.964568D-02	0.306771D 00	0.306771D 00
-0.138572D 00	0.100648D-01	0.286952D 00	0.286952D 00
-0.138456D 00	0.104839D-01	0.267356D 00	0.267356D 00
-0.138348D 00	0.109030D-01	0.247981D 00	0.247981D 00
-0.138248D 00	0.113221D-01	0.228827D 00	0.228827D 00
-0.138156D 00	0.117412D-01	0.209895D 00	0.209895D 00
-0.138072D 00	0.121603D-01	0.191185D 00	0.191185D 00
-0.137996D 00	0.125794D-01	0.172696D 00	0.172696D 00
-0.137927D 00	0.129985D-01	0.154429D 00	0.154429D 00
-0.137866D 00	0.134176D-01	0.136384D 00	0.136384D 00
-0.137813D 00	0.138367D-01	0.118560D 00	0.118560D 00
-0.137767D 00	0.142558D-01	0.100958D 00	0.100958D 00
-0.137728D 00	0.146750D-01	0.835778D-01	0.835778D-01
-0.137697D 00	0.150941D-01	0.664189D-01	0.664189D-01
-0.137672D 00	0.155132D-01	0.494818D-01	0.494818D-01
-0.137655D 00	0.159323D-01	0.327662D-01	0.327662D-01
-0.137645D 00	0.163514D-01	0.162723D-01	0.162723D-01
-0.137641D 00	0.167705D-01	0.222045D-15	0.222045D-15

```
AT R/R=0.200  DELTA-CD=  0.883 USING BRAGG CORRELATION
AT R/R=0.250  DELTA-CD=  0.863 USING BRAGG CORRELATION
AT R/R=0.300  DELTA-CD=  0.925 USING BRAGG CORRELATION
AT R/R=0.400  DELTA-CD=  1.145 USING BRAGG CORRELATION
AT R/R=0.500  DELTA-CD=  1.545 USING BRAGG CORRELATION
AT R/R=0.600  DELTA-CD=  2.202 USING BRAGG CORRELATION
AT R/R=0.700  DELTA-CD=  3.271 USING BRAGG CORRELATION
AT R/R=0.800  DELTA-CD=  5.066 USING BRAGG CORRELATION
AT R/R=0.900  DELTA-CD=  7.488 USING BRAGG CORRELATION
AT R/R=0.950  DELTA-CD= 10.925 USING BRAGG CORRELATION
AT R/R=0.975  DELTA-CD= 18.481 USING BRAGG CORRELATION
```

PROPELLER PERFORMANCE AND DESIGN SECTION

* * * STRIP ANALYSIS METHOD * * *

ADVANCE RATIO=0.900

PROPELLER CHARACTERISTICS :

```
NUMBER OF BLADES            = 4
RADIUS OF PROPELLER         = 6.7500 (FEET)
RADIUS OF HUB               = 0.5015 (FEET)
NUMBER OF SECTIONS          = 11
CHORD AT PROPELLER TIP      = 0.2460 (FEET)
```

PROPELLER SECTION CHARACTERISTICS :

R/RAD=	BLDANG=	CHORD=	T/C=	ALPHA0=	CLD=	VDIS=	R/C=
0.2000	52.900	0.5130	0.6175	-3.998	0.7900	0.85500	0.0803
0.2500	47.200	0.6750	0.3900	-3.790	0.7420	0.89750	0.0507
0.3000	41.700	0.7750	0.2790	-3.513	0.6930	0.92500	0.0363
0.4000	32.800	0.9020	0.1715	-3.167	0.6080	0.95000	0.0223
0.5000	27.000	0.9290	0.1250	-2.720	0.5250	0.96500	0.0163
0.6000	23.200	0.8780	0.0975	-2.318	0.4480	0.97750	0.0127
0.7000	20.300	0.7720	0.0798	-2.035	0.3820	0.98900	0.0104
0.8000	17.800	0.6320	0.0725	-1.810	0.3420	0.99850	0.0094
0.9000	16.600	0.5280	0.0710	-1.721	0.3300	0.99930	0.0092
0.9500	15.900	0.3980	0.0695	-1.714	0.3260	0.99950	0.0090
0.9750	15.700	0.2460	0.0676	-1.699	0.3210	0.99990	0.0088

PROPELLER OPERATION CHARACTERISTICS :

```
FREE STREAM VELOCITY        = 207.5625 (FT/SEC)
FREE STREAM MACH NO.        = 0.19695
ALTITUDE FOR OPERATION      = 10000.000 (FEET)
PRESSURE AT ALTITUDE        = 1135.8375 (LB/FT**2)
TEMPERATURE AT ALTITUDE     = 461.000 (RANKINE)
DENSITY AT ALTITUDE         = 0.0014352 (LB*SEC**2/FT**4)
REQUIRED BLADE SETTING      =  13.050 (DEGREES)
REQUIRED HORSEPOWER         =     0.000
REQUIRED POWER COEFF.       = 0.000000
```

NOTE: IF ANY CHARACTERISTICS =0.0 ,THEN NOT SPECIFIED

PROPELLER PERFORMANCE CHARACTERISTICS :

R/RAD=	BETA=	PHI=	THETA=	ALPHA=	MACH=	REYN=
0.2000	65.950	50.767	4.288	10.895	0.21678	0.506
0.2500	60.250	45.804	5.161	9.285	0.24554	0.755
0.3000	54.750	41.454	5.360	7.935	0.27397	0.967
0.4000	45.850	34.231	5.252	6.367	0.33121	1.360
0.5000	40.050	28.938	4.977	6.135	0.39130	1.655
0.6000	36.250	25.019	4.850	6.381	0.45356	1.813
0.7000	33.350	22.036	4.817	6.497	0.51732	1.818
0.8000	30.850	19.675	4.584	6.590	0.58221	1.675
0.9000	29.650	17.645	4.846	7.159	0.64695	1.555
0.9500	28.950	16.773	5.210	6.967	0.67930	1.231
0.9750	28.750	16.372	5.738	6.640	0.69511	0.779

R/RAD=	VELI=	DELCT=	DELCQ=	CL=	CD=	CL/CD=
0.2000	17.129	0.00793	0.00434	1.0758	0.49244	2.185
0.2500	23.374	0.03999	0.00684	1.0756	0.05430	19.810
0.3000	27.092	0.06063	0.01056	1.0315	0.04413	23.374
0.4000	32.086	0.10865	0.01943	0.9514	0.03849	24.716
0.5000	35.911	0.16551	0.03132	0.9420	0.05286	17.821
0.6000	40.560	0.22290	0.04843	0.9796	0.10371	9.445
0.7000	45.950	0.25964	0.07286	1.0191	0.21417	4.758
0.8000	49.201	0.33154	0.07020	1.1297	0.07178	15.738
0.9000	57.810	0.39267	0.09551	1.2988	0.13426	9.674
0.9500	65.276	0.33629	0.08583	1.3358	0.14672	9.104
0.9750	73.606	0.21505	0.05573	1.3176	0.13584	9.700

R/RAD=	E=	BMAX=	AC=	K0=	CLI/CLC=	CDI/CDC=
0.2000	0.2746	0.6459	0.1252	0.2185	0.9500	1.8827
0.2500	0.3099	0.6855	0.1080	0.1800	0.9500	1.8627
0.3000	0.3453	0.7250	0.1051	0.1680	0.9500	1.9253
0.4000	0.4225	0.7967	0.1091	0.1620	0.9500	2.1451
0.5000	0.5116	0.8518	0.1250	0.1736	0.9500	2.5455
0.6000	0.6085	0.8900	0.1533	0.2001	0.9500	3.2021
0.7000	0.7092	0.9108	0.1988	0.2451	0.9500	4.2711
0.8000	0.8096	0.9138	0.2731	0.3197	1.0000	1.0000
0.9000	0.9056	0.8988	0.3636	0.4055	1.0000	1.0000
0.9500	0.9520	0.8871	0.5070	0.5527	1.0000	1.0000
0.9750	0.9752	0.8813	0.8408	0.9061	1.0000	1.0000

```
PROPELLER PERFORMANCE OUTPUT:

     PROPELLER ADVANCE RATIO          = 0.9000
     PROPELLER R.P.M.                 =  1025.000
     TOTAL ACTIVITY FACTOR            =  275.820
     BLADE ACTIVITY FACTOR            =   68.955
     PROPELLER THRUST                 =  2289.174 (LB)
     PROPELLER TORQUE                 =  7163.657 (FT*LB)
     HORSEPOWER ABSORBED              =  1398.058
     THRUST COEFFICIENT               =  0.16455
     TORQUE COEFFICIENT               =  0.03814
     POWER COEFFICIENT                =  0.23966
     PROPELLER EFFICIENCY             =  0.61793
     THRUST COEF. WITH CORRECTION     =  0.16402
     POWER COEF. WITH CORRECTION      =  0.23968
     PROP. EFF. WITH CORRECTION       =  0.61592

NOTE: THE ABOVE TERMS INCLUDE ICING EFFECTS
```

1. Report No. NASA CR-175092	2. Government Accession No.	3. Recipient's Catalog No.
4. Title and Subtitle Analytical Determination of Propeller Performance Degradation Due to Ice Accretion		5. Report Date April 1986
		6. Performing Organization Code
7. Author(s) Thomas L. Miller		8. Performing Organization Report No. None
		10. Work Unit No.
9. Performing Organization Name and Address Sverdrup Technology, Inc. Lewis Research Center Cleveland, Ohio 44135		11. Contract or Grant No. NAS 3-24105
		13. Type of Report and Period Covered Contractor Report
12. Sponsoring Agency Name and Address National Aeronautics and Space Administration Washington, D.C. 20546		14. Sponsoring Agency Code 505-68-11

15. Supplementary Notes

Final report. Project Manager, Robert J. Shaw, Propulsion System Division, NASA Lewis Research Center, Cleveland, Ohio 44135.

16. Abstract

A computer code has been developed which is capable of computing propeller performance for clean, glaze, or rime iced propeller configurations, thereby providing a mechanism for determining the degree of performance degradation which results from a given icing encounter. The inviscid, incompressible flow field at each specified propeller radial location is first computed using the Theodorsen transformation method of conformal mapping. A droplet trajectory computation then calculates droplet impingement points and airfoil collection efficiency for each radial location, at which point several user-selectable empirical correlations are available for determining the aerodynamic penalities which arise due to the ice accretion. Propeller performance is finally computed using strip analysis for either the clean or iced propeller. In the iced mode, the differential thrust and torque coefficient equations are modified by the drag and lift coefficient increments due to ice to obtain the appropriate iced values. Comparison with available experimental propeller icing data shows good agreement in several cases. The code's capability to properly predict iced thrust coefficient, power coefficient, and propeller efficiency is shown to be dependent on the choice of empirical correlation employed as well as proper specification of radial icing extent.

17. Key Words (Suggested by Author(s)) Propeller icing; Performance degradation; Analytical prediction		18. Distribution Statement Unclassified - unlimited STAR Category 03	
19. Security Classif. (of this report) Unclassified	20. Security Classif. (of this page) Unclassified	21. No. of pages 137	22. Price* A07

*For sale by the National Technical Information Service, Springfield, Virginia 22161

National Aeronautics and
Space Administration

Lewis Research Center
Cleveland, Ohio 44135

Official Business
Penalty for Private Use $300

SECOND CLASS MAIL

ADDRESS CORRECTION REQUESTED

Postage and Fees Paid
National Aeronautics and
Space Administration
NASA-451

NASA